Universitat de Girona

STUDY OF THE ANTICANCER ACTIVITY OF A NUCLEAR DIRECTED HP-RNASE VARIANT AND DIFFERENT METAL-BASED COMPOUNDS

Marlon Rolando Bravo Bonilla

Universitat de Girona

DOCTORAL THESIS

Study of the anticancer activity of a nuclear directed HP-RNase variant and different metal-based compounds

Marlon Rolando Bravo Bonilla

2022

Universitat de Girona

DOCTORAL THESIS

Study of the anticancer activity of a nuclear directed HP-RNase variant and different metal-based compounds

Marlon Rolando Bravo Bonilla

2022

PhD program in Molecular Biology, Biomedicine and Health

Under the direction of:

Dr. Antoni Benito Mundet and Dra. Jessica Castro Gallegos

Tutoring provided by:

Dr. Antoni Benito Mundet

Thesis delivered to obtain the doctoral degree by the Universitat de Girona

Dr. Antoni Benito Mundet

Professor titular del Departament de Biologia de la Universitat de Girona i Investigador Principal del Grup de Recerca en Enginyeria de Proteïnes de la Universitat de Girona

Dra. Jessica Castro Gallegos

Professora agregada del Departament de Biologia de la Universitat de Girona i membre del Grup de Recerca en Enginyeria de Proteïnes de la Universitat de Girona

Certifiquem:

Que Marlon Rolando Bravo Bonilla ha dut a terme sota la nostra direcció el treball titulat "**Study of the anticancer activity of a nuclear directed HP-RNase variant and different metal-based compounds**" que es presenta en aquesta memòria, la qual constitueix la seva Tesi per optar al Grau de Doctor per la Universitat de Girona.

A Girona,

Dr. Antoni Benito Mundet

Dra. Jessica Castro Gallegos

Girona, 21 de abril de 2022

ACKNOWLEDGEMENTS

ACKNOWLEDGEMENTS

Recuerdo que hace casi 4 años una de las primeras conversaciones con Jess, en la que planificamos experimentos, resolvíamos dudas y le comentaba sobre los años que tengo para avanzar con la investigación; tan ingenua e inocentemente por mi parte le decía: "*es un tiempo suficiente e ¡incluso! habrá tiempo de sobra, no es un tema que me preocupe realmente*", ella solo sonrió y me dijo: "*no lo creas, cuando menos te lo esperes el tiempo habrá terminado, los años pasan volando*", al escuchar esas palabras no lo creí realmente pero en un abrir y cerrar de ojos, cuando menos me di cuenta, el tiempo no me perdonó, se había agotado y me encontraba escribiendo estas líneas.

Así pues, quiero tener la oportunidad de poder decir gracias nuevamente a Toni y Jess, por ser más que mis directores, parte de mi familia aquí, al otro lado del mundo, mi segunda hermana mayor y mi segundo padre, por la paciencia, por el tiempo, por las explicaciones, por los conocimientos que heredé, por la confianza y por darme la oportunidad de elegir el camino que cambio mi vida, a ustedes gracias de nuevo y como no puede faltar, "¡*disculpen las molestias!*"

No se me puede olvidar tampoco decir muchas gracias a los demás miembros del grupo, María, Marc y en especial a Álex, ya que sin su ayuda tampoco podría estas escribiendo estas líneas.

Para terminar, quiero agradecer a mis padres y hermanos por el apoyo, que, aunque están a casi 10,000 km de distancia nunca faltó y siempre lo sentí, finalmente a mi compañera de vida *Alicia*, no sé qué haría sin ti, sin tu ayuda sin tu apoyo y compresión, solo puedo decir lo hicimos, vamos por la siguiente y por más.

Gracias, a cada una de las personas que en el transcurso de este tiempo pasaron por mi camino y dejaron su huella, tengan por seguro que de todos aprendí.

Marlon.

FUNDING

FUNDING

This doctoral thesis was supported by:

- Programa de ayudas para la contratación de investigadores en formación de la UdG IFUdG2018 (a predoctoral contract).

- Project BIO2013-43517 from the Ministerio de Economía y Competitividad (MINECO) Spain.

- Project MPCUdG2016-18 from the Universitat de Girona.

LIST OF PUBLICATIONS

LIST OF PUBLICATIONS

Publications and communications arisen from this thesis.

Publications:

Title: A family of manganese complexes containing heterocyclic-based ligands with cytotoxic properties.
Authors: Jessica Castro, Ester Manrique, **Marlon Bravo**, Maria Vilanova, Antoni Benito, Xavier Fontrodona, Montserrat Rodríguez, and Isabel Romero
Journal: Journal of Inorganic Biochemistry (2018) 182, 124-132
JCR Impact Factor: 4.155
DOI: https://doi.org/10.1016/j.jinorgbio.2018.01.021

Title: A Nuclear-Directed Ribonuclease Variant Targets Cancer Stem Cells and Inhibits Migration and Invasion of Breast Cancer Cells.
Authors: Jessica Castro, Giusy Tornillo, Gerardo Ceada, Beatriz Ramos-Neble, **Marlon Bravo**, Marc Ribó, Maria Vilanova, Matthew J. Smalley, and Antoni Benito.
Journal: Cancers (2021) 13 (17), 4350.
JCR Impact Factor: 6.639
DOI: https://doi.org/10.3390/cancers13174350

Title: Dinuclear iron complexes of iminopyridine based ligands as selective cytotoxins for tumor cells and inhibitors of cancer cells migration.
Authors: Jessica Castro, **Marlon Bravo**, Meritxell Albertí, Anaís Marsal, María José Alonso-De Gennaro, Oriol Martínez-Ferraté, Carmen Claver, Piet W. N. M. van Leeuwen, Isabel Romero, Antoni Benito, and Maria Vilanova.
Journal: Submitted for publication.

Communications:

Bravo M, López-Ramos B, Castro J, Benito A. Caracterització del mecanisme de citotoxicitat de variants de l'HP-RNasa dirigides a nucli i avaluació de la seva capacitat per inhibir la migració cel·lular i la invasivitat. I Jornades de Biologia de Girona. Girona, Spain, March 19-20, 2020. Oral presentation.

Bravo M, Albertí M, Martínez-Ferraté O, Alonso M, Marsal A, Romero M, Rodríguez M, Leeuwen P, Benito A, Vilanova M, Castro J. New cytotoxic iron-based complexes as potential anti-tumour agents. IV Jornades d'Investigadors Predoctorals de la Universitat de Girona. Girona, Spain, July 13-16, 2020. Oral presentation.

Bravo M, López-Ramos B, Castro J, Benito A. Caracterización y evaluación de la actividad antitumoral de compuestos metálicos y variantes de la HP-RNasa y su capacidad para inhibir la migración celular y metástasis. I Jornadas Virtuales de Ciencias en Laboratorio Clínico. Loja. Ecuador, March 22-27, 2021. Oral presentation.

LIST OF ABBREVIATIONS

LIST OF ABBREVIATIONS

AcH4	Acetylated histone H4
Bcr/Abl	Breakpoint cluster region / Tyrosine Kinase ABL1 fusion gene
BFBF	Dihydrobenzofurobenzofuran
BSA	Bovine serum albumin
CAR	Chimeric Antigen Receptor
cDNA	Complementary DNA
CEMIP	Cell Migration Inducing Hyaluronidase protein
CSCs	Cancer Stem Cells
CTCs	Circulating tumor cells
CTR-1	Copper transporter 1
DACH	1,2-Diaminocyclohexane
DBDOC	Methanodibenzodioxocine
DCF	Dichlorofluorescein
DFO	Desferrioxamine
DMEM	Dulbecco's Modified Eagle Medium
DMSO	Dimethylsulfoxide
DMT-1	Divalent metal transporter 1
DTPA	Diethylene triamine pentaacetic acid
ECIS	European Cancer Information System
ECM	Extracellular matrix
ECP	Eosinophil-cationic protein / RNase 3
EDN	Eosinophil-derived neurotoxin / RNase 2
EDTA	Ethylenediaminetetraacetic acid
FBS	Fetal bovine serum
FGF-2	Fibroblast growth factor 2
GFR	Growth Factor Reduced
GLUT1	Glucose transporter 1
GST	Glutathione S-transferase
H3K27me3	Trimethylation of lysine 27 of histone H3
HP-RNase	Human pancreatic ribonuclease
HPV	Human Papilloma Virus
IC	Inhibitory concentration
JNK	c-Jun N-terminal kinase
LLC	Lewis lung carcinoma
MDR	Multidrug resistant
MET	Mesenchymal epithelial transition
MMP2	Matrix Metallopeptidase 2
MMP9	Matrix Metallopeptidase 9
MTT	Thiazolyl Blue Tetrazolium Bromide
NAC	N-acetyl cysteine

ND-RNases	Nuclear-directed ribonucleases
NK	Natural Killer lymphocyte
NLS	Nuclear localization sequence
OCT	Organic cation transporter
ONC	Onconase
p53	Tumor suppressor protein p53
PBS	Phosphate-buffered saline
PFA	Paraformaldehyde
P-gp	Glycoprotein P / Multidrug resistance protein 1
PI	Propidium iodide
pRB	Retinoblastoma protein
pTEN	Phosphatase and tensin homolog gene tumor suppressor
RAS	Oncogene "Rat sarcoma"
RI	Ribonuclease Inhibitor
RNase	Ribonuclease
ROS	Reactive oxygen species
rpm	Revolutions per minute
RPMI	Roswell Park Memorial Institute culture medium
SE	Standard error
SOD	Superoxide dismutase
TfR	Transferrin receptor
TNBC	Triple Negative Breast Cancer
TNF	Tumor Necrosis Factor
TNF-α	Tumor Necrosis Factor alpha
VEGF	Vascular endothelial growth factor
VEGFR	Vascular endothelial growth factor receptor
WHO	World Health Organization
xg	Gravitational force

LIST OF FIGURES AND TABLES

LIST OF FIGURES AND TABLES

List of figures

List of tables

ABSTRACT

ABSTRACT

Cancer is the leading cause of death due to non-communicable diseases worldwide. Despite the large number of chemotherapeutics that have been developed so far, the cure of these diseases has been limited by their recurrence, the pharmacokinetic properties of the compounds used and the high toxicity that they often generate.

In this thesis we have evaluated and characterized the antitumor activity of NLSPE5, a nuclear directed ribonuclease (ND-RNase), as well as two panels of manganese- and iron-based metal compounds. The results obtained in this study show that NLSPE5 increases the expression of the epigenetic mark H3K27me3 in the MDA-MB-231 tumor cell line, it also significantly reduces the migration and invasion capacity of this cell line and, accordingly, it reduces the expression of the N-cadherin protein.

The evaluation of the panel of metallic compounds based on manganese indicates that, Mn8 has a remarkable and selective antitumor activity against lung (NCI-H460) and ovarian (OVCAR-8) tumor cell lines. Its IC_{50} is of the same order of magnitude as *Cis*-platin. This compound kills cancer cells by generating ROS species that allow it to cleave DNA. We have also demonstrated that cells of both tested lines die by a mechanism different from necrosis and apoptosis and that its antitumor activity is not linked to any cell-cycle phase.

Finally, the evaluation and characterization of the iron-based metal compounds shows that all the variants tested have an IC_{50} value lower than that of *Cis*-platin and carboplatin in the tumor cell lines tested. Moreover, all the compounds interact with DNA promoting double strand breaks through the production of ROS as with the Mn8 compound. Among them, the compound 10 shows the highest selectivity for tumor cells, alters the proportion of the phases of the cell cycle in a cell type-dependent manner, induces cell death by apoptosis and significantly decreases the migration capacity of the MDA-MB-231 tumor cell line.

RESUMEN

RESUMEN

El cáncer es la principal causa de muerte debido a enfermedades no transmisibles a nivel mundial. A pesar del gran número de quimioterapéuticos que se han desarrollado hasta el momento, la curación de estas enfermedades se ha visto limitada por su recurrencia, por las propiedades farmacocinéticas de los compuestos utilizados y por la elevada toxicidad que suelen generar.

En esta tesis se ha evaluado y caracterizado la actividad antitumoral de NLSPE5, una ribonucleasa dirigida al núcleo, así como de dos paneles de compuestos metálicos basados en manganeso y hierro. Los resultados obtenidos en este estudio muestran que NLSPE5 aumenta la expresión de la marca epigenética H3K27me3 en la línea celular tumoral MDA-MB-231, también es capaz de reducir significativamente la capacidad de migración e invasión de esta línea celular y, por último, reduce la expresión de la proteína N-cadherina.

La evaluación del panel de compuestos metálicos a base de manganeso indica que el Mn8 tiene una notable y selectiva actividad antitumoral contra las líneas celulares tumorales de pulmón (NCI-H460) y de ovario (OVCAR-8). Su IC_{50} es del mismo orden de magnitud que el *Cis*-platino. Este compuesto genera especies reactivas de oxígeno y gracias a ellas provoca la ruptura del ADN induciendo la muerte celular. También se ha demostrado que las células de ambas líneas ensayadas mueren por un mecanismo diferente al de necrosis y al de apoptosis, y que su actividad antitumoral no está vinculada a ninguna fase del ciclo celular.

Por último, la evaluación y caracterización de los compuestos metálicos basados en hierro muestra que todas las variantes tienen un valor de IC_{50} inferior al del *Cis*-platino y el carboplatino en las líneas celulares tumorales ensayadas. Además, todos los compuestos interaccionan con el ADN promoviendo su ruptura a través de la producción de ROS, como ocurre con el compuesto Mn8. Entre todos ellos, el compuesto 10 es el que muestra la mayor selectividad para las células tumorales, altera la proporción de las fases del ciclo celular de forma dependiente del tipo celular, induce la muerte celular por apoptosis y disminuye significativamente la capacidad de migración de la línea celular tumoral MDA-MB-231.

RESUM

RESUM

El càncer és la principal causa de mort a nivell mundial degut a malalties no transmissibles. Malgrat el gran nombre de fàrmacs que s'han desenvolupat fins ara, la curació d'aquestes malalties s'ha vist limitada per la seva recurrència, per les propietats farmacocinètiques dels compostos utilitzats i per l'elevada toxicitat que sovint generen.

En aquesta tesi s'ha avaluat i caracteritzat l'activitat antitumoral de NLSPE5, una ribonucleasa dirigida al nucli, així com la de dos panells de compostos metàl·lics basats en manganès i ferro. Els resultats obtinguts en aquest estudi mostren que NLSPE5 és capaç de reduir significativament la capacitat de migració i invasió de la línia cel·lular tumoral de càncer de mama MDA-MB-231. Aquesta reducció ve acompanyada per una disminució de l'expressió de la proteïna N-cadherina. També es mostra que els canvis d'expressió globals observats pel tractament de les cèl·lules tumorals amb NLSPE5 són deguts en part a canvis en el patró epigenètic de les cèl·lules ja que el tractament amb aquesta proteïna augmenta la presència de la marca epigenètica H3K27me3 a la línia MDA-MB-231.

L'avaluació del panell de compostos metàl·lics a base de manganès indica que el Mn8 té una activitat antitumoral notable i selectiva contra les línies cel·lulars tumorals de pulmó (NCI-H460) i d'ovari (OVCAR-8). La seva IC_{50} és del mateix ordre de magnitud que la del *Cis*-platí. Aquest compost genera espècies reactives d'oxigen dins de la cèl·lula i gràcies a elles provoca el trencament del ADN induint la mort cel·lular. També s'ha demostrat que les cèl·lules tumorals tractades amb Mn8 moren per un mecanisme diferent a la necrosi i l'apoptosi, i que la seva activitat antitumoral no està vinculada a cap fase del cicle cel·lular.

Finalment, l'avaluació i la caracterització dels compostos metàl·lics basats en ferro mostra que tots ells tenen un valor d'IC_{50} inferior al del *Cis*-platí i el carboplatí per les línies cel·lulars tumorals assajades. A més, tots els compostos interaccionen amb l'ADN promovent la seva ruptura a través de la producció de ROS, com passa

amb el compost Mn8. De tots els compostos assajats, el 10 és el que mostra la major selectivitat per a les cèl·lules tumorals. Aquest compost altera la proporció de les fases del cicle cel·lular de forma depenent del tipus cel·lular, indueix la mort cel·lular per apoptosi i disminueix significativament la capacitat de migració de la línia cel·lular tumoral MDA-MB-231.

TABLE OF CONTENTS

TABLE OF CONTENTS

INTRODUCTION

1. INTRODUCTION

1.1 Cancer

According to the World Health Organization (WHO), cancer refers to a large group of diseases that can affect any part of the body characterized by molecular changes and mutations that allow the cell to have an abnormal and uncontrolled growth [1,2], allowing them to migrate and invade other areas of the body. This later process is called metastasis and is the main cause of cancer death [3]. Since cancer is not a single disease, but many disorders with a natural evolution, it displays a high diverse therapeutic response [4].

1.1.1 Current global perspective

The number of deaths caused by cancer have been growing rapidly in recent years worldwide. The reasons are both diverse and complex, reflecting the growth and aging of the population as well as changes in the prevalence and distribution of the main risk factors for developing this pathology [5–7].

The data of incidence and mortality of cancer in Europe according to the European Cancer Information System (ECIS) for the year 2020 are shown in **Figure 1**. As it can be seen during that year an estimated 2.68 million new cases and 1.26 million deaths were recorded [8].

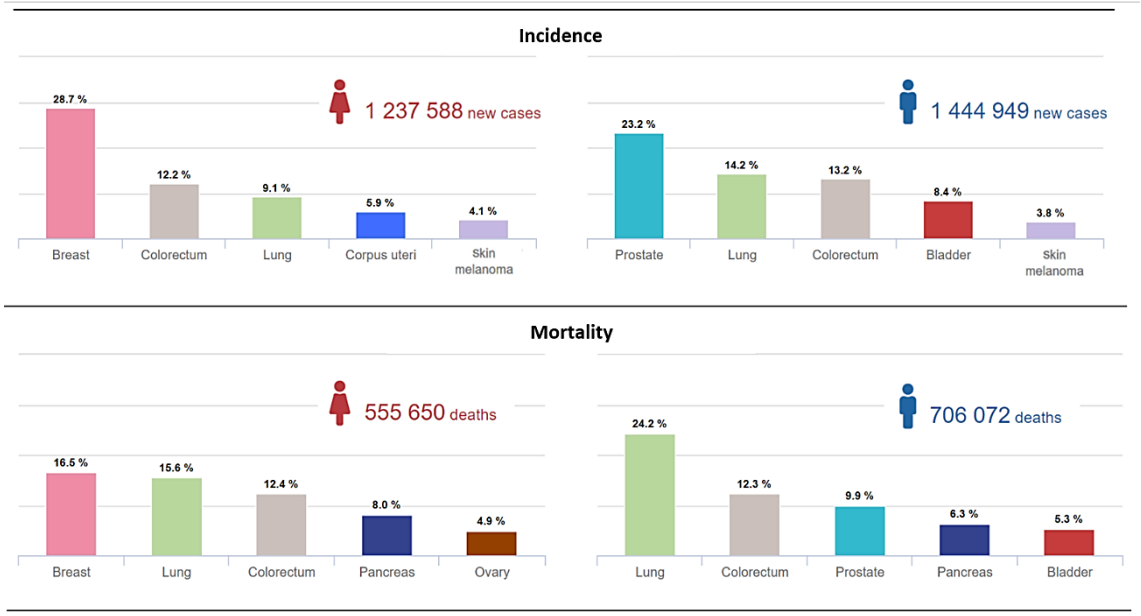

Figure 1. Cancer incidence and mortality in Europe. Distribution of cases and deaths for the top ten most common cancers (excluding non-melanoma skin cancer) in Europe in 2020 for both sexes. Figure extracted and modified from: ECIS from https://ecis.jrc.ec.europa.eu © European Union, 2022

In Spain ECIS data show that during 2020 a total of 260,455 new cases of cancer were detected, 110,946 in women and 149,509 in men, while the number of deaths were 112,335, corresponding to 44,990 deaths in women and 67,345 deaths in men. Breast cancer was the most commonly diagnosed cancer in women (incidence of 30.72%) and prostate cancer in men (incidence of 23.15%). However the most common cancer causing death is colorectal cancer in women with a mortality rate of 15.18% and lung cancer in men with a mortality rate of 25.76% [8].

1.1.2 Molecular basis

Carcinogenesis, the process by which a normal cell becomes cancerous, is mediated by mutations in the genetic material of the cell [2,9]. It is estimated that about 20,000 DNA damage events and 10,000 replication errors occur in a normal cell daily, [10] but in normal conditions the immune system has mechanisms such as tumor immunosurveillance that allow it to eliminate tumor cells. However, some of

them can develop new characteristics that allow them to evade these mechanisms and develop cancer [11].

Due to the great diversity of types of cancer it is very difficult to clearly establish which are the pathways that are altered in the cell to become tumorous and whether these are shared in all types of cancers. Hanahan and Weinberg [2,12] proposed that all manifestations in the phenotype of cancer cells are mainly due to the presence of eight essential characteristics that are common to all cancer cells and are responsible for the cancer development and their evasion of the tumor immunosurveillance system. These characteristics are: 1. self-sufficiency in growth signals, 2. insensitivity to growth-inhibitory signals, 3. evasion of programed cell death (apoptosis), 4. limitless replicative potential, 5. sustained angiogenesis, 6. tissue invasion and metastasis, 7. reprogramming of energy metabolism and, 8. evasion from immune destruction.

The following is a brief description of each of the eight features of the tumor cells mentioned above. First, the most paradigmatic characteristic of tumor cells is their high rate of multiplication corresponding to "*Self-sufficiency in growth signals*". Unlike the cells that form normal tissues, in cancer cells the mechanisms that regulate cell cycle entry and subsequent cell division are out of control. This loss of homeostasis is mainly due to the occurrence of mutations or increased expression of tyrosine kinase cell surface receptors. These changes allow the tumor cell to maintain its cell cycle always active [12–14].

There are several ways by which tumor cells can become *"Insensitive to signals that inhibit cell growth"* but the two most studied are mutations in the retinoblastoma protein (pRB) and p53 protein. The pRB protein is responsible for regulating the passage from G1 to S phase of the cell cycle. It has been observed that this protein is mutated in 100% of retinoblastoma cases, while in lung, bladder, osteosarcoma, liver, and esophagus cancers it is also mutated but to a lesser extent [15]. p53 is a transcription factor that like pRB regulates the cell cycle. The functionality of this protein is critical since it has the ability to induce the

repair of DNA when damage has occurred or can initiate the process of apoptosis if the damage is irreparable. p53 is mutated in 50% of all human cancers [16,17].

The homeostasis of a tissue depends on the balance between cell proliferation and cell death, a balance that is carried out by a mechanism of programed cell death called apoptosis. "*Evasion of apoptosis*" is another hallmark of human cancers that promotes tumor formation and progression, as well as resistance to treatment. Tumor cells evade apoptosis by activating anti-apoptotic and cell survival programs that ultimately block cell death [18].

Under normal conditions, most cells have a limited number of cell divisions, a phenomenon called *Hayflick limit* [19,20]. Tumor cells have an "*Unlimited replicative potential*" because they express telomerase that adds repetitive segments to the ends of telomeric DNA, preventing it from shortening. This protein is not found in most normal cells, while in tumor cells it is present in about 90% of them. The expression of this protein is enhanced by the presence of mutations in the p53 protein and allows tumor cells to become immortal.

Throughout human development, the formation of new blood vessels, called angiogenesis, is necessary to supply nutrients and oxygen and also to remove waste products [21]. Accordingly, tumor cells maintain a mechanism of "*Sustained angiogenesis*". This mechanism would be mediated through different growth factors and cytokines such as vascular endothelial growth factors (VEGFs), fibroblast growth factors (FGFs), tumor necrosis factor alpha (TNF-α) and interleukin 8 (IL-8) [22–24].

Most of the cancer-related deaths are due to the capacity of the tumor cells for "*Tissue invasion and metastasis*". Invasion occurs when the tumor cell invades nearby tissue, while the process by which tumors cells spread far from the primary tumor is called metastasis. Two of the best characterized proteins linked to this capacity are E-cadherin and N-cadherin. These proteins are essential for cell adhesion to the extracellular matrix (ECM) and it has been shown that the

increased expression of N-cadherin and the decreased expression of E-cadherin play a central role in tumor cell migration and invasion [12,25,26]. Another phenomenon linked to invasive cells is the phenotypic change towards mesenchymal cells, a process called Epithelial-Mesenchymal Transition (EMT). In this process tumor cells lose their adherent junctions, change their epithelial morphology, increase their motility, and increase the expression of enzymes that degrade the ECM [25]. On the other hand, the fibroblasts surrounding the tumor cells generate a pro-tumor microenvironment called *reactive stroma* that favors the carcinogenic process and the EMT process [12,27]. The invasive process leading to the development of a "successful" metastasis is an inefficient process. In breast cancer only 0.01% of the cells released into circulation (circulating tumor cells, CTCs) produce a bone metastasis [27]. The presence of CTCs is necessary, but not sufficient, for the development of metastases, as CTCs have been found in disease-free patients up to 20 years after successful treatment [27]. In recent years, the usefulness of measuring CTCs and their functional characterization for prognostic and predictive purposes in cancer patients has been proposed, although the detection methods available for their mass introduction still need to be improved [28].

Cells under aerobic conditions normally degrade glucose to carbon dioxide, a process that begins in the cytoplasm to end in the mitochondrial matrix. However, in tumor cells a phenomenon called *Warburg effect* [29] is observed, in which cells undergo a "*Reprogramming of energy metabolism*" towards glycolysis. *Warburg effect* is defined as an increase in the rate of glucose uptake and preferential production of lactate, even in the presence of oxygen in the medium [30–32]. In the tumor cell an overexpression of glucose transporters is observed, mainly GLUT1. It is believed that the cell performs this reprogramming to meet the bioenergetic and biosynthetic demands of its rapid growth. It is also proposed that under these conditions the cell would be protected from hypoxia-normoxia fluctuations that derive from the reorganization of the tumor vasculature during its growth [12,33].

The human body has an immune surveillance system that includes the innate and adaptive immune system, which normally detects and removes, among others, tumor cells. The presence of adaptive immune system cells within the tumor in

some types of cancer is a prognostic indicator. In colon and ovarian tumors, the presence of cytotoxic T lymphocytes and Natural Killer (NK) cells have a better prognosis than those without the presence of cytotoxic lymphocytes [12]. Accordingly, failures in this surveillance system could explain why tumor cells acquire an "*Evasion of immune destruction*" leading to a higher incidence of certain types of tumors in immunocompromised individuals [34,35]. Normally, tumor cells are recognized by immune system cells because they express on their surface a protein pattern different from that expressed by normal cells. Despite the mechanisms that detect and eliminate tumor cells, their recognition remains difficult since there is a degree of immunotolerance by part of the immune system. In addition, due to genomic mutations, their antigenic profile is constantly changing and hand in hand with this change, there is an overexpression of cytokines and chemokines. The cytokines and chemokines produced act as immunomodulators, regulating their microenvironment and favoring the recruitment of monocytes, macrophages and highly suppressive cells (e.g. regulatory T lymphocytes) thus suppressing the activity of the immune system and favoring angiogenesis [12,34].

Accumulating evidence from previous studies has suggested that malignant tumors are highly heterogeneous and likely contain a small subset of tumor cells with self-renewal capacity and differentiation potential called cancer stem cells (CSCs). CSCs are proposed to be implicated in different tumor hallmarks such as angiogenesis, tumor growth, metastasis, drug resistance and immune dysregulation and as a consequence, the elimination of this cell subpopulation represent a current challenge in cancer therapy [36–40].

1.1.3 Cancer treatment approaches

Over the past few years, significant progress has been made in understanding the development of cancer, which has led to important advances in its treatment. Common cancer treatment methods include surgery, radiation

therapy, immunotherapy, hormonal therapy, targeted therapies and chemotherapy [41–43]. Surgery is the "first line" treatment for solid cancers such as breast and lung [44] and aims to remove all cancerous tissue. However, it is ineffective in patients with advanced tumor pathology or when surgery failed to remove the entire tumor mass [45,46]. Radiation therapy aims to kill cancer cells using high-energy radiation (photons, protons or particle radiation). Although radiation damages both normal and tumor cells, the main goal of this therapy is to maximize exposure to tumor cells while minimizing the radiation dose to adjacent normal cells.

Cancer immunotherapy takes advantage of the immune system's ability to recognize and eliminate cancer cells. The two main therapeutic approaches used in cancer immunotherapy are based on the enhancement of the patient's own antitumor immunity with cytokines or vaccines and on the administration of tumor-reactive immune cells such as chimeric antigen receptor (CAR) T cells [47].

Hormonal therapy applies to cancers whose development is dependent or is sensitive to hormones. There are three major types of hormonal therapies based on the type of cancer:

1. Breast cancer hormone therapy that uses competitive inhibitors of estrogen receptor that lowers the levels of estrogen and progesterone.

2. Prostate cancer hormonal therapy such as anti-androgens, luteinizing hormone blockers, and gonadotrophic releasing hormone blockers, that are used to reduce serum testosterone levels.

3. Ovarian and womb cancer hormonal therapy in which an estrogen receptor blocker is used, mainly Tamoxifen [42].

This therapy it is commonly combined with other treatments, such as surgery, radiation, or chemotherapy, and is considered a systemic treatment because it affects tumor cells throughout the body.

On the other hand, the goal of targeted therapy is to deliver drugs to specific genes or proteins to cancer cells or to the tissue environment that promotes cancer

growth. The efficacy of the therapy lies in the selective release of drugs at the site of disease, minimizing unwanted side effects in normal tissues. Targeted therapy involves the development of drugs that block cancer cell proliferation or induce apoptosis or autophagy. Targeted therapy involves the use of monoclonal antibodies or small oral drugs [43].

Finally, chemotherapy is the use of chemicals to fight against cancer and is the most common clinical choice of treatment [48]. Chemotherapeutic agents are administered intravenously or orally, and then travel through the bloodstream to attack cancers cells that have spread from the primary tumor to distant parts of the body. These compounds act by killing rapidly dividing cells and their efficacy depends on the type and stage of cancer. Nevertheless, their use is often limited by their toxicity to other tissues in the body [49]. A brief list of the compounds most commonly used as chemotherapeutics in various types of cancer is depicted in **Table 1**.

Table 1. Most common types of chemotherapeutics used for cancer treatment.

Compound type	Mechanism of action	Examples	Ref.
Alkylating agents	React with electron-rich atoms in biological molecules (such as amino acids, nucleic acids DNA/RNA) to form covalent bonds. Substitute alkyl groups for hydrogen atoms on DNA, resulting in the formation of cross links within the nucleic acid and the misreading of the DNA code. This leads to the inhibition of DNA, RNA, and protein synthesis, which ultimately induces apoptosis.	Nitrosourea compounds (e.g. carmustine), Alkyl sulfates (e.g. busulfan, treosulfan), Ethyleneimine derivatives (e.g. thiotepa), Epoxides (e.g. etoglucide), Triazene compounds (e.g. dacarbazine, temozolomide) and Metal salts (e.g. *Cis*-platin, carboplatin, oxaliplatin)	**50–52**
Antimetabolite agents	These agents act mainly during the S phase of the cell cycle generally by mimicking natural purines and pyrimidines and affecting DNA synthesis.	Folate analogs (e.g. aminopterin), Purine analogs (e.g. mercaptopurine) and Pyrimidine analogs (e.g. fluorouracil, gemcitabine, capecitabin)	**53–58**
Antimitotic natural agents	These agents act on the microtubules of the cell and they are generally classified into two groups, microtubule stabilizing agents and microtubule destabilizing agents. Stabilizing agents act by promoting the assembly of tubulin into microtubules or by inhibiting the disassembly of the mitotic spindle once it has formed. Destabilizing agents inhibit the polymerization process of microtubules activating the chromatic spindle checkpoint, thus, blocking the passage from metaphase to anaphase.	Destabilizers: Vinka alkaloids (e.g. vinblastine, vincristine) and Colchicine and its derivatives (e.g. combretastatins). Stabilizers: Taxanes such as paclitaxel, docetaxel and cabazitaxel	**59–66**
Cytotoxic antibiotics	Form covalent bonds with nucleic acids interfering with DNA synthesis.	Puromycin, anthracyclines such as daunorubicin, doxorubicin among others.	**53,67–71**

1.2 Antitumor drugs based on ribonucleases

The flow of genetic information is channelized through DNA ↔ RNA → Protein and is controlled by enzymes of RNA metabolism such as RNA polymerases and ribonucleases (RNases) [72]. RNases are classified using different functional or evolutive criteria. Depending on how they cleave RNA, these enzymes can be classified as exoribonucleases if they cleave nucleotides from the 5′ or 3′ end of RNA molecules, or as endoribonucleases, which cleave RNA at an internal phosphodiester bond [73]. Also, they are classified depending on their sequence homology. Using this criteria, RNases are classified into three major families: the RNase A superfamily (which includes RNases from mammals, birds, reptiles, and amphibians), the T1 family and the T2 family.

The RNase A superfamily is extremely dynamic, with high rates of gene duplication and gene loss, resulting in a variable number of genes in different species [74]. RNases of this superfamily usually consist of a signal peptide of about 25 amino acids, a mature peptide of about 130 residues containing three catalytic residues (one lysine and two histidines) and six to eight cysteines forming three to four disulfide bonds. The homology between the RNases that are part of the RNase A superfamily can be between 20% to almost 100% [74]. Within this family we can find six classical members: pancreatic ribonuclease (RNase 1), eosinophil-derived neurotoxin (EDN, or RNase 2), eosinophil-cationic protein (ECP, or RNase 3), RNase 4, angiogenin (RNase 5), and RNase 6 (or k6) [74]. More recently, different studies have expanded the superfamily to include seven additional members, RNases 7 to 13 [74]. In addition to RNA regulation, RNases have other biological activities such as participation in angiogenesis, immunosuppression, and antiviral and antibacterial processes [75]. The interest in studying RNases as antitumor agents began in the early 1950s, when it was reported that bovine pancreatic ribonuclease (RNase A) was shown to have antitumor activity both *in vitro* and *in vivo* [76].

Human pancreatic ribonuclease (HP-RNase or RNase 1) is a glycoprotein secreted mainly by the pancreas, although it has also been found in kidney, liver, brain, spleen and endothelium. Additionally, it is found in seminal plasma and urine [77]. HP-RNase is considered the human counterpart of the RNase A with which it shares a 70% of sequence identity and the ability to cleave RNA, specifically on the 3'-side of pyrimidine bases. Both enzymes show an increased activity over poly(C) than with poly(U) and also an optimal activity at pH near 8.0. However, HP-RNase presents a higher activity both on double stranded RNA and on destabilizing DNA [78–80].

From then on, it has been shown that different members of the RNase superfamily have selective cytotoxic activity for tumor cells, constituting an approach to anticancer therapy [81,82]. The mechanism of cytotoxicity of different RNases has been partially characterized. These RNases interact with a specific or a nonspecific component of the target cell and are endocytosed. Then, at some point of the endocytic pathway they translocate to the cytosol avoiding lysosomal degradation. Once there, the RNase has to evade the action of the ribonuclease inhibitor (RI) to preserve its ribonucleolytic activity and therefore to be able to degrade different kinds of RNAs and induce cell death by apoptosis [83]. The RI is a protein present in the cytosol of mammalian cells that bind some RNases with high affinity and is thought to act as safeguard against an eventual entry of foreign RNases into the cells [84,85]. Therefore, to kill the cells, these RNases must evade by some mechanism the action of RI. For instance, Onconase (ONC), a RNase of amphibian origin, display antitumor activity because it binds with very low affinity to RI and thus evading its inhibition.

The mechanism by which the tumor cells are more sensitive to the RNases is not completely known, but it has been postulated that RNases may be selectively recognized or internalized by malignant cells because their membrane is highly anionic. This hypothesis is derived from the observation that the molar ratio between ethanolamine phospholipids and choline phospholipids in the plasma membrane increases following neoplastic transformation [83,86]. Very recently, both RNase A and its human counterpart, the HP-RNase, have been described to interact

with a neutral hexasaccharide glycosphingolipid, Globo H, a component of a glycolipid or a glycoprotein located on the outer membrane of epithelial cells and detected in high levels in the outer membrane of several tumor cells [76,87]. Other hypotheses to explain the selectivity of RNases towards tumor cells would indicate that RNases follow a different internalization pathway that is present only in tumor cells, or that this specificity might depend on the fact that malignant cells might be more sensitive than normal cells to the toxic effects of RNA hydrolysis. [83].

Based on this knowledge, different groups have envisaged different strategies to endow RNases with antitumor activity. Some of them have designed RNases capable of avoiding interaction with the RI by introducing steric hindrances and preventing the formation of the RNase-RI complex [84,88]. Other groups have endowed the RNases with higher capacity to reach the cytosol and saturate all the RI present into the cell [76].

HP-RNase is an interesting enzyme to endow with antitumor activity because it shows low renal toxicity and immunogenicity, and displays higher ribonucleolytic activity than ONC, cleaving more efficiently a wide range of cellular RNAs [89–91]. Although HP-RNase is not cytotoxic for tumor cells because it cannot evade the RI, different research groups have developed cytotoxic HP-RNase variants [88,92] some of which entered in Phase I clinical trials (Evade™ RNases from Quintessence Biosciences Company).

1.2.1 Nuclear directed-RNases (ND-RNases)

In the last 15 years, our group has developed a new strategy to endow HP-RNase with cytotoxic activity that consists in redirecting the protein to the nucleus, which is an RI-free organelle, by introducing a nuclear localization signal (NLS) into its sequence [76]. These RNases are named nuclear directed-RNases (ND-RNases). Apart of endowing the RNase with cytotoxic activity, another benefit of bringing the molecule inside the nucleus is the increase of the specificity towards

neoplastic cells whose nuclear transport is seven times more active than that of non-transformed cells [93].

PE5, the first developed ND-RNase, is an HP-RNase variant which has five substitutions at the N-terminal end (Arg4Ala, Lys6Ala, Gln9Glu, Asp16Gly and Ser17Asn) and also incorporates two other mutations: Gly89Arg and Ser90Arg [94]. Despite being sensitive to the RI, PE5 is cytotoxic against many human tumor cell lines [95,96] because it carries a non-contiguous extended bipartite NLS constituted by at least three basic regions of the protein, comprising Lys1 and the Arg clusters 31-33 and 89-91. Although these regions are separated by more than 90 residues in the primary structure, they are close in the three-dimensional structure of the protein and their topological disposition is equivalent to that of a classical bipartite NLS [97]. Once PE5 has been internalized and reaches the cytosol, this NLS is recognized by α-importin, which drives the protein into the nucleus, specifically into the nucleolus, where PE5 cleaves nuclear RNA, leaving cytosolic RNA undamaged [97]. PE5 is recognized by α-importin and by RI, and the regions of the enzyme implicated in the binding to both proteins are overlapped. This means that once PE5 has internalized and reaches the cytosol, it can interact with both proteins but not at the same time [98]. Although the affinity of PE5 for RI would be higher than that of α-importin, PE5 molecules captured by α-importin would be released into the nucleus and exit the two competing equilibria. The lack of free PE5 molecules would shift the PE5-RI equilibrium toward dissociation, making the free PE5 molecules ready to be captured by α-importin. As a result, PE5 will progressively accumulate in the nucleus [98]. The replacement of the critical residues of the NLS significantly reduces the cytotoxicity of PE5, indicating that the NLS endows this HP-RNase variant with cytotoxic activity [99]. The cytotoxic properties of PE5 have been studied using NCI/ADR-RES cells. Treatment of this cell line with PE5 generates classical hallmarks of apoptosis such as plasma membrane blebbing, apoptotic body formation, chromatin condensation, nuclear fragmentation, phosphatidylserine translocation and caspase activation [96]. This cell death is mediated by the increase of the expression of $p21^{WAF1/CIP1}$ together with the underphosphorylation of JNK [96]. Interestingly, PE5 reduces the expression level of P-gp in the multidrug resistant (MDR) cell lines NCI/ADR-RES and NCI-H460/R. It

has also been reported that the combination of PE5 and doxorubicin is synergistic in NCI/ADR-RES [100]. Studies using human cDNA microarrays to determine the gene expression pattern of PE5-treated NCI/ADR-RES cells have shown that PE5 especially decreases the expression of genes involved in metabolic pathways that are deregulated in tumor cells (glycolysis, lipid synthesis and degradation, and amino acid synthesis pathways). This decrease is accompanied by the under expression of oncogenes and overexpression of tumor suppressor genes. PE5 also increases the expression of genes involved in the removal of reactive oxygen species (ROS) and decreases the expression of genes associated with the acquisition of MDR [101].

New ND-RNases have been lately constructed from PE5 to improve their properties. Firstly, an additional NLS of the SV40 large T antigen, which was known to bind efficiently to α-importin [102], was introduced in PE5 to increase its cytotoxicity. The new variant, called NLSPE5, is ten times more cytotoxic than PE5. Although *in vitro* it slightly evades RI, in treated cultured cells it is unable to degrade cytosolic RNA, which also demonstrates that its cytotoxicity depends on the ability to degrade nuclear RNA [98,103]. The effects of NLSPE5 on tumor cells are analogous to those of PE5 in the NCI/ADR-RES cell line: it induces a two-fold increase in the levels of $p21^{WAF1/CIP1}$ and cyclin E, leaving cyclin D1 unaltered, the proportion of early and late apoptotic cells at different incubation times is of the same order as PE5 and, finally, NLSPE5 also activates procaspases 3, 8 and 9, following the same pattern as PE5 [98].

Subsequent assays [104] showed that NLSPE5 has lower IC_{50} values than ONC for tumor cell lines while for non-tumor cell lines the IC_{50} values of NLSPE5 are much higher. The ratio between the IC_{50} values of non-tumor and tumor cells ranges from 5 to 18-fold when we compare the two least affected cell lines and the two most affected by NLSPE5. In contrast, these values for ONC only range between 0.25 and 1.8-fold. For the CCD-18Co non-tumor cells, it was shown that the resistance to RNase-induced apoptosis coincides with the overexpression and cytoplasmic subcellular localization of $p27^{KIP1}$ [104]. A more recent study shows that

NLSPE5 shows high selectivity for 3D cultured tumor cells and significantly decreases the viability and self-renewal capacity of CSCs [105].

1.3 Metal-based antitumor compounds

Metal ions are necessary for several organ functions, as well as for the treatment of diseases. Among these metal ions we can include not only metals essential for life such as iron, copper, or zinc, but also metals previously described as dangerous such platinum [106].

Designing ligands that will interact with free or protein-bound metal ions is also a recent focus of medicinal inorganic research. The development of new metal compounds as potential antitumor agents is a complicated task, due to the possible accumulation of these ions in the organism, their biodistribution, excretion and pharmacological specificity. A mechanistic understanding of how metal complexes achieve their activities is crucial to their clinical success, as well as to the rational design of new compounds with improved potency [107]. In the case of metal-based drugs, the metal centers, being positively charged, are favored for binding to negatively charged biomolecules such as proteins and nucleic acids [107], whereas the ligands can play an important role in target site recognition. The presence of a chelating ligand can control reactivity towards different biomolecules (DNA, enzymes) and play a key role in the interaction with them through hydrogen bonds or intercalation [108]. In addition, lipophilic ligands are useful for increasing cellular uptake while the shape of the ligands can be tailored to improve DNA affinity, facilitate binding with receptors on the surface of tumor cells, and inhibit enzymes involved in cancer progression. The ligands also determine the type of DNA-adduct that is formed, as well as the mode of cell-death that ensues [108,109]. In conclusion the ligands impart their own functionality and can tune properties of the overall complex that are unique from those of the individual ligand or metal [110].

1.3.1 Platinum based compounds and its reversals

Platinum-based compounds, such as carboplatin, *Cis*-platin and oxaliplatin, are being used in the treatment of approximately 10–20% cancers [111]. Recently, scientists have focused on studying the specific biochemical interactions responsible for the pharmacological effects of platinum-based compounds, partly elucidating the differences between the mechanism of action of each metal compound [112].

In terms of structure, *Cis*-platin, carboplatin and oxaliplatin are complex Pt (II) combinations. *Cis*-platin has a structure of two ammine groups and two chloro ligands that are oriented in a cis planar configuration around the central platinum ion. Carboplatin differs from *Cis*-platin in that it has a 1,1-cyclobutanedicarboxylate bidentate ligand in place of the two chloride ligands. Oxaliplatin has a more complex structure in which the ammine monodentate ligands are replaced by the 1,2-diaminocyclohexane (DACH) bidentate ligand and the Cl- ligands by the oxalate bidentate ligand [113].

Cis-platin is an alkylated agent that acts by covalent binding to DNA. In aqueous biological media the chloro- ligands are replaced by water and interact with DNA to form inter- and intra-strand cross-links. These new connections are formed between two adjacent purine bases (between two guanines or between guanine and adenosine) located on the same strand or on different strands leading to distortion of the DNA structure. Subsequently, replication and transcription are disrupted, and although these DNA- *Cis*-platin products are recognized by many DNA repair complexes the cell goes into apoptosis [114]. Cells incorporate *Cis*-platin using cupper transporter 1 (CTR1), a transmembrane protein implicated in cupper homeostasis [115] and only 1% of intracellular *Cis*-platin can bind DNA. It is hypothesized that *Cis*-platin's toxicity in slowly proliferating or terminally differentiated cells may be primarily due to drug-protein interactions [116]. Indeed, *Cis*-platin can react with a lot of substrates in the cytoplasm such as glutathione, methionine, metallothionein and other proteins, through their cysteine residues. *Cis*-platin displays an important cytotoxic activity by tipping the redox scale in

favor of oxidative stress, leading to mitochondrial membrane permeabilization and DNA damage [114,117].

Cis-platin has become the mainstay in combination therapy of advanced and metastatic testicular germ-cell cancer, and it is also used against small cell and non-small cell lung cancers as well as cervical, bladder and esophageal cancers. A set of severe side-effects during *Cis*-platin therapy is known: nephrotoxicity, neurotoxicity, nausea, ototoxicity and vomiting. Nephrotoxicity is even with vigorous hydration and forced diuresis the most common dose-limiting factor, occasionally leading to irreversible kidney damage [118].

The second-generation platinum drug carboplatin, whose cyclobutanedicarboxylic acid has a slower kinetic for binding to biological molecules, was developed to reduce the dose-limiting toxicity of *Cis*-platin. As a result of reduced reactivity, the neurotoxicity and ototoxicity after carboplatin treatment are much less pronounced but the dose is limited by myelosuppression, with thrombocytopenia, being more severe than neutropenia and anemia [119]. Carboplatin is used to treat many types of solid cancers, such as ovarian cancer and advanced non-small and small cell lung cancers [120,121]. However, carboplatin has limited efficacy against testicular germ-cell cancers, squamous cell carcinoma of head and neck and bladder cancer. As a consequence, *Cis*-platin still remains the drug of choice for treating these diseases [119].

Oxaliplatin, a third-generation platinum drug, was developed to overcome the resistance that some types of cancer, such as metastatic colorectal cancer, present to *Cis*-platin and carboplatin. The ligand oxalate significantly reduces oxaliplatin reactivity and consequently limits its toxicity [119] whereas DACH lipophilic characteristics increase passive absorption of oxaliplatin when compared to *Cis*-platin and carboplatin [122]. This higher lipophilicity could explain why oxaliplatin uses other cellular incorporation pathways such as organic cation transporters OCT1 and OCT2. Overexpression of these transporters significantly increases oxaliplatin cellular accumulation (with no effect on *Cis*-platin and

carboplatin). Colorectal cancer cells express high levels of OCT transporters, and this may explain why oxaliplatin is efficient in these types of cancers.[114,119].

Following the success of platinum-based compounds and considering their disadvantages including activity against a limited number of tumors, severe side-effects, and the problem of developing drug resistance during treatment, other compounds containing different metals such as manganese, iron, ruthenium, copper, and gold, among others, have been investigated with the aim of discovering novel cytotoxic compounds with a higher therapeutic index [112].

1.3.2 Manganese compounds

Manganese is an essential metal that is necessary for normal functioning of a variety of physiological processes including amino acid, lipid, protein and carbohydrate metabolism [123,124]. Mn ion is a widely distributed metal which is a required cofactor for many ubiquitous enzymes [125].

It has been shown that Mn (II) ions are mainly taken up and transported by the divalent metal transporter DMT-1 and by transferrin (Tf) receptor (TfR). The fact that these proteins are highly expressed in some tumor tissues [126,127] endows Mn (II)-based compounds with a molecular mechanism to target tumor cells. Mn (II) salts have been reported to exert anti proliferative effects on several cancer cell lines and Mn (II) complexes containing thiosemicarbazone or hydrazone groups have been reported as antitumor agents generally by the induction of apoptotic cell death at rather high concentrations [126,128–132]. Finally, it is possible for special Mn (II) complexes to target cancer cells through an ATP-related Ca transporter [126].

Currently, coordination sites occupied by good leaving groups are labile sites for substitution reactions with target sites. It has been considered that manganese complexes containing these N-chelating ligands, such as pyridines,

bipyridines, and pyrazoles [133–136], and chloride, triflate or nitrate as labile ligands, could be highly cytotoxic for tumor cell lines as it has been observed for the α-$[Ru(azpy)_2Cl_2]$ compound, which contains the same type of ligands [137]. It has recently been demonstrated that the application of the aforementioned ligands to Mn (II) endows this metal with antiproliferative characteristics in several tumor cell lines [108].

1.3.3 Iron compounds

Iron is a naturally occurring element in the human body involved in many biological processes. For instance, Fe promotes energy generation and oxygen transport in living cells [138], and it also participates in metabolic processes including DNA synthesis. However, Fe concentrations in body tissues must be tightly regulated because excessive Fe leads to tissue damage as a result of formation of free radicals, β-thalassemia, Friedreich's Ataxia and cancer [139,140]. Organic molecules as Fe chelators have been studied as effective treatments against some cancer types, such as colorectal cancer [141].

Cancer cells require larger quantities of Fe than normal cells, which is reflected by the marked overexpression of TfR necessary for the uptake of Fe into these cells [142]. The increased Fe uptake plays a pivotal role during the intensive DNA synthesis in neoplastic cells [143]. The increased Fe dependence of cancer cells suggest that Fe depletion may be an effective strategy to inhibit the rapid proliferation of cancer cells [144]. Fe compounds with antitumor properties show low toxicity to normal cells and multiple anticancer mechanisms which, interestingly, are different from those of platinum complexes [145]. The most studied families of Fe compounds as anticancer agents are those of organometallic complexes of ferrocene and the inorganic coordination complexes of Fe (II) and Fe (III) [145].

Among the metal complexes with antitumor activity described in the literature, multinuclear ones show great potential as anticancer agents [146].

Multinuclear complexes exhibit novel modes of DNA binding that are distinct from *Cis*-platin, such as the ability for long-range DNA crosslinking within or between strands, bisintercalation, binding to the major or minor groove, and electrostatic binding [146]. A number of bimetallic mixed complexes containing a ferrocene and another transition metal have been synthesized showing improved cytotoxicity compared with the corresponding ferrocenyl motifs [147]. Other Fe compound 1D-polymeric Fe (III) complexes containing N-donor heterocyclic ligands have been tested over a panel of tumor cell lines, showing interesting cytotoxic values although the compounds are not stable in the medium [148]. Unlike polymeric and mixed bimetallic Fe complexes, few binuclear Fe complexes have been tested as antitumor agents and although they have nuclease activity, they are not highly cytotoxic [149].

OBJECTIVES

2. OBJECTIVES

Cancer continues to be one of the most lethal illnesses worldwide. To improve cancer survival, it is necessary to develop new antitumor agents that could affect those cells responsible of metastasis and drug resistance and that could be more selective towards tumor cells. In this line, our group is developing both, proteins such as human RNase variants and metal-based compounds, as antitumor drugs. ND-RNases such as NLSPE5, have a highly anticancer potential due to their non-mutagenic activity, their selectivity for cancer cells, their low immunogenicity, their action against multiple important tumor processes in addition to their lower renal retention and much higher ribonucleolytic activity than other cytotoxic RNases. As with RNases and due to the great success of antitumor compounds based on metals such as platinum, the development of new metallic compounds has been a great avenue of research that seeks to maximize the beneficial effect and limit the side effects that these compounds commonly present. For this, our research group has been interested in developing antitumor complexes based on transition metals such as Mn (II) and Fe (II).

Considered these aspects, the main objectives of the present work can be summarized as follows:

- To study the effect of NLSPE5 on the expression of different epigenetic marks.

- To study the effects of NLSPE5 on the migration and invasiveness of a highly invasive breast cancer cell line.

- To determine the *in vitro* cytotoxicity and selectivity for tumor cells of a panel of new Mn and Fe compounds in the human ovarian adenocarcinoma OVCAR-8 and lung carcinoma NCI-H460 cell lines.

- To determine the effect of the most cytotoxic and selective for tumor cells Mn and Fe compounds on the cell cycle phase distribution and the induction of apoptosis.

- To study the molecular mechanism of cytotoxicity of the selected Mn and Fe based compounds.

- To determine the effect on cell migration of cancer cells of the most effective Fe compound.

METHODS

3. METHODS

3.1 RNase variant

Plasmid expressing the HP-RNase variant NLSPE5 (pNLSPE5) has been previously described [101]. NLSPE5 is a PE5 variant that incorporates the NLS of SV40 large T-antigen (PKKKRKVE) at its N-terminus plus a two-residue linker (AS) [101]. PE5 is a HP-RNase variant [95] that carries seven substitutions: Arg4Ala, Lys6Ala, Gln9Glu, Asp16Gly, Ser17Asn, Gly89Arg and Ser90Arg [80,95]. As a result of these modifications, PE5 has a conformational bipartite NLS [97,99].

3.1.1 RNase expression and purification

NLSPE5 was produced and purified from *Escherichia coli* BL21(DE3) cells [150] transformed with pNLSPE5 essentially as described previously [80,151]. Briefly, transformed cells were grown in Luria-Bertani medium supplemented with 100 μg/ml ampicillin until an absorbance at 550 nm near 1.5 was reached. Protein expression was induced by the addition of isopropyl thiogalactoside (Fermentas, USA) to 1 mM. After 3-4 h, cells were harvested by centrifugation at 7,500 xg for 7 min. Pellet from 2 L of induced culture was resuspended in 30 ml of 10 mM ethylenediaminetetraacetic acid (EDTA), 50 mM Tris-acetate (pH 8.0). Cells were lysed using a French press and inclusion bodies were harvested by centrifugation at 12,000 xg for 45 min at 4ºC. Pellets were then solubilized in 10 ml of 6 M guanidinium chloride, 2 mM EDTA, 100 mM Tris-acetate (pH 8.5). Reduced glutathione was added to a final concentration of 0.1 M, the pH was adjusted to 8.5 with solid Tris, and the samples were incubated at room temperature for 2 h under a nitrogen atmosphere to assist protein solubilization. Insoluble material was removed by centrifugation at 14,500 xg for 30 min at 4ºC and solubilized protein was diluted dropwise into 0.5 M L-arginine, 1 mM oxidized glutathione, 2 mM EDTA, 100 mM Tris-acetate (pH 8.5) and incubated at 4°C for at least 48 h. Then, protein was concentrated by tangential ultrafiltration using a Prep/Scale TFF cartridge (Millipore, USA) and dialyzed against 50 mM sodium acetate (pH 5.0).

The sample was centrifuged at 15,000 xg for 30 min at 4ºC to remove insoluble material, loaded onto a Mono-S HR 5/5 FPLC column (Amersham Biosciences, USA) equilibrated with 50 mM sodium acetate (pH 5.0), and eluted with a linear gradient from 0 to 1 M NaCl. Fractions eluting at approximately 0.6 M NaCl contained pure and properly folded NLSPE5. They were collected and dialyzed against ultra-pure water, lyophilized, and stored at -20 °C until its use. A yield of 15–25 mg of protein per 1 L of culture was obtained. The molecular mass of each variant was confirmed by Matrix-assisted laser desorption/ionization time-of-flight (MALDI-TOF) mass spectrometry in the *Serveis Tècnics de Recerca (STR*) of the University of Girona (UdG) (Girona, Spain). The protein concentration was determined by ultraviolet spectroscopy using an extinction coefficient at 280 nm of 7950 M^{-1} cm^{-1} for this variant calculated as reported previously [152].

3.2 Manganese compounds

A panel of Mn complexes with ligands containing nitrogen as donor atoms (Mn1-8) and their ligands (L-Mn1-8, respectively) were synthesized by members of the *Catalysis and Sustainability Research Group* of the Department of Chemistry of the UdG. Except Mn7[which is based on Mn (III)], the complexes were Mn (II)-based compounds containing the pyrazolic ligands 2-(1-methyl-3-pyrazolyl) pyridine (pypz-Me) and ethyl 2-(3-(pyridine-2-yl)-1H-pyrazol-1-yl) acetate (pypz-CH_2COOEt), together with chlorido or triflate as monodentate ligands (**Figure 2**). Compounds Mn1 and Mn2 have the general formula $[MnX_2(pypz\text{-}Me)_2]$, where X corresponds to Cl^- and $CF_3SO_3^-$, respectively. Compound Mn3 has the formula $[Mn(CF_3SO_3)_2(pypz\text{-}CH_2COOEt)_2]$. Compounds Mn4-7 contain the bidentate 2-(3-pyrazolyl) pyridine (pypz-H) ligand whereas compound Mn8 the chiral bidentate nitrogen ligand (−)-pinene[5,6]bipyridine ((−)-L) (**Figure 2**).

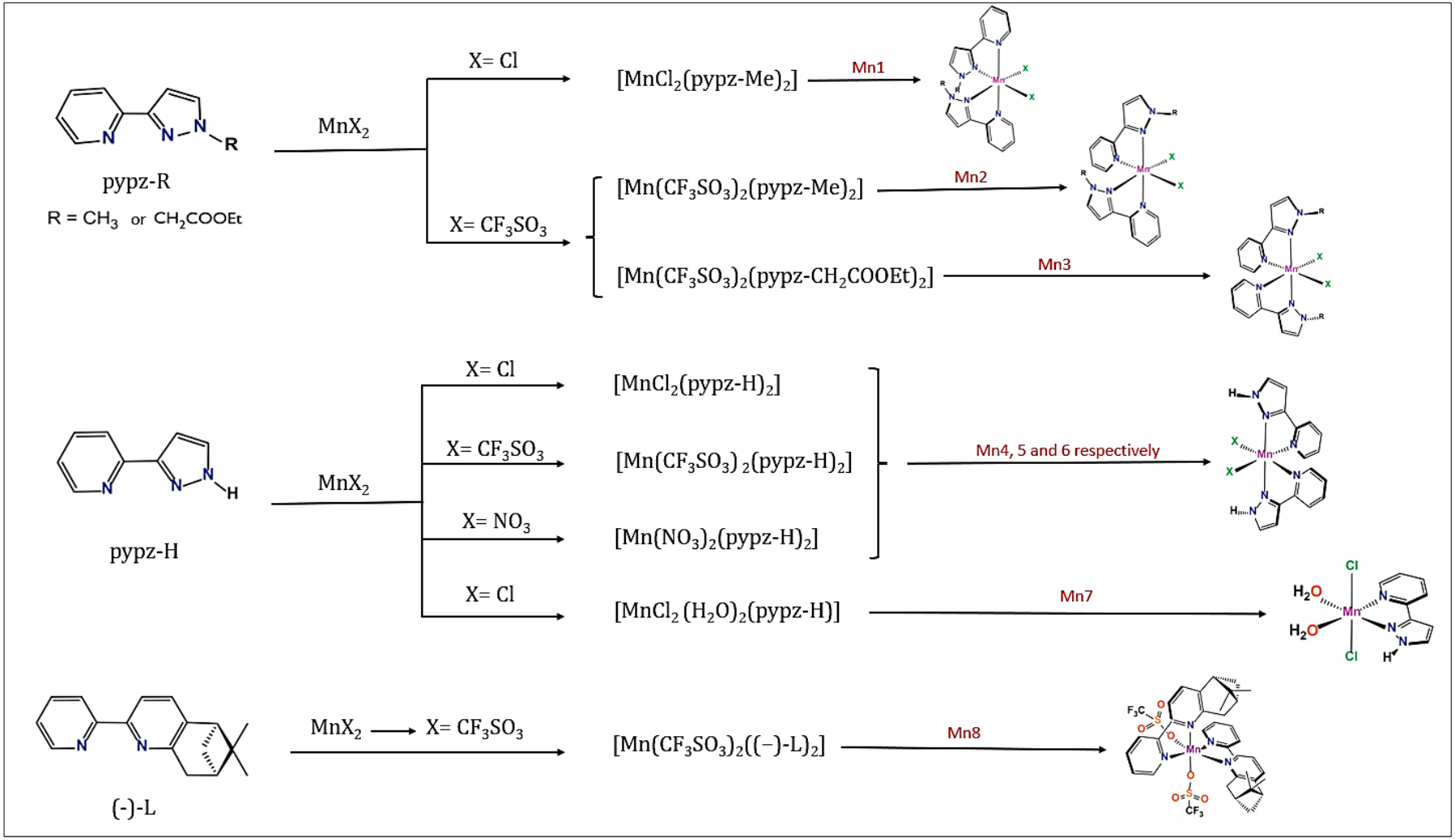

Figure 2. Synthesis and structure of different metallic Mn compounds. Figure extracted and modified from Rich *et al.*[134], Manrique *et al.*[136] and Castro *et al.* [108].

3.2.1 Preparation of manganese compounds

Mn compounds and their ligands were first reconstituted in dimethylsulfoxide (DMSO) at 25 mg/ml and then the samples were diluted dropwise onto sterile and bidistilled water to reach a final concentration of 4% DMSO. Then, the concentration of the compounds and ligands was determined using their extinction coefficients. The extinction coefficient of each compound and ligand was calculated experimentally by measuring their absorbance at the wavelength where each one presents its maximum (λmax). A linear regression equation between absorbance at λmax and different concentrations of each compound or ligand was calculated in each case to obtain the different molar extinction coefficients from the slope (see **Table 2**). Finally, stock solutions were then diluted to the desired final concentrations with sterile complete medium immediately before each experiment.

Table 2. Molar extinction coefficients of the different Mn compounds and their ligands.

Mn Compound	**Extinction coefficient** (M^{-1} cm^{-1})
Mn1 $[MnCl_2(pypz\text{-}Me)_2]$	17,526
Mn2 $[Mn(CF_3SO_3)_2(pypz\text{-}Me)_2]$	23,274
Mn3 $[Mn(CF_3SO_3)_2(pypz\text{-}CH_2COOEt)_2]$	21,380
Mn4 $[MnCl_2(pypz\text{-}H)_2]$	19,082
Mn5 $[Mn(CF_3SO_3)_2(pypz\text{-}H)_2]$	16,291
Mn6 $[Mn(NO_3)_2(pypz\text{-}H)_2]$	13,353
Mn7 $[MnCl_2(H_2O)_2(pypz\text{-}H)]$	18,186
Mn8 $[Mn(CF_3SO_3)_2((-)\text{-}L)_2]$	23,541
Mn ligand	
pypz-Me	6,719
pypz-CH_2COOEt	12,452
pypz-H	6,717
(−)-L	15,467

3.3 Iron compounds

A series of imino- and amino-pyridine ligands based on dihydrobenzofurobenzofuran (BFBF) and methano-dibenzodioxocine (DBDOC) backbones were synthesized at the *Institut Català d'Investigació Química (ICIQ)* [153] (see **Figure 3**). These ligands form bimetallic and binuclear complexes with Fe (II) and have been designated as compound 7-12. The compounds contain six different ligands (L1-6) and present octahedral coordination due to the two nitrogens present in each ligand. Thus, each Fe atom can coordinate with the labile ligands (which in this case are acetonitrile). The counterions for the six compounds studied are tetrafluoroborate $[BF_4]_4$. Compound 10 and compound 11 differ in that at position 6 the former has a methyl group and the latter a methoxy group. Compound 12 has a phenyl group as radical.

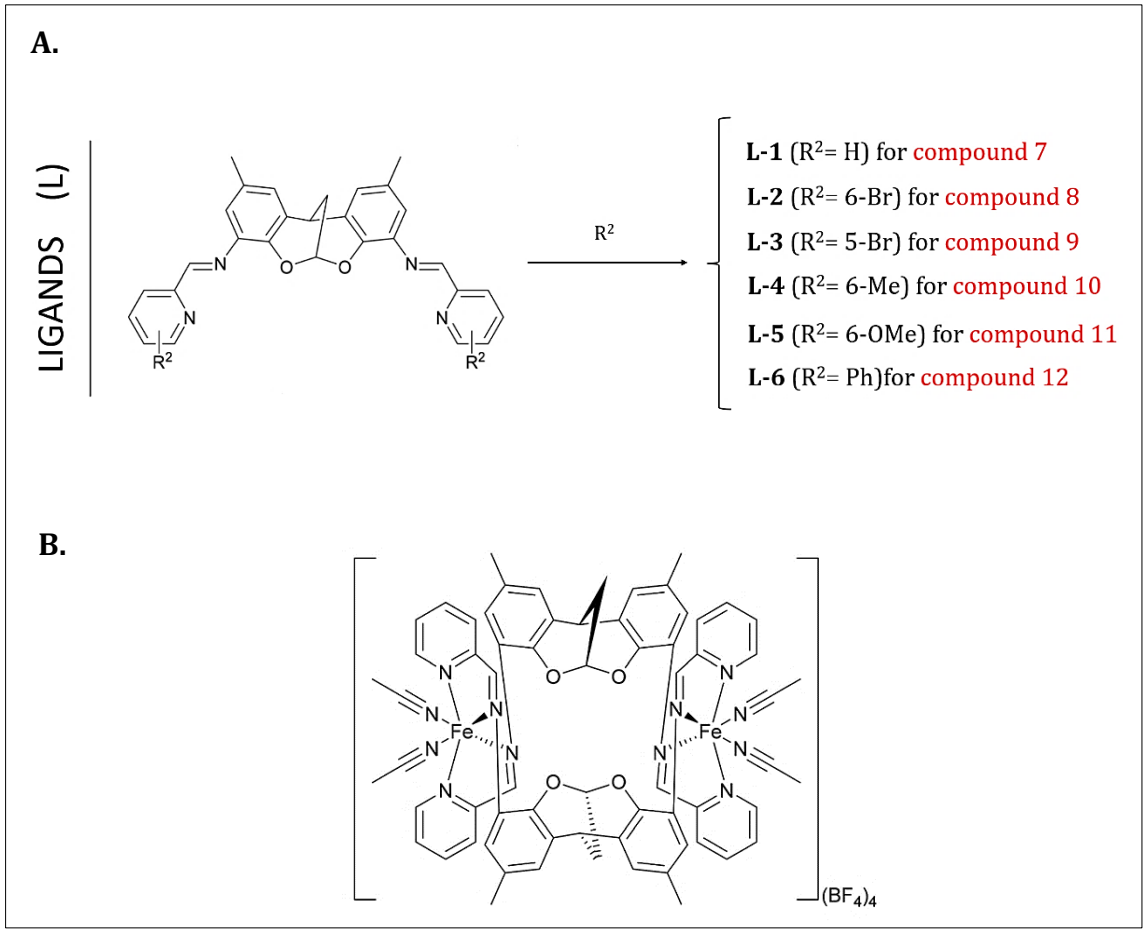

Figure 3. Chemical structure of Fe compounds. **A.** Structure of the ligands used, where R^2 represent the different substituents in each compound. **B.** Representative arrangement of two ligand molecules within the iron compound. Image taken and modified from Martínez-Ferraté *et al*. [153].

3.3.1 Preparation of iron compounds

Compounds and their ligands were first reconstituted in DMSO at 4.4 mg/ml and then left under magnetic stirring protected from light until the compound was completely dissolved. Then the samples were diluted dropwise onto sterile and bidistilled water and then each compound was filtered and its concentration calculated by measuring the absorbance at 280 nm. For each compound, a stock solution of 100 μM at 4% DMSO was prepared and then diluted to the desired final concentrations with sterile complete medium immediately before each experiment.

3.4 Cell lines and culture conditions

Human mammary gland adenocarcinoma cell line MDA-MB-231 [154] and normal human colon fibroblasts CCD-18Co [155] were obtained from Eucellbank (Universitat de Barcelona, Spain). Human non-small cell lung cancer cell line NCI-H460 [156], and human ovarian cancer cell line OVCAR-8 [157] were obtained from the National Cancer Institute - Frederick DCTD tumor cell line repository. Tumor cell lines were routinely grown on RPMI 1640 media (Gibco, USA) supplemented with 10% fetal bovine serum (FBS) (Gibco, Germany), 50 U/mL penicillin, 50 μg/mL streptomycin and 1% L-Glutamine (Gibco, Germany). CCD-18Co cells were cultured in DMEM medium (Gibco, Germany) supplemented with 10% FBS, 50 U/mL penicillin, 50 μg/mL streptomycin and 1% L-Glutamine. Cells were maintained at 37ºC in a 5% CO_2 humidified atmosphere, remained free of *Mycoplasma,* and were propagated in adherent culture according to established protocols.

3.5 Cell proliferation assays

3.5.1 Cytotoxicity assays in 2D

Cells were seeded into 96-well plates at the appropriate density: 2,500 cells for MDA-MB-231, 2,800 cells for NCI-H460, 10,000 cells for CCD-18Co and 2,600

cells for OVCAR-8. Cells were seeded and incubated for 24 h and then were treated with various concentrations of the cytotoxic molecule for a further 72 h. *Cis*-platin (Pfizer, Spain) and carboplatin (Teva, Spain) were included as controls in some experiments. To determine the effect of the cytotoxic compounds on the viability of the cell lines, an assay that monitors the reduction of Thiazolyl Blue Tetrazolium Bromide (MTT) (Sigma, USA) to formazan was used. Data were collected by reading at 570 nm in a multi-well plate reader (Synergy 4 hybrid, Biotek, USA). The IC_5, IC_{10}, IC_{20}, and IC_{50} values represent the concentrations of the assayed compounds required to inhibit cell proliferation by 5, 10, 20, and 50%, respectively, and were calculated by interpolation from the obtained growth curves. The mean standard error (SE) was calculated from at least three independent experiments with three replicas in each one.

3.5.2 Cytotoxicity assay in 3D

MDA-MB-231 single cells resuspended in RPMI 1640 media containing 2.5% of Growth Factor Reduced (GFR) Matrigel™ (Corning, USA) were seeded at a concentration of 1,000 cells/well into 96-well plates coated with a thin solidified layer of GFR Matrigel™. After 2 days of incubation for growing on GFR Matrigel™, cells were treated with different concentrations of NLSPE5 in media containing 2.5% GFR Matrigel™ for 72 h. Cell viability was determined by the CellTiter-Glo method, essentially following the manufacturer's instructions (Promega, USA). All data are described as the mean ± SE of at least three independent experiments.

3.6 Transwell migration and invasion assays

The migration assay protocol depends on the compound tested. For NLSPE5, 200,000 MDA-MB-231 cells were seeded into 6-well plates and after 24 h of incubation, cells were pretreated with 0.05, 0.1, and 0.2 μM of NLSPE5 (corresponding to an IC_5, IC_{10} and IC_{20}, respectively) for 24 h at 37ºC. Then cells were trypsinized and 12,500 viable cells were suspended in 0.4 ml RPMI 1640

medium with 0.5% FBS and the same concentration of NLSPE5 and seeded into the upper chamber of a 24-well transwell insert (8 μm pore size; Sarstedt, Germany) for 48 h at 37ºC. For the evaluation of compound 10, no pretreatment was performed. Cells were seeded directly into the transwell chamber and treated with 0.1 μM (corresponding to an IC_{20} in 2D cultures) of compound 10 for 24, 48 and 72 h. The number of cells and volumes used are the same as described above. In both cases the lower chamber contained 0.5 ml RPMI 1640 medium with 10% FBS as a chemoattractant. Then, non-migrated cells were wiped from the upper surface of the membrane with a cotton swab and migrated cells remaining on the bottom surface were fixed with 4% paraformaldehyde (PFA) for 30 min. Cells were stained with 0.2% crystal violet solution for 20 min at room temperature and ten randomly selected fields at 200X magnification were counted using an Olympus CKx41 inverted microscope. The invasion assays were performed using the same procedure as the migration assay except that the number of cells seeded into the upper chamber of the transwell was of 25,000 and the chamber filter was coated with GFR Matrigel™.

3.7 Wound closure cell migration assay

MDA-MB-231 cells (600,000 on 2 ml) suspended in culture media were seeded into a 6-well plate and allowed to grow to 80% confluence. Then, a straight scratch was made using a 200 μl pipette tip, and cells were washed with cold PBS before treating with different concentrations of NLSPE5 in media with 0.5% FBS. Images were captured at 0, 16, 24, 40, and 48 h after wounding using an Olympus CKx41 inverted microscope. The wound area was quantified using the ImageJ software (National Institute of Health, USA), with a wound healing tool macro (Montpellier RIO Imaging, France). Treatment effects were described as the mean ± SE of three independent experiments.

3.8 Protein sample preparation for Western Blots

The effect of NLSPE5 on the expression of different proteins implicated in migration and evasiveness and on the epigenetic regulation was evaluated in 3D cell cultures cultured in GFR Matrigel™. This methodology better reproduces the multicellular architecture and cell relationships that occur *in vivo* and, therefore, is a better predictor of *in vivo* responses to NLSPE5 [158–161]. MDA-MB-231 single cells resuspended in media containing 2.5% of GFR Matrigel™ were seeded at a density of 15,000 cells/well into 48-well plates coated with a thin solidified layer of GFR Matrigel™. After 3 days of incubation, cells were treated with 0.5 μM NLSPE5 (corresponding to an IC_{30} in 3D cultures) in media containing 2.5% GFR Matrigel™ for 72 h. After treatment, wells were rinsed thoroughly with PBS supplemented with a protease inhibitor cocktail (ab65621, Abcam, UK). Then, GFR Matrigel™ was liquefied by incubating for 1 h on ice with Cell Recovery Solution (Corning, USA). Cell spheroids were collected by centrifugation at 6,000 rpm and lysed using a lysis buffer (9803, Cell Signaling Technology, USA). Cell lysates were stored at −80 °C. Protein concentrations were quantified with a Pierce BCA protein assay kit (Thermo Fisher Scientific, USA).

3.9 Western Blot analysis

50 μg protein extracts were submitted to SDS-PAGE and transferred to PVDF membranes. Then membranes were blocked with BSA 5% for 2h and probed overnight with primary antibodies directed against the following proteins: N-cadherin (dilution 1/500; sc-393933, Santa Cruz Biotechnology), E-cadherin (dilution 1/500; sc-8426, Santa Cruz Biotechnology), MMP2 (dilution 1/200; sc-13595, Santa Cruz Biotechnology), MMP9 (dilution 1/200; sc-21733, Santa Cruz Biotechnology), H3K27me3 (dilution 1/1,500; ab6002, Abcam), AcH4 (dilution 1/500; 06-866, Millipore) and Actin (dilution 1/300; sc-8432, Santa Cruz Biotechnology). The secondary antibodies (mouse anti-rabbit peroxidase conjugate (dilution 1/10,000; sc-2357, Santa Cruz Biotechnology) or goat anti-

mouse IgG peroxidase conjugate (dilution 1/15,000; DC02L, Calbiochem) were incubated for 2 h at room temperature. Blots were developed with immobilon chemiluminescent HRP substrate (Millipore, USA) and images were captured by a FluorChem SP system (Alpha Innotech, USA). The intensity of each band was quantified using the ImageJ software (National Institutes of Health (NIH), USA).

3.10 Detection of Reactive Oxygen Species

Reactive oxygen species (ROS) generation was determined by flow cytometry using the carboxy-2',7'-dichlorodihydrofluorescein diacetate probe (carboxy-H_2DCFDA) (Invitrogen, USA). Carboxy-H_2DCFDA is oxidized to green fluorescent dichlorofluorescein (DCF) by ROS. NCI-H460 and OVCAR-8 cell lines were seeded in 6-well plates (70,000 cells/well) in phenol red-free RPMI (Gibco, USA) and incubated for 24 h before treatments. Cells were treated with different concentrations of Mn8 or its ligand (2, 5 and 9 μM for NCI-H460 and 5, 12 and 24 μM for OVCAR-8) or compound 10 (0.7, 1.5 and 3 μM for NCI-H460 cells and 2, 4.5 and 9 μM for OVCAR-8 cells) for 48 or 72 h at 37 °C. After treatments, cells were washed with PBS and incubated with 1 μM carboxy-H_2DCFDA for NCI-H460 cells or 0.5 μM for OVCAR-8 cells in PBS for 30 min at 37 °C in the dark. Then, cells were trypsinized with phenol red-free trypsin, collected by centrifugation at 2,200 rpm and analyzed on a NovoCyte flow cytometer (ACEA Biosciences, USA). The geometric mean fluorescence intensity of 10,000 cells was established using NovoExpress software (ACEA Biosciences, USA).

To further investigate the involvement of ROS in the cytotoxic mechanism of the metallic compounds, the effect of the antioxidant agent N-Acetyl-L-Cysteine (NAC) (Sigma, USA) on the cytotoxicity of those compounds was also investigated. 2,600 cells/well of NCI-H460 or 2,800 cells/well of OVCAR-8 were seeded in 96-well plates 24 h prior to treatments. After 24 h cells were treated with Mn8, its ligand and with compound 10 for 48 or 72 h at 37°C. When indicated, cells were co-treated with the compounds plus 2.5 mM NAC. Finally, the viability of NAC-

treated cells was compared to that of cells without NAC treatment by the MTT method previously described.

3.11 Cell cycle phase analysis

Cell cycle phase analysis was performed by propidium iodide (PI) staining. NCI-H460 (50,000 cells/well, 6-well plates) and OVCAR-8 cells (100,000 cells/well, 6-well plates) were seeded and incubated for 24h. Then, cells were treated with Mn8 or its ligand (2 or 9 μM for NCI-H460 and 5 or 24 μM for OVCAR-8) or compound 10 (0.3 μM for NCI-H460 and 0.8 μM for OVCAR-8) for 72 h and then harvested and fixed with 70% ethanol overnigth at −20 °C. Fixed cells were harvested by centrifugation and washed in cold PBS. The collected cells were resuspended in PBS (1–2 × 10^6 cells/mL), treated with RNase A (100 μg/mL) and incubated with PI (40 μg/mL) (Molecular Probes, USA) at 37 °C for 30 min before flow cytometric analysis. A minimum of 10,000 cells within the gated region was analyzed on a NovoCyte flow cytometer. Cell cycle phase distribution was analyzed using the NovoExpress software.

3.12 Phosphatidylserine exposure assay

Quantitative analysis of apoptotic cell death caused by Mn8, its ligand or compound 10 was performed by flow cytometry using the Alexa Fluor 488 annexin V/PI Vybrant Apoptosis Assay Kit (Molecular Probes, USA) following the manufacturer's instructions. Briefly, NCI-H460 (70,000 cells/well) and OVCAR-8 (80,000 cells/well) cells were seeded into 6-well plates and then treated with compound 10 (0.64 μM for NCI-H460 or 1.65 μM for OVCAR-8) or with Mn8 or its ligand (9 μM for NCI-H460 and 24 μM for OVCAR-8) for 72 h in a serum-starved medium. After treatment, attached and floating cells were harvested by centrifugation, washed in cold PBS, and subjected to Annexin V-Alexa Fluor 488 and PI staining in binding buffer at room temperature for 15 min in the dark.

Stained cells were analyzed on NovoCyte flow cytometer using NovoExpress software. A minimum of 10,000 cells within the gated region were analyzed.

3.13 DNA interaction analysis

Interaction of metal based compounds with DNA was monitored by agarose gel electrophoresis. Stock solutions of Mn8 and its ligand or compound 10 were freshly prepared in 4% DMSO. To investigate whether the presence of ROS could mediate the interaction of the compound with DNA, 1 μL of 30% H_2O_2 (w/v) was added to the reaction. Samples were prepared by mixing 0.5 μL of 0.5 μg/μL supercoiled pUC18 DNA (Thermo Scientific) with appropriate aliquots of Mn8, its ligand or compound 10 (25, 50 75 or 100 μM) in a final volume of 20 μL. A sample of untreated pUC18 DNA was used as negative control. The samples were then incubated at 37 °C for 24 h and then 4 μL of 6× loading buffer (10 mM Tris-HCl, pH 7.6, 0.03% bromophenol blue, 0.03% xylene cyanol FF, 60% glycerol, 60 mM EDTA) were added to each sample. The mixed solutions were loaded on a 0.8% agarose gel in 0.5× TBE buffer (89 mM Tris-borate, pH 8.3, 2 mM EDTA) and electrophoresis was carried out for 70 min at 100 V. Gels were stained with ethidium bromide (1 μg/mL in TBE) for 15 min and the DNA bands were visualized under UV light. For comparison purposes, the *Cis*-platin (0.1 μg/μL) effect was evaluated under the same experimental conditions.

3.14 Statistical analysis

Statistical analysis was carried out using IBM SPSS 24 software for Windows (USA). t-Test and one-way ANOVA test were performed, taking a significance level of 0.05.

RESULTS

4. RESULTS

4.1 ND-RNase NLSPE5

Previous works from the research group have shown that ND-RNases display pleiotropic effects on different cancer cell lines. Here we have investigated about how some of these pleiotropic effects are produced and how NLSPE5 affects cancer cell migration and invasion.

4.1.1 NLSPE5 affects the epigenetic marks of MDA-MB-231 cell line

Our research group has previously described that ND-RNases affect the expression of different genes involved in the maintenance of the malignant phenotype such as overexpression of tumor suppressor genes, down-regulation of oncogenes and enzymes involved in the regulation of metabolic pathways such as glycolysis or nucleotide synthesis, etc. [101]. ND-RNases are affecting gene expression at different levels since we have previously observed that it affects the rRNA level [99] or the miRNA pool [162].

We wondered whether the described changes of gene expression could be also due to an effect over the epigenetic regulation of gene expression. We firstly investigated whether NLSPE5 was cytotoxic against the breast cancer cell line MDA-MB-231 cultured in 3D by measuring the effect of increasing concentrations of this ND-RNase on its growth after an incubation period of 72 h (**Figure 4**). On this cell line NLSPE5 is highly cytotoxic being the IC_{50} of 1.32 ± 0.16 μM.

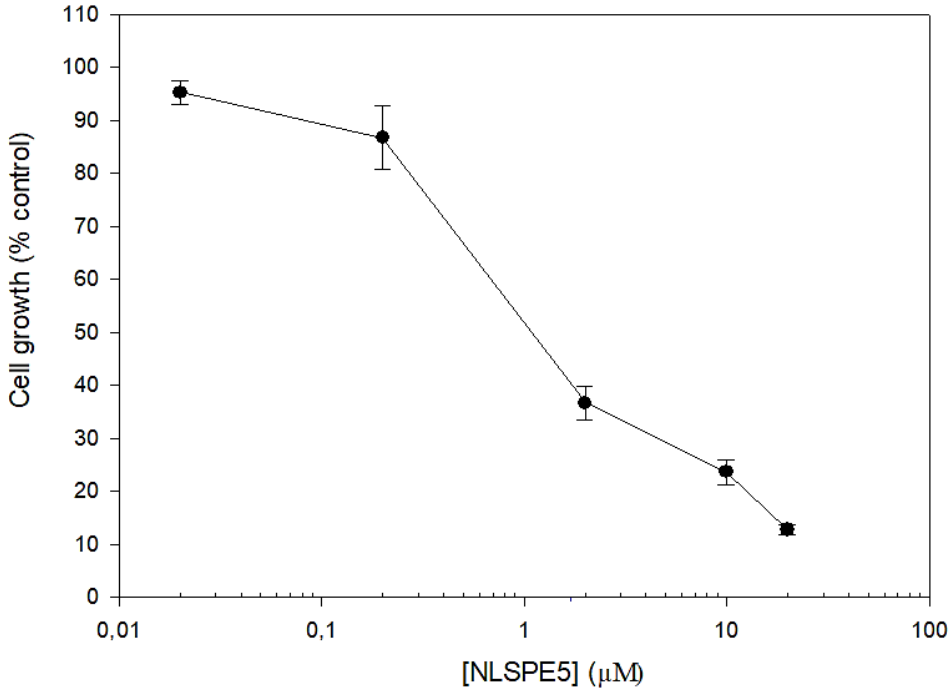

Figure 4. Effect of NLSPE5 on the growth of the MDA-MB-231 cell line cultured in 3D after an incubation period of 72 h using CellTiter-Glo method. Cell growth was calculated from fluorescence values as a percentage of growth respective to control cells. The curve shown in the figure comes from a single representative experiment. At least three independent experiments yielded comparable results.

Subsequently, the effect of ND-RNase NLSPE5 on the expression level of two epigenetic marks such as H3K27me3 and AcH4 was investigated by Western Blot. Cell extracts of the MDA-MB-231 cell line cultured in 3D with GFR Matrigel™ and treated with 0.5 µM NLSPE5 (a concentration equivalent to the IC_{30} in 3D cultures) for 72 h were subjected to immunoblotting with antibodies against AcH4 (histone H4 acetylation) and H3K27me3 (trimethylation of lysine 27 of histone H3).

Trimethylation of lysine 27 in histone H3 is known to be associated with gene silencing [163] whereas in general, the acetylation of each of the four lysines of histone H4 is associated to gene activation [164–166]. As shown in the **Figure 5**, the level of histone H4 acetylation was unchanged, whereas the methylation of K27 in histone H3 was significantly increased by almost 50% when compared to the control.

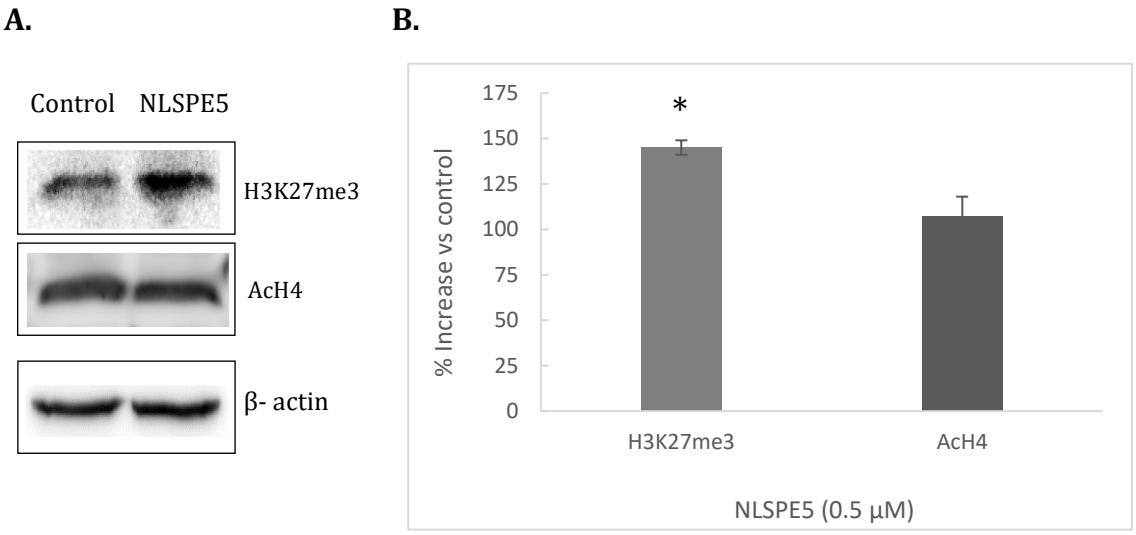

Figure 5. Effect of the treatment of MDA-MB-231 cells with NLSPE5 on the expression of H3K27me3 and AcH4. Cellular protein was collected and analyzed by western blot using the antibodies described in the methodology section. **A.** Representative image of each protein analyzed. **B.** Densitometric analysis of protein expression normalized with β-actin from three independent experiments. Values of untreated cells are considered as 100%. Differences versus untreated control cells were considered significant at * $p < 0.05$.

4.1.2 NLSPE5 affects the migration and invasion capacity of the MDA-MB-231 cell line

One of the characteristics of cancer cells is their ability to migrate from the primary tumor to other parts of the body and invade other tissues. Since ND-RNases affect multiple pathways of cancer cells, we wondered whether they could inhibit these two processes. To investigate this, we chose the MDA-MB-231 cell line that presents a triple negative phenotype (TNBC), one of the most aggressive phenotypes of breast cancer and with the most unfavorable prognosis [167,168]. First, we determined the level of cytotoxicity of NLSPE5 in 2D cultures by measuring the effect of increasing concentrations of NLSPE5 on their growth after a 72 h incubation period (**Figure 6**). Under these conditions, NLSPE5 is highly cytotoxic with an IC_{50} of 0.39 ± 0.07 µM.

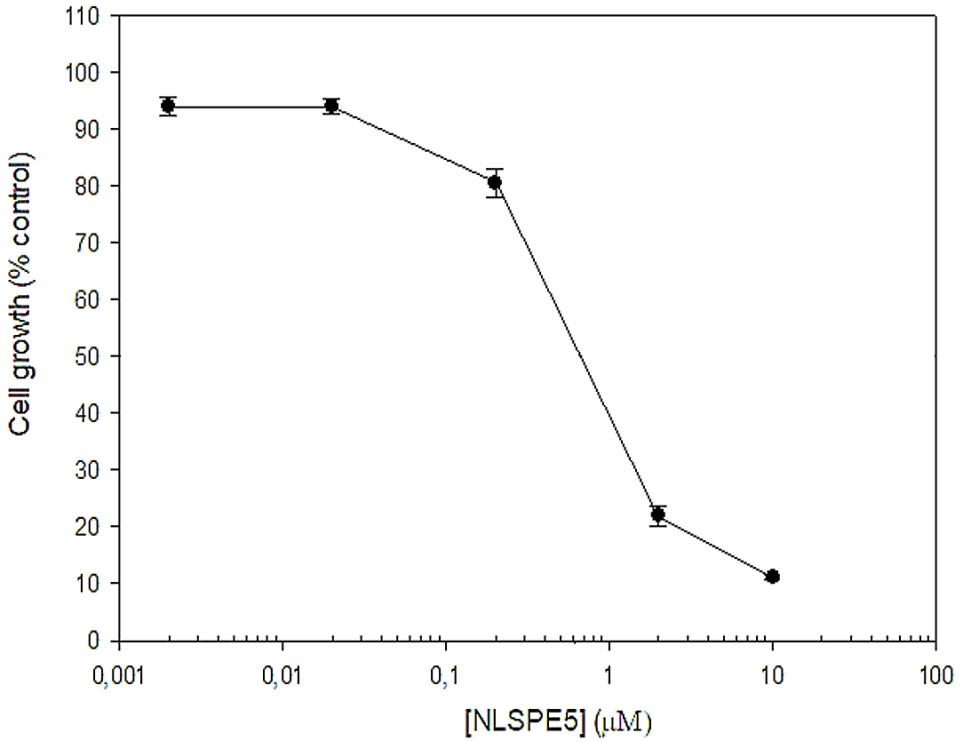

Figure 6. Effect of NLSPE5 on the growth of the MDA-MB-231 cell line cultured in 2D after an incubation period of 72 h using the MTT assay. Cell growth was calculated from absorbance values as a percentage of growth respective to control cells. The curve shown in the figure comes from a single representative experiment. At least three independent experiments yielded comparable results.

To measure the effect that NLSPE5 has on the migration and invasion capacity of this cell line, transwell and wound closure assays were performed. Migration analysis in transwell chambers showed that after 72 h of incubation, NLSPE5 significantly decreased the migration of MDA-MB-231 cells (**Figure 7-A**) even at concentrations of 0.1 µM and 0.2 µM (**Figure 7-B**).

A.

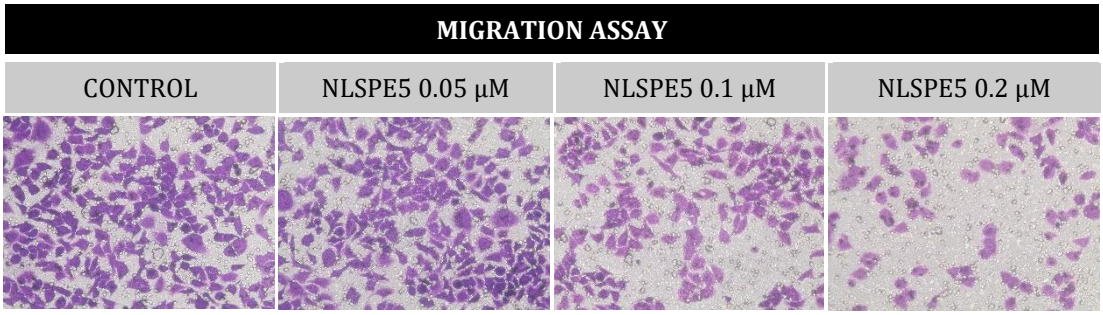

B.

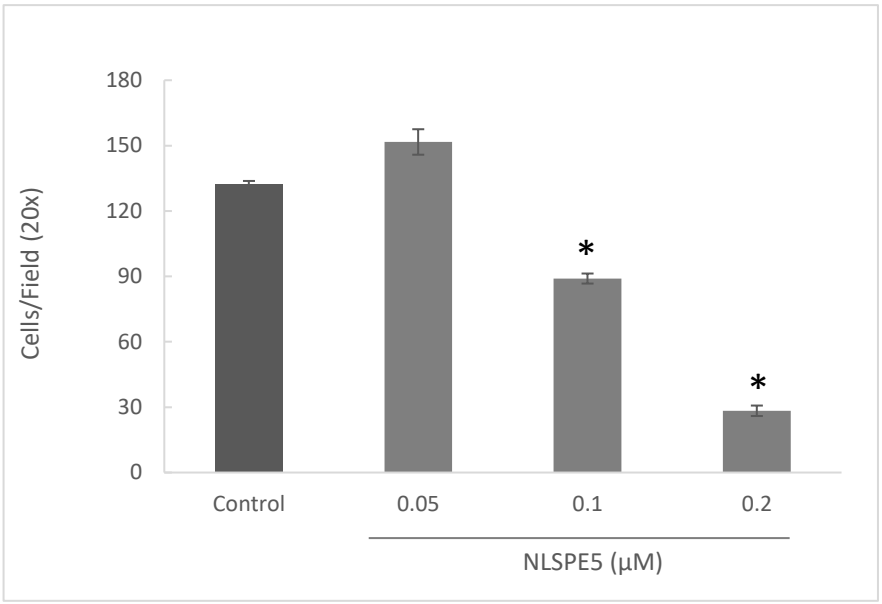

Figure 7. Effect of NLSPE5 on migration of MDA-MB-231 cells in a transwell chamber assay. **A.** Representative images of migrating cells untreated and treated with NLSPE5 for 72 h and **B.** quantitative analysis of cell density. Cells were stained with crystal violet. *P< 0.05. Data are shown as mean ± SE of at least three independent experiments.

This effect was confirmed with the wound closure assay (**Figure 8-A**). Again, treatment with NLSPE5 significantly delayed healing at all time points tested (16, 24, 40, and 48 h) in a dose dependent manner (**Figure 8-B**).

A.

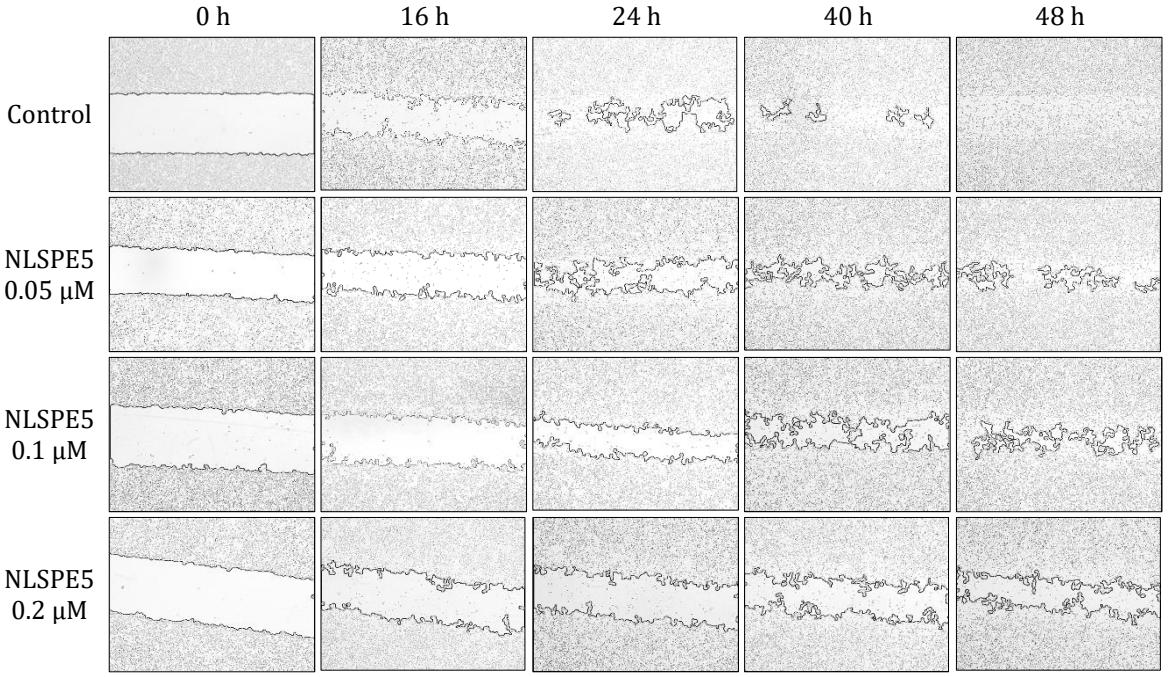

B.

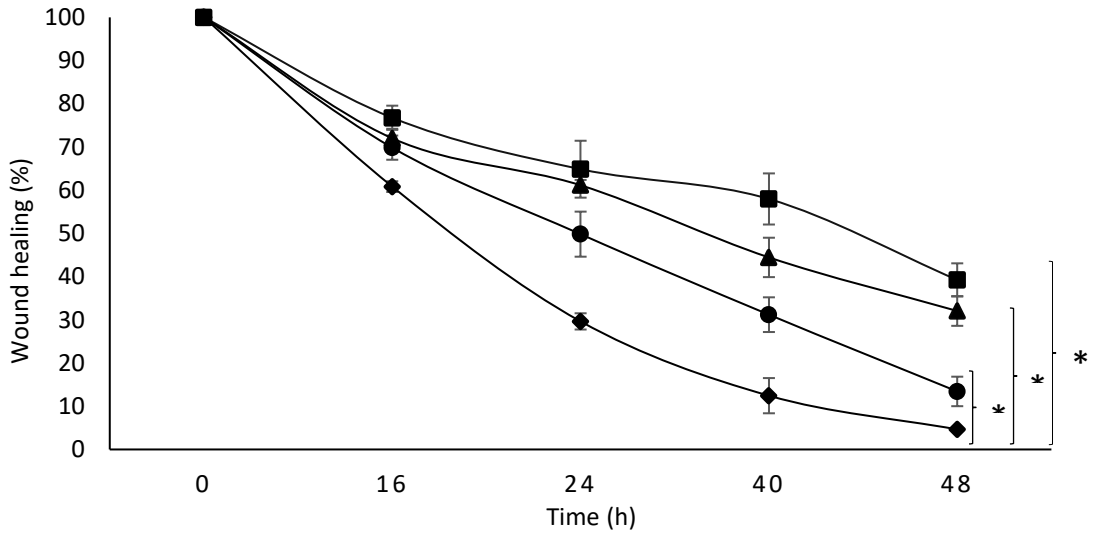

Figure 8. Effect of NLSPE5 on cell migration in the wound closure assay. **A.** Representative images from wound healing assay of MDA-MB-231 cells untreated or treated with NLSPE5 at different incubation times. **B.** Percentage of wound area respective to 0 h at indicated time points of MDA-MB-231 cell cultures untreated (♦) and treated with NLSPE5 at 0.05 µM (●), 0.1 µM (▲) and 0.2 µM (■). Data are shown as mean ± SE of three independent experiments. Differences versus untreated control cells were considered significant at * $p < 0.05$.

Transwell assays with GFR Matrigel™ were used to examine the impact of NLSPE5 on the invasiveness capacity of the MDA-MB-231 cell line. After 72 h of incubation, less NLSPE5 treated cells were present on the other side of the well when compared to control (**Figure 9-A**) demonstrating that a concentration of the ND-RNase as low as 0.1 µM significantly reduced the invasion potential of the cell line (**Figure 9-B**).

A.

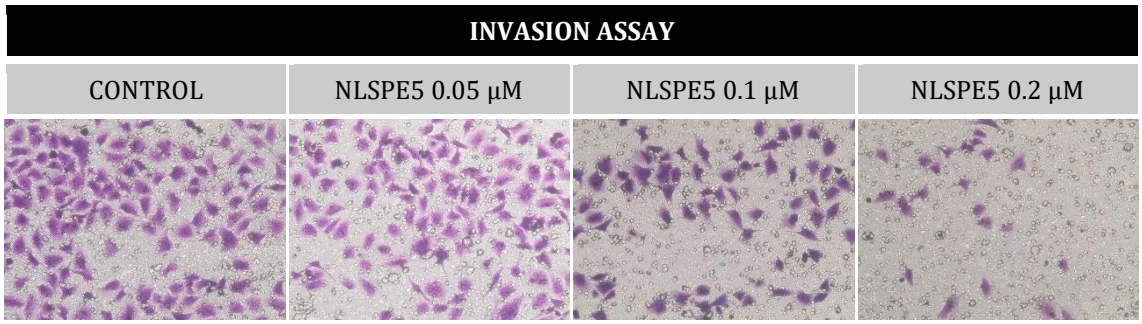

B.

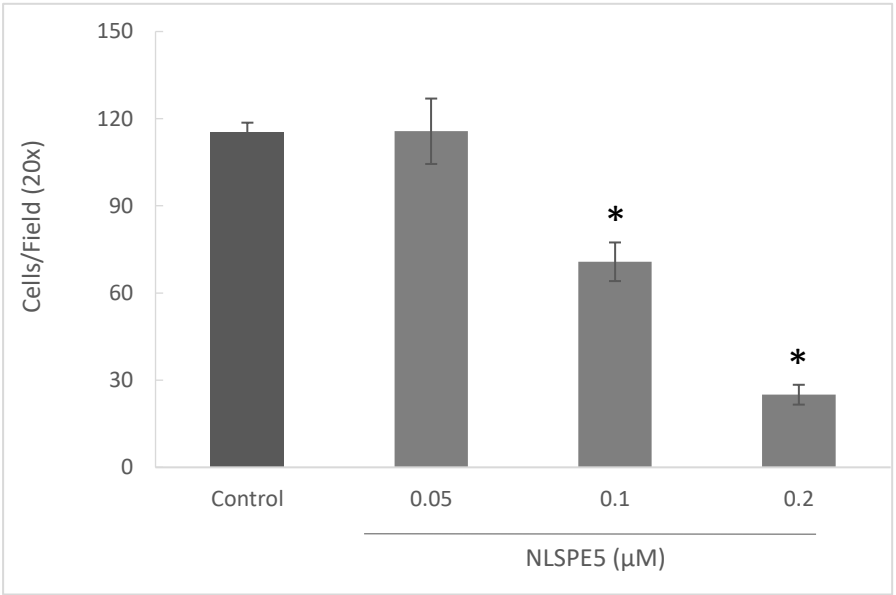

Figure 9. Effect of NLSPE5 on invasiveness of MDA-MB-231 cells using transwell chambers. **A.** Representative images of migration assays of cells untreated or treated with NLSPE5 for 72 h and **B.** Quantitative analysis of cell density. Cells were stained with crystal violet. Differences versus untreated control cells were considered significant at *P< 0.05. Data are shown as mean ± SE of at least three independent experiments

4.1.3 NLSPE5 reduces the expression of N-cadherin

Additionally, the effect of NLSPE5 on the expression level of proteins related to migration and invasiveness were investigated by Western Blot. Cell extracts of MDA-MB-231 cells cultured in 3D with GFR Matrigel™ and treated with 0.5 μM NLSPE5 for 72 h were subjected to immunoblotting with antibodies against E-Cadherin, N-Cadherin, MMP2 and MMP9 (**Figure 10**). As it can be seen, upon treatment with NLSPE5 a significant decrease of 44% of the N-cadherin is observed with respect to untreated cells. The rest of the proteins do not show significant variations of their expression levels when compared with protein extracts of control cells.

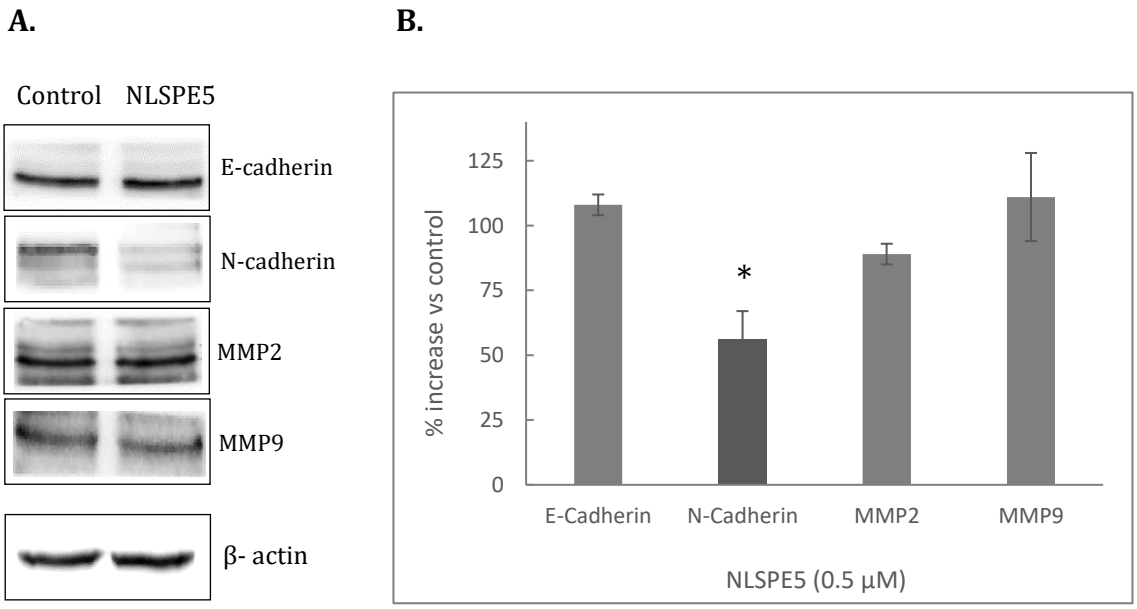

Figure 10. Effect of the treatment of MDA-MB-231 cells with NLSPE5 on the expression of E-Cadherin, N-Cadherin, MMP2 and MMP9. Protein extracts from MDA-MB-231 cells treated and untreated with NLSPE5 were analyzed by Western Blot using the antibodies indicated in the figure. **A.** Representative Western Blots of each analyzed protein. **B.** Densitometric analysis of protein expression normalized to that of β-actin from three independent experiments. Values of untreated cells are considered as 100%. Differences versus untreated control cells were considered significant at * $p < 0.05$.

4.2 Manganese Compounds

4.2.1 Mn compounds are cytotoxic and selective for tumor cells

Transition-metal complexes with ligands containing nitrogen as donor atoms constitute an important class of coordination compounds that are able to perform a wide range of transformations [169–171]. The exponential development of bioinorganic chemistry along the last three decades has manifested the unique properties they present for the design of new pharmaceutical compounds being *Cis*-platin and carboplatin two metal-based compounds that are widely used in cancer therapy. Mn and Fe complexes have potentially fewer side effects compared to *Cis*-platin. For these reasons we have investigated the cytotoxic properties of a panel of Mn complexes.

Cytotoxicity assays of Mn compounds (Mn1-Mn8) were performed on two tumor cell lines, NCI-H460 and OVCAR-8. Each ligand was also tested (**Table 3**). The effect of increasing concentrations of these compounds on cell viability was measured after an incubation period of 72 h. In addition to the manganese compounds, platinum derivatives such as *Cis*-platin and carboplatin were used for comparison.

Most of the compounds present a slight cytotoxic activity in a dose dependent manner. However, as shown in **Table 3**, the compound Mn8 and, to a lower extent its ligand, present a much higher cytotoxicity comparable in the case of Mn8 to that observed for *Cis*-platin in both cell lines. Compared to carboplatin, the cytotoxicity observed for Mn8 is about eight times higher for the NCI-H460 cell line and 24 times higher for the OVCAR-8 cell line.

Table 3. IC_{50} values (μM) of the different manganese compounds and its ligands tested in the indicated cell lines. Data presented are mean ± SE of triplicate values from at least three independent experiments.

	IC_{50} (μM)	
Mn compound	**NCI-H460**	**OVCAR-8**
Mn1 $[MnCl_2(pypz\text{-}Me)_2]$	160.8 ± 20.2	> 600
Mn2 $[Mn(CF_3SO_3)_2(pypz\text{-}Me)_2]$	94.3 ± 10.9	318.3 ± 53.0
Mn3 $[Mn(CF_3SO_3)_2(pypz\text{-}CH_2COOEt)_2]$	51.3 ± 7.2	212.5 ± 37.5
Mn4 $[MnCl_2(pypz\text{-}H)_2]$	124.7 ± 2.6	373.1 ± 62.7
Mn5 $[Mn(CF_3SO_3)2(pypz\text{-}H)_2]$	189.2 ± 29.2	492.4 ± 93.4
Mn6 $[Mn(NO_3)_2(pypz\text{-}H)_2]$	157.2 ± 32.1	> 600
Mn7 $[MnCl_2(H_2O)_2(pypz\text{-}H)]$	132.2 ± 23.5	413.1 ± 45.8
Mn8 $[Mn(CF_3SO_3)_2((-)\text{-}L)_2]$	1.7 ± 0.4	4.7 ± 0.4
Cis-platin	1.0 ± 0.1	6.9 ± 1.2
Carboplatin	12.8 ± 2.2	110.0 ± 4.2
Manganese ligand		
pypz-H (for Mn4, Mn5, Mn6 and Mn7)	> 600	> 600
pypz-Me (for Mn1 and Mn2)	> 600	> 600
pypz-CH_2COOEt (for Mn3)	160.5 ± 21.3	> 600
(−)-L (for Mn8)	3.3 ± 0.1	15.9 ± 3.8

In all cases Mn compounds have much more cytotoxicity than free ligands, confirming that the antitumor activities of the pyrazole and bipyridine ligands can be enhanced by coordinating the corresponding ligand to Mn. It can be also observed that the NCI-H460 cell line is much more sensitive to Mn compounds than the OVCAR-8 cell line.

Considering the interesting results of Mn8, we decided to further characterize this compound and its ligand (L-Mn8). We firstly investigated whether the cytotoxic properties of Mn8 were specific for tumor cell lines. For this, we analyzed the sensitivity of Mn8 as well as that of its ligand to the non-tumor cells CCD-18Co.

As it can be seen (**Table 4**), the IC_{50} of both Mn8 and its ligand for CCD-18Co were higher than the highest concentration available of the compounds (30 μM). This indicates that Mn8 as well as its ligand are clearly selective for cancer cells.

Table 4. IC_{50} value (μM) of Mn8 and its ligand on the non-tumor cells CCD-18Co. Data presented are mean ± SE of triplicate values from at least three independent experiments.

	IC_{50} (μM)
Mn compound	**CCD-18Co**
Mn8 $[Mn(CF_3SO_3)_2((-)\text{-}L)_2]$	>30
L-Mn8 [(−)-L]	>30

4.2.2 Mn8 and its ligand triggers ROS generation

Mn constitutes a co-factor for several enzymes such as superoxide dismutase (Mn-SOD), catalase, ribonucleotide reductase, and peroxidase [172]. We decided to investigate whether ROS plays a key role in the cytotoxicity activity of Mn8. For this, we firstly studied whether this compound increased the ROS levels in OVCAR-8 and NCI-H460 cells. Both cell lines were treated at different concentrations of Mn8 and its ligand for 48 or 72 h and the amount of ROS produced was measured with the carboxy-H_2DCFDA probe through flow cytometry (**Figure 11**).

A.

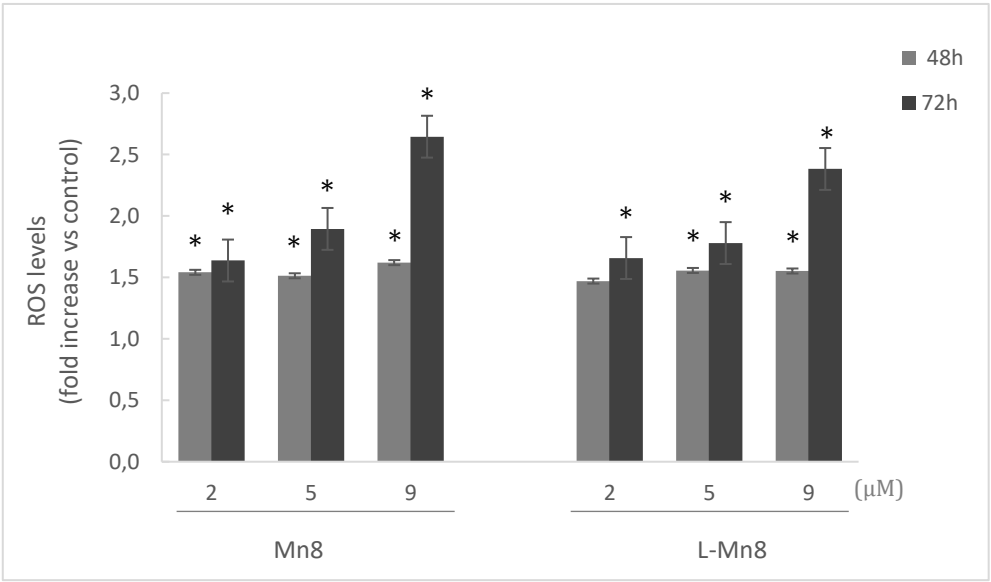

B.

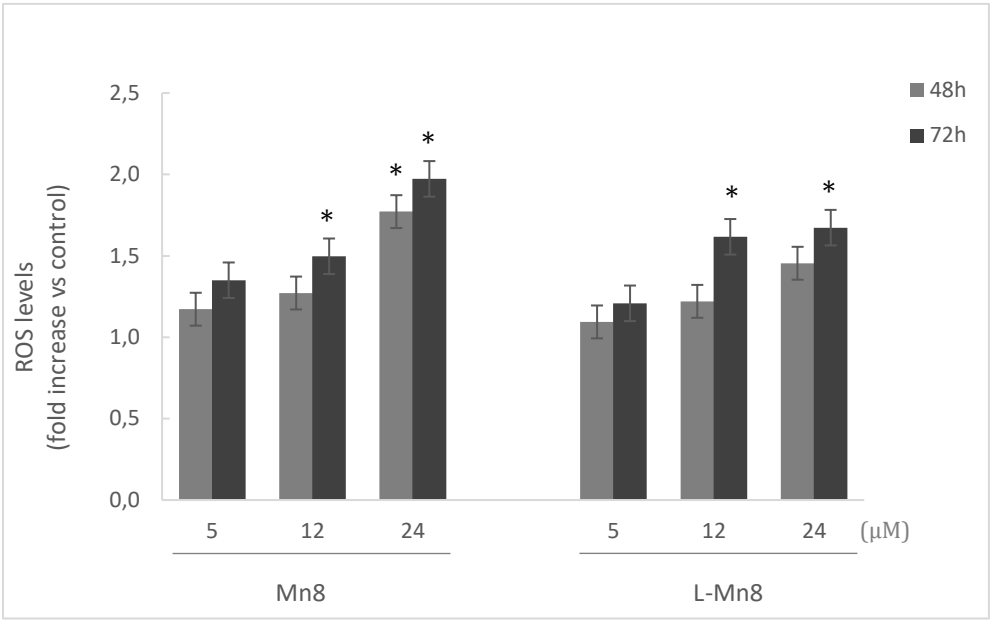

Figure 11. ROS production triggered by Mn8 and its ligand (L-Mn8) in NCI-H460 (**A)** and OVCAR-8 **(B)** cell lines. Cells were treated for 48 and 72 h with Mn8 or its ligand and ROS generation was measured by flow cytometry after labeling the cells with carboxy-H_2DCFDA. ROS levels are indicated as fold increase vs. control (untreated cells). Values were analyzed from 10,000 total events. Data are presented as the mean ± SE of at least three independent experiments. Differences from untreated control cells were considered significant at *$p < 0.05$.

As shown in **Figure 11**, Mn8 increases ROS levels in both cell lines in a dose- and time-dependent manner. Surprisingly, L-Mn8 also increases ROS levels although to a lower extent. The levels of ROS produced in the NCI-H460 cells were higher than those observed in the OVCAR-8 cell line.

Next, we investigated whether increased ROS production could explain the cytotoxic effect observed for Mn8 and its ligand. Using the MTT assay we measured the viability of the NCI-H460 cell line treated with different concentrations of Mn8 or its ligand, in the presence and absence of the reducing agent NAC. This reducing agent counteracts the production of ROS in the cells. **Figure 12** shows that the presence of NAC reduces the cytotoxic effect of Mn8 and its ligand at all concentrations tested.

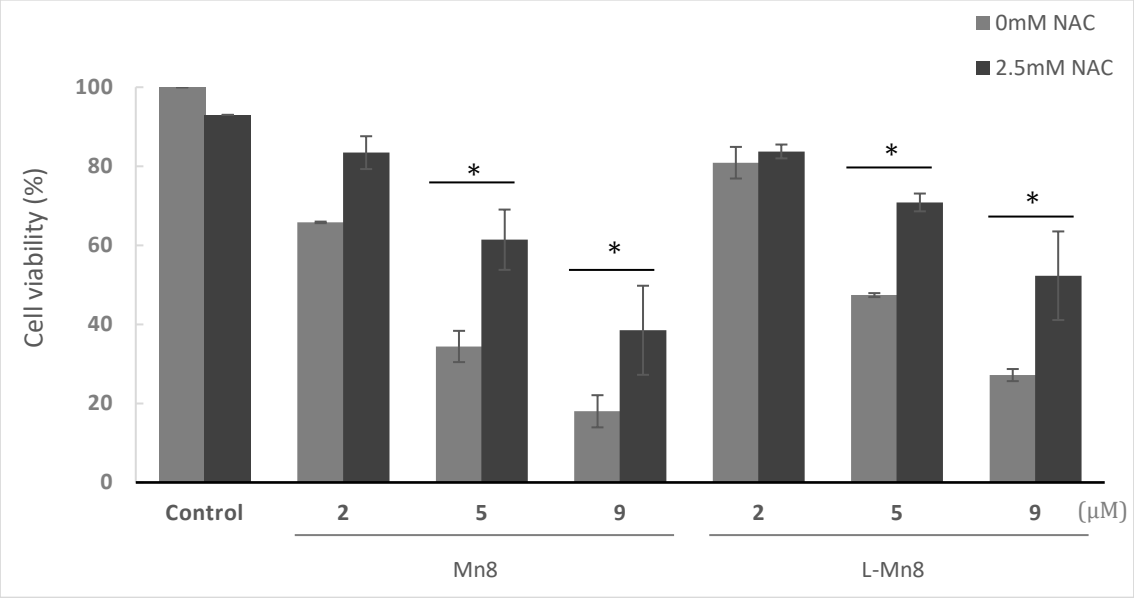

Figure 12. Cellular viability of NCI-H460 cells after treatment with Mn8 or its ligand in the presence and absence of NAC. Cellular viability was measured by the MTT assay. Data are presented as mean ± SE of at least three independent experiments. Differences in the cell viability values of cells with and without NAC treatment were considered significant at *p < 0.05.

4.2.3 Mn8 interacts with DNA in the presence of ROS

Since the effect of Mn8 over NCI-H460 cells is not completely suppressed when the cells are incubated with NAC, this indicates that Mn8 could affect tumor cells through other mechanisms, we checked the ability of Mn8 and its ligand to interact with DNA. For this, four different concentrations of the compound and its ligand were incubated with plasmid DNA (pUC18) at 37 °C for 24 h and the effects were analyzed in an agarose gel electrophoresis. The results are shown in **Figure 13**. DNA interaction with the compound can be visualized as a decrease of the degree of compaction of the supercoiled form (CCC) of DNA band that shifts to a lower mobility position and an increase of the compaction of the relaxed form (OC) DNA that increases its mobility. Both bands tend to converge in a coalescence point. The analysis can also reveal whether the compound breaks the DNA since in this case an increase of the OC band is observed (single strand breaks) or part of the pUC18 DNA can appear as the linear form (double strand break) or as DNA fragments (multiple double strand breaks) [173]. As it can be seen in **Figure 13-A**, neither Mn8 nor its ligand can interact with DNA at any of the concentrations

tested since the bands that are observed are identical to the negative control. On the other hand, on the positive control, which corresponds to DNA incubated with *Cis*-platin, both DNA bands are near to reach the coalescence point. We wondered about the possibility that DNA interaction required the presence of ROS so we repeated the agarose gel assays but this time adding H_2O_2 to each sample. As it is observed in **Figure 13-B**, in the presence of H_2O_2 even the lower concentration used of Mn8 alters the ratio between the CCC and the OC forms. At the concentration of 75 μM an intermediate band can be observed that corresponds to the linear form of the tested plasmid and at the highest concentration of Mn8, corresponding to 100 μM, we observe how the DNA has been completely degraded. This indicates that Mn8 cleaves the DNA in the presence of H_2O_2. Regarding the ligand, no changes were observed in the DNA at any of the concentrations tested in the presence of H_2O_2 (**Figure 13-C**).

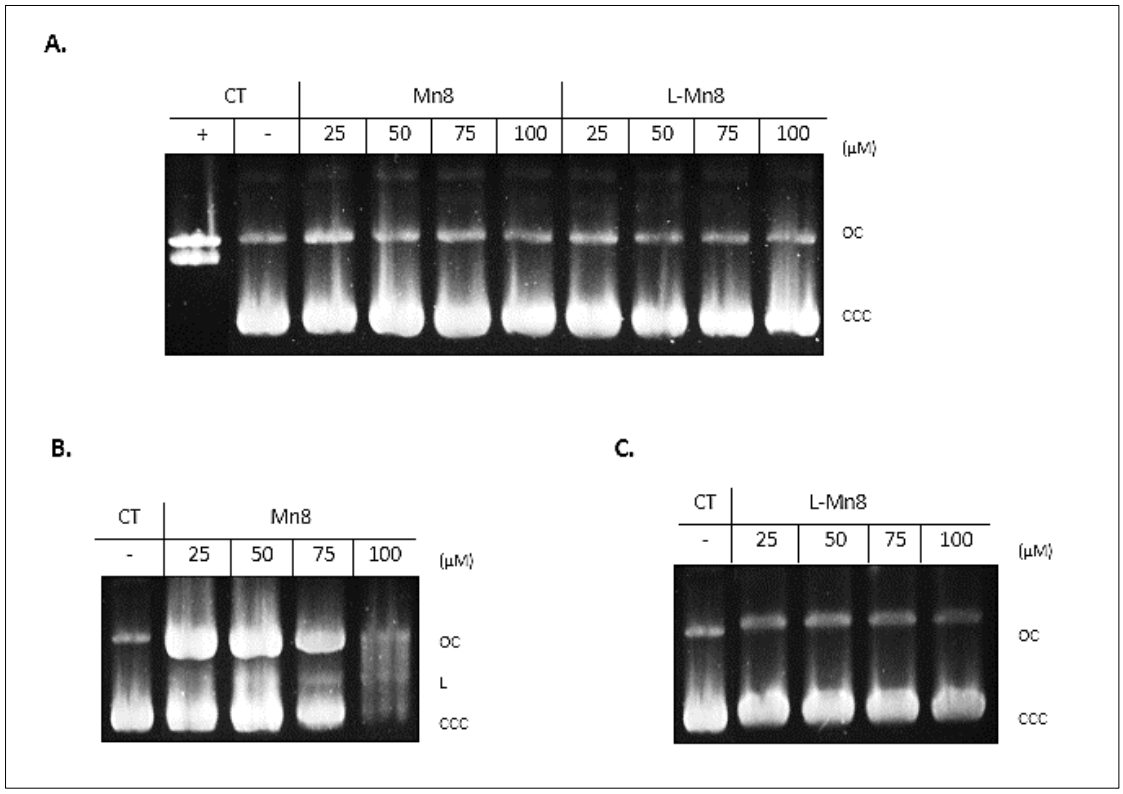

Figure 13. Agarose gel electrophoresis of pUC18 plasmid DNA treated with different concentrations of Mn8 and its ligand (L-Mn8) in the absence (**A**) and presence (**B**) of H_2O_2. No changes in DNA mobility were observed at any of the L-Mn8 concentrations tested in the presence of H_2O_2 (**C**). *Cis*-platin (0.1 μg/μL) was included as positive control. OC=open circular form; CCC=covalently closed circular form; L=linear form.

4.2.4 Effects of Mn8 and its ligand on the cell cycle phase distribution

We investigated by flow cytometry the effect of two concentrations of Mn8 and its ligand on the cell cycle progression of NCI-H460 and OVCAR-8 cell lines (**Figure 14**). The cells were incubated for 72 h with Mn8 or its ligand and after this time the proportion of each cell cycle phase was compared with that of the control. No changes were observed in the phases of the cell cycle except for a slight increase in the G_0/G_1 phase in both cell lines, accompanied with a decrease of the S and G_2/M cell cycle phases.

A.

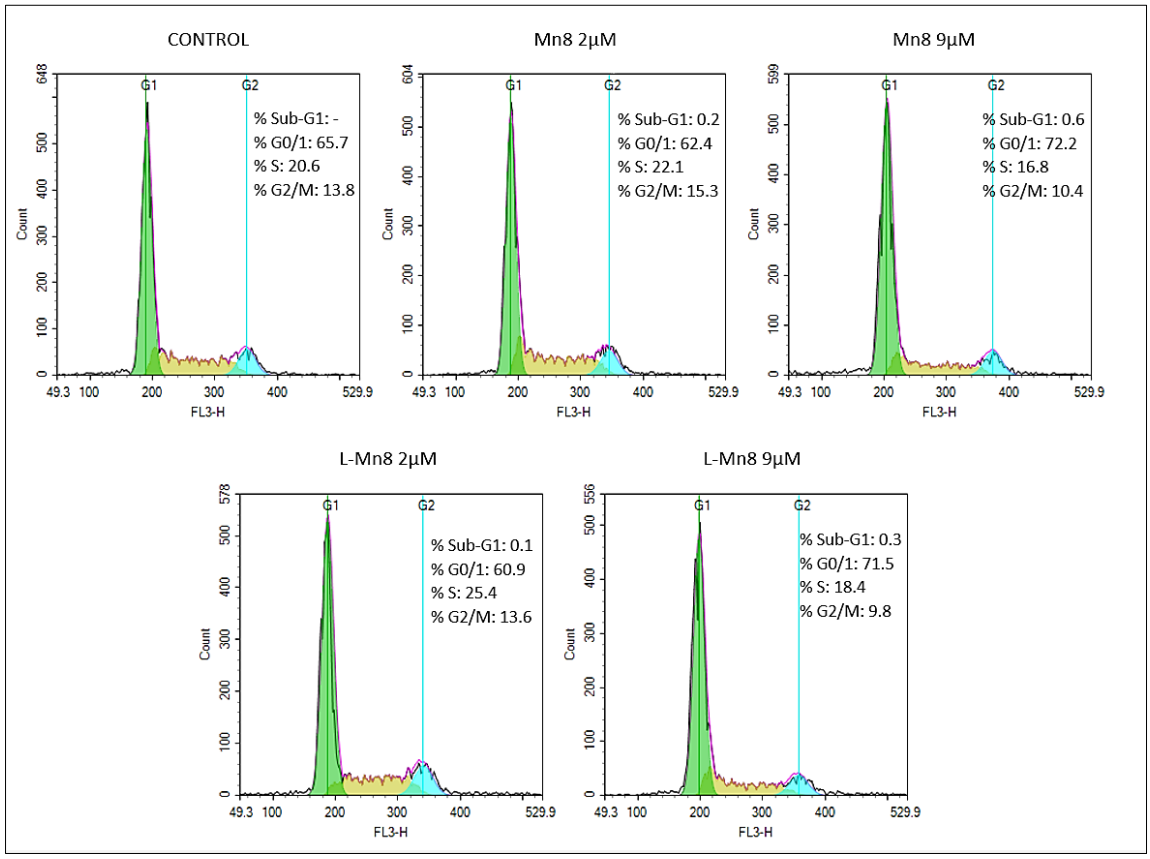

B.

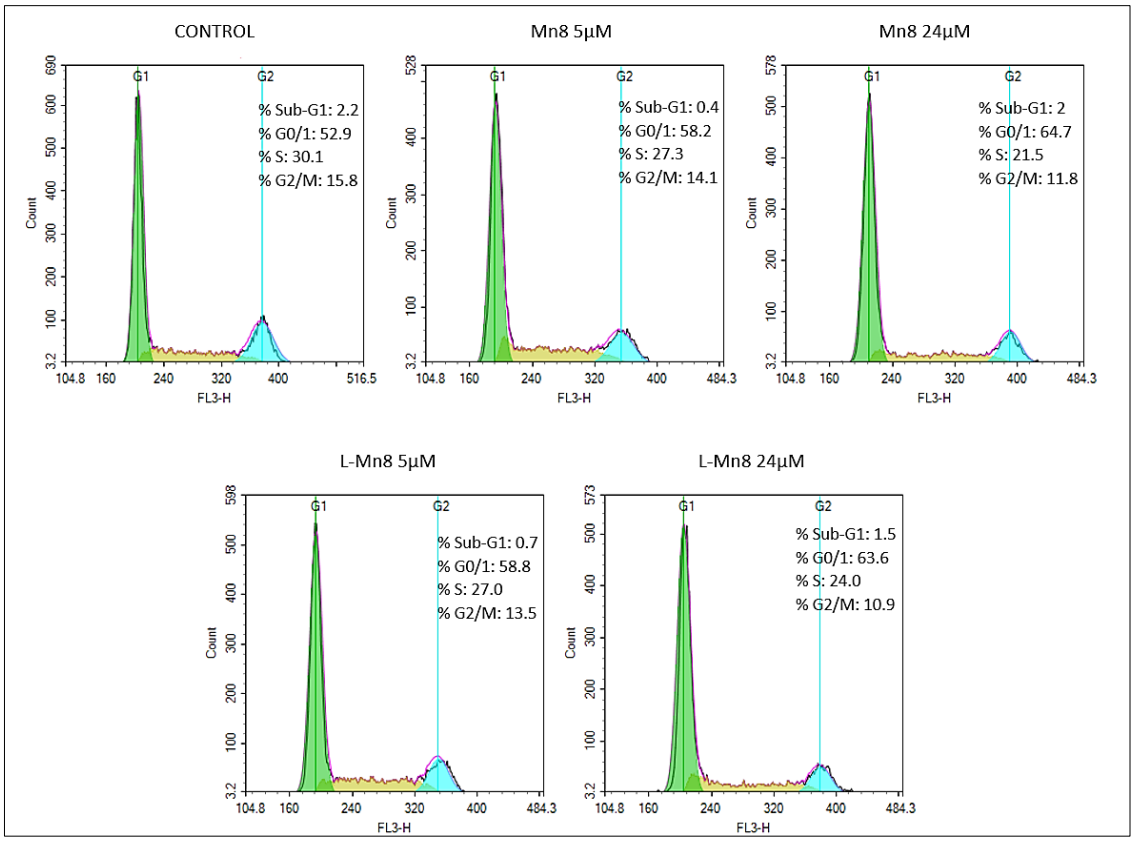

Figure 14. Representative histograms of the effects of Mn8 and its ligand on cell cycle phase distribution of NCI-H460 **(A)** and OVCAR-8 **(B)** Cells compared to control untreated cells after treatment for 72 h. Cells were permeabilized and stained with PI and cell DNA content was analyzed by flow cytometry. Inset data are the mean of three independent assays and are expressed as percentages (%) of the total cell cycle. Values were analyzed from at least 10,000 total events.

4.2.5 Study of the apoptotic effect of Mn8 and its ligand

We studied the cell death induced by treatment with Mn8 and its ligand. To determine whether cells treated with this compound showed characteristic features of apoptosis, NCI-H460 and OVCAR-8 cell lines were treated with Mn8 or its ligand for 72 h, subsequently stained with annexin V-Alexa Fluor 498 and PI and analyzed by flow cytometry (**Table 5**). Cells undergoing early apoptosis are positive for annexin V and negative for PI (annexin V+/PI−), late apoptotic cells are annexin V+/PI+ and necrotic cells are annexin V−/PI+.

Table 5. Analysis of the apoptosis of NCI-H460 and OVCAR-8 cells treated with Mn8 and L-Mn8 measured by Annexin V-Alexa Fluor 488/PI staining.

	NCI-H460			**OVCAR-8**		
	Control	**Mn8**	**L-Mn8**	Control	**Mn8**	**L-Mn8**
Early apoptotic cells (%)	5.35±4.05	3.34±2.32	3.71±2.36	3.00±0.92	3.95±0.77	6.91±0.54
Late apoptotic cells (%)	14.10±2.20	25.15±3.65	18.65±1.85	19.15±0.35	16.60±6.60	17.50±0.40
Necrotic cells (%)	0.59±0.13	1.88±0.26	1.77±0.05	1.11±0.25	0.78±0.15	1.01±0.31
Viable cells (%)	80.00±1.70	69.65±6.25	75.85±0.55	76.70±1.50	78.65±7.55	74.55±1.25

All data were expressed as mean ±SE of three different experiments. Values were analyzed from 10,000 total events.

As it can be seen in the **Table 5**, Mn8 does not induce apoptosis in the OVCAR-8 cell line, since the values obtained are very similar to those of the control. On the other hand, in the NCI-H460 cell line, which is more sensitive to Mn8, there is a slight increase in the percentage of cells in late apoptosis after 72 h of treatment. Taking into account that we used a concentration five times the IC_{50}, it is very likely that cells are dying through a mechanism different to apoptosis. On the other side, cells in necrotic state in both cell lines are less than 2%, therefore the mechanism of cell death is neither necrosis, which is beneficial for its potential use as antitumor agent.

4.3 Iron Compounds

Binuclear Fe compounds that present imino- and amino-pyridine ligands based on BFBF and DBDOC backbones have been studied in this thesis to check whether these structures and coordination displayed antitumor activity.

4.3.1 Fe compounds display selective cytotoxicity for different tumor cell lines

We analyzed the cytotoxicity of these compounds (unfortunately, the ligands were not available for evaluation) on two tumor cell lines, NCI-H460 and OVCAR-8, after 72 h of treatment (**Table 6**). Again, as with the Mn compounds, *Cis*-platin and carboplatin were used for comparison.

Table 6. IC_{50} values (μM) of the different Fe complexes assayed in the NCI-H460 and OVCAR-8 tumor cell lines

	IC_{50} (μM)	
Fe compounds	**NCI-H460**	**OVCAR-8**
Compound 7 $[Fe_2\mathbf{1}_2(CH_3CN)_4](BF_4)_4$	0.43 ±0.03	1.39 ±0.14
Compound 8 $[Fe_2\mathbf{2}_2(CH_3CN)_4](BF_4)_4$	0.48 ±0.13	1.27 ±0.39
Compound 9 $[Fe_2\mathbf{3}_2(CH_3CN)_4](BF_4)_4$	0.60 ±0.04	1.78 ±0.16
Compound 10 $[Fe_2\mathbf{4}_2(CH_3CN)_4](BF_4)_4$	0.64 ±0.05	1.65 ±0.26
Compound 11 $[Fe_2\mathbf{5}_2(CH_3CN)_4](BF_4)_4$	0.50 ±0.10	1.40 ±0.30
Compound 12 $[Fe_2\mathbf{6}_2(CH_3CN)_4](BF_4)_4$	0.49 ±0.08	1.24 ±0.27
Cis-platin	1.10 ±0.14	6.91 ±1.21
Carboplatin	12.80 ±2.23	110.0 ±4.2

Data are presented as mean ± SE of at least three independent experiments conducted in triplicate.

As shown in **Table 6**, all the tested Fe complexes are cytotoxic for the two tumor cell lines assayed. As we have previously shown for Mn8, the NCI-H460 cell line presents lower IC_{50} values, thus denoting more sensitivity to the different metallic complexes. All the Fe compounds have a similar IC_{50}, which is lower than that of *Cis*-platin and carboplatin. As with the Mn8 compound, to check the

selectivity for tumor cells, we proceeded to measure their cytotoxicity on the non-tumor cells CCD-18Co (**Table 7**).

Table 7. IC_{50} values (μM) and the selectivity index of the different Fe complexes assayed in CCD-18Co non-tumor cells.

	IC_{50} (μM)	SI**	
Fe compounds	**CCD-18Co**	**NCI-H460**	**OVCAR-8**
Compound 7 $[Fe_2\mathbf{1}_2(CH_3CN)_4](BF_4)_4$	7.78 ±5.67	18.1	5.6
Compound 8 $[Fe_2\mathbf{2}_2(CH_3CN)_4](BF_4)_4$	7.00 ±3.43	14.6	5.5
Compound 9 $[Fe_2\mathbf{3}_2(CH_3CN)_4](BF_4)_4$	7.20 ±3.40	12.0	4.1
Compound 10 $[Fe_2\mathbf{4}_2(CH_3CN)_4](BF_4)_4$	21.55 ±3.18	33.7	13.1
Compound 11 $[Fe_2\mathbf{5}_2(CH_3CN)_4](BF_4)_4$	12.04 ±1.44	24.1	8.6
Compound 12 $[Fe_2\mathbf{6}_2(CH_3CN)_4](BF_4)_4$	4.05 ±0.62	8.1	3.2
Cis-platin	31.23 ±5.76	28.4	4.5
Carboplatin	240.0 ±25.2	18.8	2.1

The data presented are the mean IC_{50} ± SE of a minimum of three independent experiments. **SI, selectivity index, is the ratio between IC_{50} values for non-tumor cells and the corresponding tumor cell line.

As shown in **Table 7**, the cytotoxicity of the Fe compounds against non-tumor cells CCD-18Co is lower compared to *Cis*-platin and carboplatin although variability is observed among the compounds. Of all the tested compounds, compound 10 shows the highest cytotoxicity and selectivity, which are higher than those presented by *Cis*-platin and carboplatin for both tumor cell lines.

4.3.2 Compound 10 triggers ROS generation

We investigated by flow cytometry whether treatment with the compound 10 caused an increase of ROS levels in NCI-H460 and OVCAR-8 cells. For this purpose, cells were treated for 48 or 72 h with different concentrations of that compound and then labeled with carboxy-H_2DCFDA. **Figure 15** shows that compound 10 triggers a significant time and concentration-dependent increase of ROS levels in both cell lines. Although the OVCAR-8 cell line is more resistant to

compound 10, it induces the highest levels of ROS (two-fold induction compared to the NCI-H460 cell line), which indicates that the cytotoxic effect induced by the compound 10 is not solely mediated by the production of ROS inside the cells.

A.

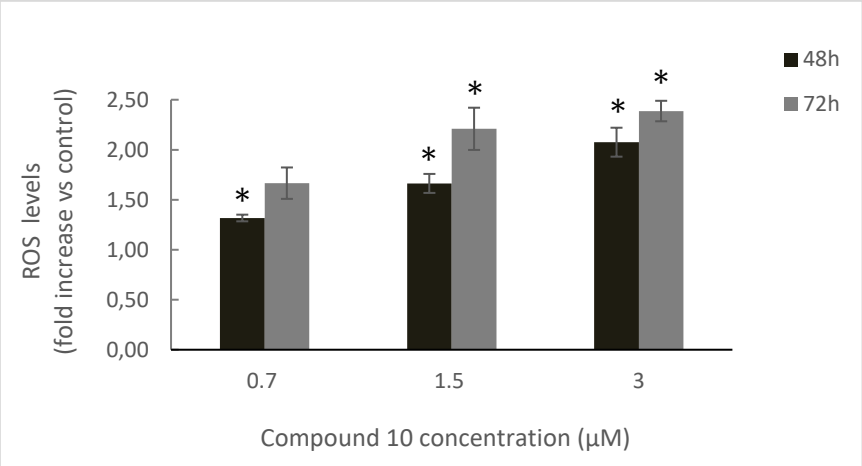

B.

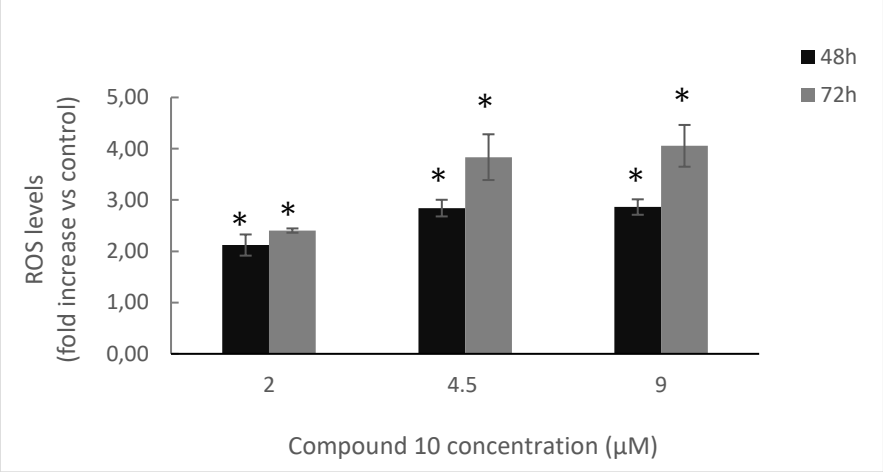

Figure 15. ROS production triggered by compound 10 in NCI-H460 **(A)** and OVCAR-8 **(B)** cell lines. Cells were treated for 48 and 72 h with different concentrations of compound 10 and analyzed by flow cytometry after labeling with carboxy-H_2DCFDA. ROS levels are indicated as fold increase vs. control (untreated cells). Values were analyzed from 10,000 total events. Data are presented as the mean ± SE of at least three independent experiments. Differences from untreated control cells were considered significant at *$p < 0.05$.

We therefore investigated whether the reducing agent NAC affected the cytotoxicity induced by compound 10. For this, we performed an MTT assay to

measure the viability of both cell lines after treating them with different concentrations of compound 10 in the presence and absence of NAC (**Figure 16**). The results in **Figure 16** show that NAC does not counteract the effect produced by compound 10. These results indicate that the cytotoxicity observed with compound 10 is not mainly linked to the production of ROS in the cells and other hypotheses had to be investigated.

A.

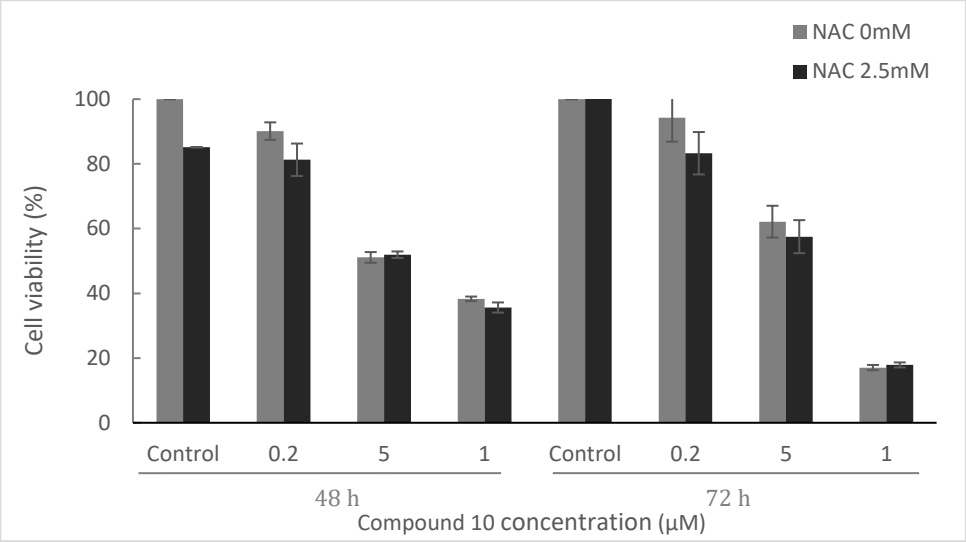

B.

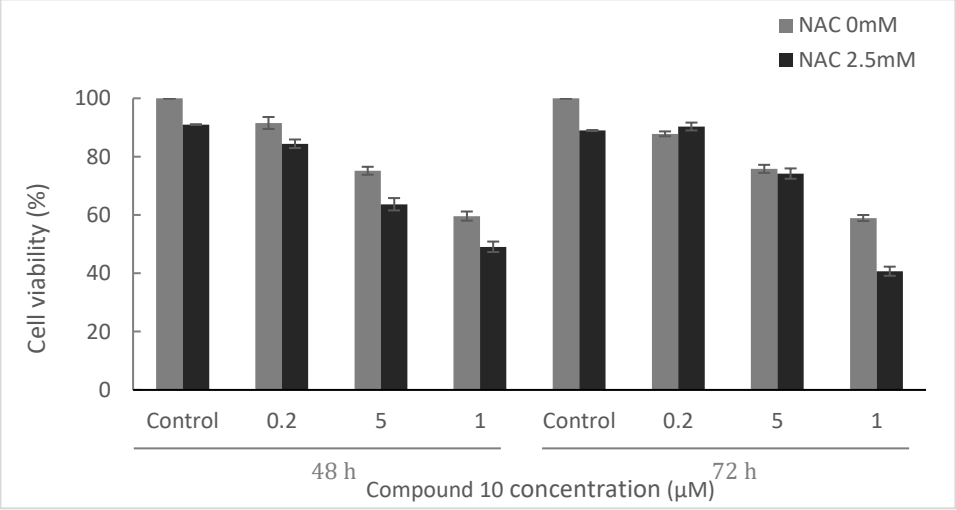

Figure 16. Cellular viability of NCI-H460 **(A)** and OVCAR-8 **(B)** cells after treatment with different concentrations of compound 10 in the presence and absence of NAC. Cellular viability was measured by the MTT assay. Data are presented as the mean ± SE of at least three independent experiments.

4.3.3 Tested dinuclear Fe compounds have the ability to interact with DNA

We tested the ability of all dinuclear Fe compounds to interact with plasmid DNA (pUC18). The interaction was detected in an agarose gel electrophoresis assay. **Figure 17-A** shows that in the agarose gel all the compounds tested produced two types of bands. The first bands correspond to the supercoiled form (CCC) of plasmid DNA and the second ones corresponds to the relaxed form (OC), as it is observed in the negative control (pUC18 alone). This indicates that any of the dinuclear Fe compounds has the ability to interact with DNA. In the case of *Cis*-platin, these two bands tend to reach the point of coalescence between the CCC form and the OC form. Since the interaction of Mn8 required the presence of ROS we checked whether this was also the case. Therefore, the assay was repeated but including H_2O_2 as a ROS initiator (**Figure 17-B**). In this situation all the compounds induce the appearance of an additional band corresponding to the linear form (L) of pUC18, which is formed when the compound breaks both strands of DNA. In addition, at the highest concentrations, compounds 8, 10 and 12 promote total DNA degradation observed by the disappearance of all the bands. Considering the level of cytotoxicity, the selectivity of the SI and the ability of the compounds to interact with DNA, we followed the characterization with only compound 10.

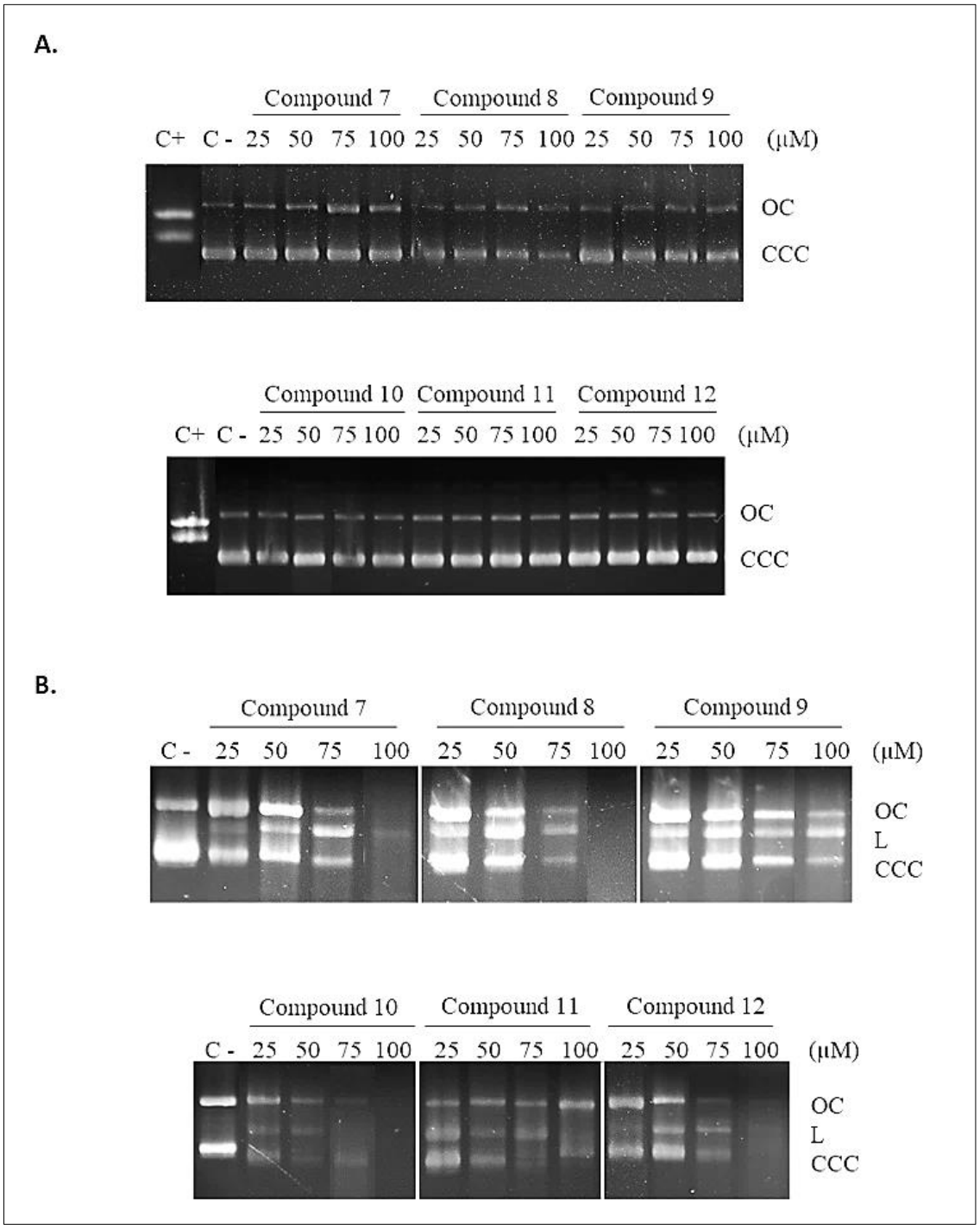

Figure 17. Agarose gel electrophoresis assay of the interaction of the different Fe compounds with DNA. Plasmid pUC18 was treated with different concentrations of the different compounds in the absence **(A)** and presence **(B)** of H_2O_2. Positive control (C+) corresponds to *Cis*-platin (1 μg/μL) and negative control (C-) corresponds to pUC18 alone. OC = open circular form; CCC = covalently closed circular form; L = linear form.

4.3.4 Effect of compound 10 on the cell cycle phase distribution

The effect of the compound 10 on cell cycle phase distribution was investigated by flow cytometry (**Figure 18**), on the NCI-H460 and OVCAR-8 cell lines. As it can be observed, the exposure to this compound of NCI-H460 cells does not change the distribution of the cell cycle phases compared to the untreated control cells. In contrast, in the OVCAR-8 cell line, compound 10 causes a shift in the cell population from the G_0/G_1 phase to the S and G_2/M phases compared to control, indicative of cell cycle arrest in these latter phases of cell cycle. These results seem to indicate that the compound 10 has a cytotoxic effect and in the case of the OVCAR-8 cell line it also produces an antiproliferative effect.

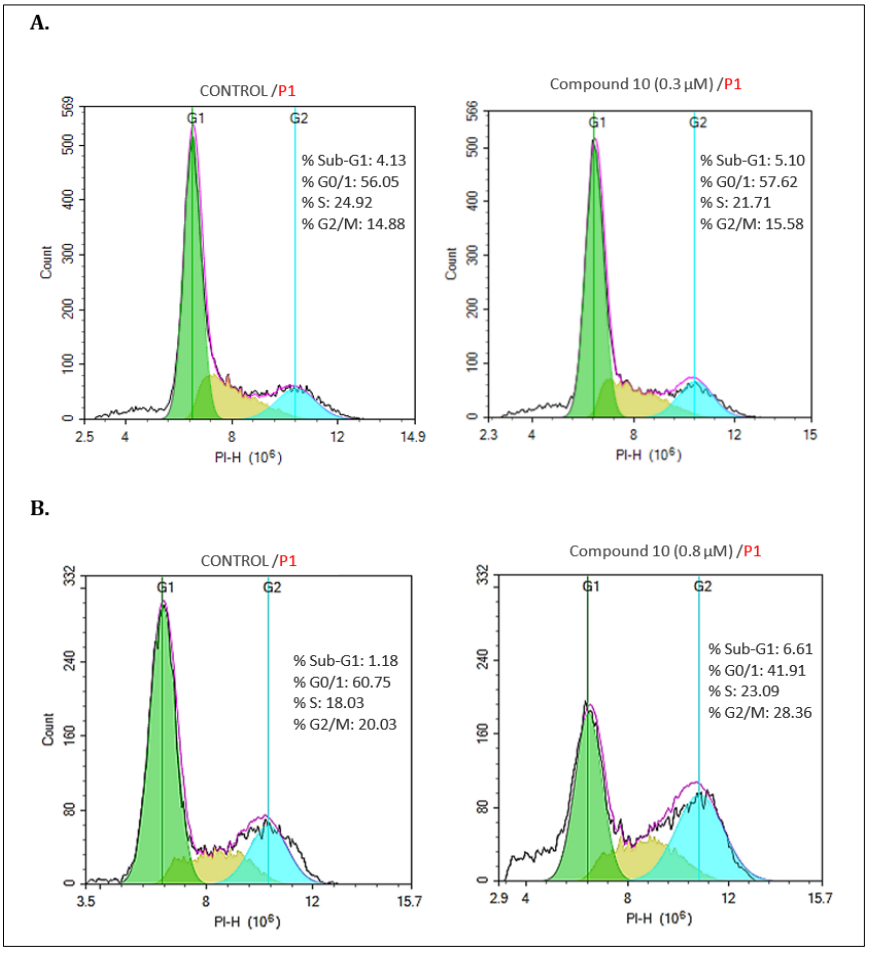

Figure 18. Representative histograms of the effects of compound 10 on cell cycle phase distribution of NCI-H460 **(A)** and OVCAR-8 **(B)** cells lines compared to control untreated cells after treatment for 72 h. Cells were permeabilized and stained with PI and cell DNA content was analyzed by flow cytometry. Inset data are the mean of three independent assays and are expressed as percentages (%) of the total cell cycle. Values were analyzed from at least 10,000 total events.

4.3.5 Study of the apoptotic effect of Compound 10

We investigated whether the compound 10 induces apoptosis in the tumor cell lines NCI-H460 and OVCAR-8. For this, cells were incubated with a concentration equivalent to their IC_{50} and then stained with annexin V-Alexa Fluor 498 and PI and analyzed by flow cytometry (**Table 8**).

Table 8. Analysis of the apoptosis of NCI-H460 and OVCAR-8 cells treated with compound 10 measured by Annexin V-Alexa Fluor 488/PI staining.

	NCI-H460		**OVCAR-8**	
	Control	**Compound 10**	Control	**Compound 10**
Early apoptotic cells (%)	2.58 ± 0.27	13.72 ± 4.34	4.48 ± 0.46	36.12 ± 2.32
Late apoptotic cells (%)	15.83 ± 1.40	68.61 ± 3.04	6.46 ± 0.36	30.82 ± 2.60
Necrotic cells (%)	1.41 ± 0.74	1.29 ± 0.27	0.80 ± 0.09	1.27 ± 0.08
Viable cells (%)	80.19 ± 1.08	16.37 ± 2.32	88.26 ± 0.78	31.79 ± 3.27

All data were expressed as mean ±SE of three different experiments. Values were analyzed from 10.000 total events.

As it can be seen in **Table 8**, compound 10 clearly increases early and late apoptosis in both cell lines. In the case of the NCI-H460 cell line, which is much more sensitive to compound 10, the number of cells in late apoptosis is clearly higher than the number of cells in early apoptosis, while for the OVCAR-8 cell line both values are very similar. Noteworthy as with the metallic Mn compound the percentage of necrotic cells in both cell lines is less than 2%.

4.3.6 Effect of compound 10 on the migration capacity

We measured the effect of compound 10 on the migration capacity of the MDA-MB-231 cell line using transwell chambers. We used this cell line since former NCI-H460 and OVCAR-8 did not migrate in the used assays. For these assays, cells were treated with 0.1 µM (corresponding to an IC_{20}) of compound 10. As shown in **Figure 19**, after treatment for 24, 48 and 72 h, a significant decrease in cell migration was observed at all time points assayed.

A.

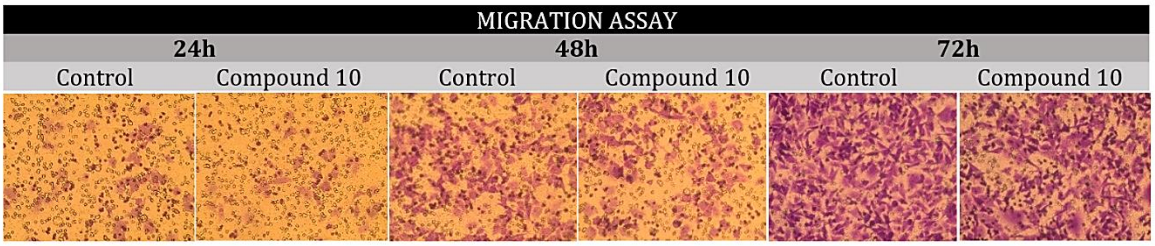

B.

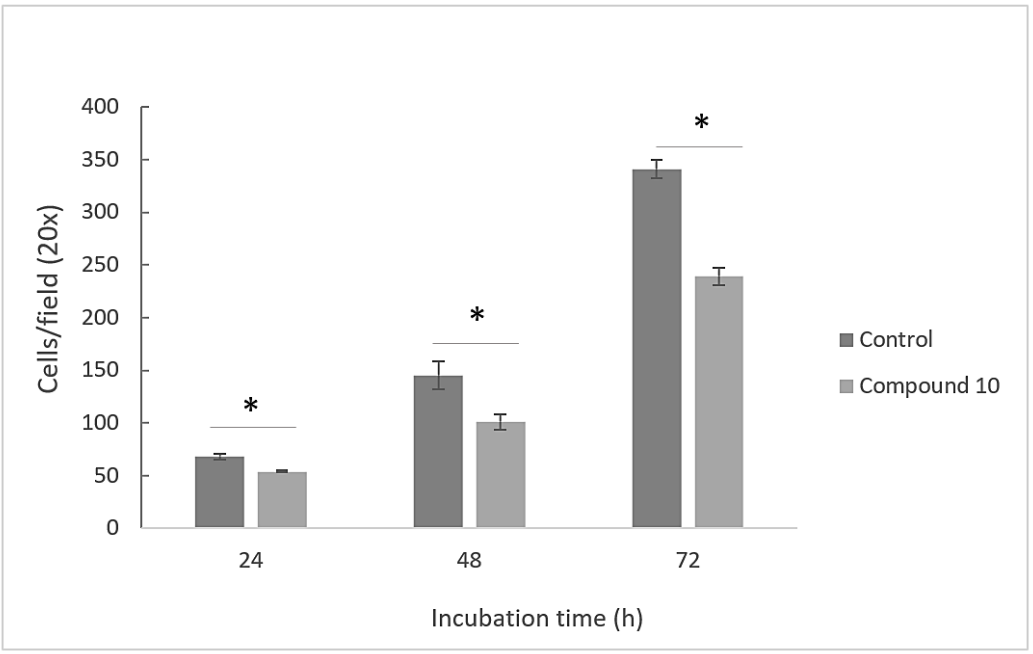

Figure 19. Effect of compound 10 on migration of MDA-MB-231 cells using a transwell chambers. **A.** Representative images of migration assays in cells untreated and treated with compound 10 for 24, 48 and 72 h and **B.** quantitative analysis of cell density in each treatment. Cells were stained with crystal violet. *P< 0.05. Data are shown as mean ± SE of at least three independent experiments.

DISCUSSION

5. DISCUSSION

Cancer is the leading cause of death worldwide [174]. According to data from the Global Cancer Observatory (GLOBOCAN) [175] by the year 2020, around 19.3 million new cases of cancer were diagnosed, and in the same year there were almost 10 million deaths due to this pathology. Despite enormous advances in anticancer treatment, cancer mortality rates remain alarmingly high because, although most patients initially respond well to chemotherapy, chemoresistance is acquired later, resulting in recurrence [176]. Moreover, most treatments produce peripheral toxicity and a host of adverse effects.

Considering the above, there is a clear need of discovering new antitumor compounds that may be efficient *in vivo* without displaying toxic side effects. The present research work has focused on the analysis, evaluation, and characterization of two types of antitumor drugs. Firstly, we have evaluated the anti-metastatic effects of a cytotoxic ND-RNase and secondly, we have investigated the antitumor properties of two panels of manganese- and iron-based metal compounds and their possible application in antitumor therapies.

5.1 Anticancer effects of NLSPE5

RNases are highly promising biological agents for use in cancer therapy. Unlike many chemotherapeutic compounds, which interfere with DNA synthesis and cell division, antitumor RNases have the advantage of being non-mutagenic agents that exert their effects by interfering with RNA functions such as protein synthesis or gene regulation. Since these RNases affect multiple RNA molecule classes, another interesting feature of antitumor RNases is that they cause pleiotropic effects in cells. That is, that they target multiple biological pathways involved in the maintenance of tumorigenesis [101]. In addition, pleiotropy may difficult the acquisition of tumor resistance to RNases and could explain the synergisms found between them and other antitumor agents. In this work, we have deepened the

study of how the ND-RNase NLSPE5 affects cancer cells by analyzing its effect on epigenetic regulation. Also, we have analyzed how NLSPE5 affects both the migration and invasion capacity of tumor cells.

Genetic and epigenetic alterations play a key role in cancer initiation and progression. Within the histone alterations, H3K27me3 is a critical determinant of chromatin accessibility and gene expression [177]. The results of treatment of the MDA-MB-231 cell line in 3D culture with the ND-RNase NLSPE5 resulted in an increase in the expression of the repressive epigenetic mark H3K27me3 by approximately 50% compared to the control.

Different authors have shown that antitumor RNases act through a decrease or increase of expression of multiple key genes. Vert *et al*. [101], in their study on the protein-engineered ribonuclease PE5, ancestor of NLSPE5, showed by microarray transcriptional analysis that this RNase have pleiotropic effects on the ovarian tumor cell line NCI/ADR-RES. One of these effects is the down-regulation of multiple genes encoding enzymes involved in metabolic pathways that are deregulated in cancer cells. Also by analyzing the complete transcriptome of murine Lewis lung carcinoma (LLC) after RNase A treatment, Mironova *et al*.[178] detected an increase in carbohydrate metabolism, the inositol phosphate cascade and oxidative phosphorylation, as well as an up-regulation in the reorganization of cell adhesion, cell cycle control, apoptosis and transcription. Otherwise, cancer-related signaling pathways involved in the progression of non-small cell lung cancer were reduced after treatment. Likewise, this treatment caused the down-regulation of genes that inhibit the biogenesis of some miRNAs, in particular the let-7 family of miRNAs.

Almost for ND-RNases, these multiple effects are very possibly a consequence of the multiple targets of this drug. It has been previously described that ND-RNases affect the expression of rRNA [101] and miRNA [162], altering gene expression. Since HP-RNase has endonuclease activity towards dsRNA [79], it would be not surprising that ND-RNases, as it occurs with ONC [179], cleave tRNAs. Interestingly, it

has been recently proposed a new class of ncRNAs derived from tRNA fragments (tRFs) [180] that may inhibit cancer proliferation [181]. Here, we show that ND-RNases can affect gene expression through modification of post-translational pattern of histones. This is likely an indirect effect and possibly ND-RNases would be affecting the expression of different transcription factors that would alter the methylation of histone H3. Up-regulation of H3K27me3 has been related to important pathways in cell metabolism, differentiation, and embryogenesis, and therefore the increase of this epigenetic mark could partly explain the effects produced by the ND-RNases. As has been previously observed, the decrease in H3K27me3 is a characteristic marker of some types of breast and prostate cancer, and constitutes a marker of aggressiveness of the disease [182]. Hsieh *et al*. [183], found that loss of H3K27me3 is highly specific for aggressive breast cancer subtypes such as the TNBC, of whom MDA-MB-231 is a model cell line. They demonstrated that treatment with a demethylase inhibitor (GSK-J4) increased H3K27me3 expression levels in this tumor cell line, leading to a potent decrease of expression of Cell Migration Inducing Hyaluronidase protein (CEMIP) and consequently an inhibition of the malignant cell phenotype. Interestingly, it is known that increased levels of this protein are associated with a better prognosis and survival in patients with breast, prostate or non-small cell lung [182–184].

Gene dysregulation as well as cell migration are innate characteristics of cancer cells that can lead to cancer metastasis, which is the major cause of cancer mortality. Current research has focused its efforts on the development of compounds that target cellular processes that contribute to metastasis such as cell migration and invasion. Here, we have analyzed how NLSPE5 affects these properties using 3D tumor spheroids since they reflect more accurately the solid tumor microenvironment and can better model the interaction between the extracellular matrix and host cells [185]. The IC_{50} value obtained for the MDA-MB-231 cell line cultured in 3D is somewhat higher than that obtained in 2D culture but this observation has already been reported in different studies [189,190]. Sometimes, this fact has been attributed primarily to signals from dynamic cellular interactions between neighboring cells and ECM input into the cellular decision-making process [191], but could also be due to a lower drug uptake through the

spheroid structure and to hypoxia, which can lead to the activation of genes involved in cell survival and drug sensitivity [192]. We show that NLSPE5 reduces the migration and invasion capacity of the MDA-MB-231 cell line, which, as mentioned above, is highly invasive and presents a TNBC phenotype. In accordance with the reduction of migratory and invasive capacities, NLSPE5 also reduces the expression of a marker of cell migration/invasion [186] such as is the N-cadherin protein. Derycke *et al.* [187] and Wu *et al*. [188] have demonstrated that N-cadherin protein plays a key role in tumor metastasis by promoting cell to cell interaction and thus providing a mechanism for transendothelial migration. Therefore, the decrease in N-cadherin expression observed after treatment of the MDA-MB-231 cell line could partly explain the inhibitory effect on migration and invasion capacity that NLSPE5 has on these breast cancer cells.

5.2 Evaluation and characterization of manganese-based compounds

Cis-platin is a paradigmatic transition-metal based compound nowadays used worldwide for the treatment of numerous cancers including bladder, head and neck, lung, ovarian, and testicular cancers [193]. However, its toxic side-effects have pushed on the research of alternative compounds using less toxic metals. Among them, Mn complexes have potentially fewer side effects compared to platinum or ruthenium. Mn is a widely distributed metal and is a necessary cofactor for many ubiquitous enzymes [125]. Most Mn (II) ions are taken up and transported through the transferrin receptor system, which is overexpressed in several types of tumor cells [194,195], making these receptors potential therapeutic targets. Based on these data, compounds containing Mn (II) have been designed and synthesized with the aim of developing new chemotherapeutic agents. Complexes containing manganese may be valuable antitumor agents though they have been only scarcely studied for such purpose [126,131,132,196–198]. In this research we have investigated the antitumor activity of a panel of new manganese compounds containing pyridine-pyrazole and (-)-pinene[5,6]bipyridine ligands together with different

monodentate labile ligands. Our results show that most of the tested Mn-based metal compounds exhibit mild cytotoxic activity. However, among them, compound Mn8, and to a lesser extent its ligand, exhibit a much higher cytotoxicity that is comparable to *Cis*-platin in both assayed cell lines. When comparing the cytotoxicity of Mn8 with carboplatin the difference is much greater, being 8-fold and 24-fold for the lung cancer line NCI-H460 and ovarian cancer line OVCAR-8, respectively. It should also be mentioned that in all cases the biological activity is much higher in the Mn compound than in its free ligand, indicating that the antitumor activity of the ligand is enhanced in coordination with Mn. This has already been reported previously [199–201] with other ligands coordinated to Mn ion that resulted in cytotoxic activity against other tumor cell lines. Ligands may play important roles in target site recognition; the presence of a chelating ligand may control the reactivity toward different biomolecules such as DNA or enzymes and play a key role in the interaction with them through hydrogen bonding or intercalation. In addition, hydrophobicity may enhance cellular uptake, since compounds Mn2 and Mn3 (bearing the apolar –Me and $–CH_2COOEt$ substituents at the bidentate ligands) and Mn8 (which contains the pinene-bipyridine ligand) are more cytotoxic than the rest of the complexes that contain more polar pypz-H ligands.

At the same time, Mn8 compound has an IC_{50} value for CCD-18Co non-tumor cells higher than 30 μM, which indicates that it is selective for cancer cells. Other Mn compounds have been previously described to be selective. Among them Liu *et al.* [131] synthesized a bis(2-pyridylmethyl)amino-2-propionic acid) bound to Mn (II) compound that is much more cytotoxic for several tumor cell lines (HeLa, HepG2, A549, MCF-7, U251, LoVo, A875 and ECA-109) than for the immortalized non-tumor liver line WRL-67.

Numerous studies have shown that ROS act as a double-edged blade since whereas a modest amount of ROS leads to tumor promotion, an excessive level assists to tumor suppression. Cancer cells have increased ROS levels, therefore, a further increase of the ROS level in these cells could raise it above a cellular tolerability threshold and induce cell death. The redox imbalance observed after

treatment with Mn-based compounds has been reported in many cases [131,199,200,202,203].

In agreement with these observations, Mn8, and to a lesser extent its ligand, induce intracellular ROS formation in a dose- and time-dependent manner. NCI-H460 cells produce higher oxidative activity than OVCAR-8 cells when incubated with Mn8. This is in accordance with the cytotoxicity results obtained since the IC_{50} of the former cells is lower than that of OVCAR-8. The role of ROS in mediating the cytotoxicity of Mn8 was checked by investigating the effect of the antioxidant agent NAC on cell viability. It was found that the presence of this compound significantly, but not completely, reduces the anti-proliferative/cytotoxic effect of Mn8 and its ligand, indicating that the cytotoxicity observed when treating tumor cells is mediated by the production of intracellular ROS. Therefore, the possibility that other mechanisms could be involved in this process could not be ruled out and we therefore investigated an alternative cytotoxic mechanism.

Different Mn cytotoxic compounds have been described to interact with DNA. As example, Gao *et al*. [204] synthesized 1H-cyclopentadipyridine-2,5-dione bound to Mn (II) and demonstrated that their complex had the ability to interact with plasmid DNA decreasing its supercoiled state and increasing its relaxed state. Because of that, we investigated whether Mn8 has the ability to interact with DNA. We showed that this compound is able to interact with DNA only in the presence of H_2O_2 and at the highest concentrations, Mn8 is able to completely degrade the plasmid DNA used in the assay. How ROS are implicated in the mechanism of cleaving the DNA cannot be inferred from our results. However, we envisage two possibilities: H_2O_2 could be altering the structure of Mn8 allowing the resulting compound to interact with the DNA or, alternatively, H_2O_2 could be acting as a substrate of the cleavage reaction produced by Mn8.

Although several investigations have shown that Mn compounds are able to influence the cell cycle of tumor cells, mainly by arresting cells in the G_0/G_1 phase[201,205,206] we have not observed important changes in the cell cycle phase

distribution in either of the two cell lines tested. Only a slight increase in the G_0/G_1 phase was observed followed by a slight decrease in S and G_2/M phase after 72 h of treatment at the highest concentration tested. These results indicate that the cytotoxic/antiproliferative activity observed for Mn8 is not restricted to any cell cycle phase and likely it is displaying a cytotoxic but not anti-proliferative activity.

The results of the assay to detect apoptosis after treatment with Mn8 and its ligand show that in the most sensitive cell line, Mn8 slightly increases the percentage of cells undergoing apoptosis respective to control cells. We could not detect apoptosis in OVCAR-8- treated cells in accordance with the lack of a subG_1 fraction in the cell cycle analysis. This seems to indicate that this compound, in contrast to other Mn-based compounds[129,199,201,204,206,207], possibly induce cell death through other mechanisms that are also different from necrosis.

Thus, considering the different results discussed above, it could be considered that we have identified a Mn compound that is a promising alternative to the current metal-based antitumor agents.

5.3 Evaluation and characterization of iron-based compounds

Fe is an essential element for almost all living organisms as it is involved in a wide variety of metabolic processes such as oxygen transport, DNA synthesis and electron transport [208]. Fe is usually present in the body in the +2 or +3 oxidation states but higher oxidation states of +4 and +5 have been suggested in Fe - containing enzymes in the course of biological oxidation reactions [209]. Fe compounds with antitumor properties have been found to cause low toxicity to normal cells, in addition to exhibiting anticancer mechanisms that are different from those observed in platinum complexes [145]. The most studied families of Fe compounds as anticancer agents are those of organometallic ferrocene complexes and inorganic Fe (II) and Fe (III) coordination complexes [145]. Although these complexes have received a great deal of attention, the field of Fe metalloids is not limited to them. Unlike polymeric and mixed bimetallic Fe complexes, few

binuclear Fe complexes have been tested as antitumor agents until now. Here, we have used a battery of binuclear Fe related compounds carrying pyridylic rings in order to investigate their antitumor activity. Since they have similar structures, we were interested in ascertaining how the different substituents on the pyridylic rings could induce differences in the cytotoxic activity of the compounds.

We evaluated the panel of new Fe-based metallic compounds against NCI-H460 and OVCAR-8 cell lines. Our results show that all the compounds have a dose-dependent cytotoxic activity against both tumor cell lines. It is noteworthy that the compounds are more cytotoxic than *Cis*-platin and carboplatin for both cell lines. As with the Mn compounds, the most sensitive cells to these compounds is the lung cancer cell line NCI-H460. Unfortunately, the assayed complexes did not display differences in their cytotoxicity for tumor cells and therefore we could not analyze how the different substituents were affecting the biologic properties of the binuclear Fe complexes. Previous studies [210–215] have shown that the addition of coordination ligands to Fe molecules provide these new complexes with cytotoxic characteristics. Wong *et al*. [214] constructed new pentadentate pyridyl ligands bound to an Fe (II) atom that were cytotoxic against a panel of breast, cervical, nasopharyngeal, and liver tumor cell lines. The cytotoxicity observed was higher than that reported for *Cis*-platin in all cell lines and in all compounds assayed.

We decided to investigate the selectivity for tumor cells of the set of organometallic compounds. The assays were carried out with CCD-18Co non-tumor cells. Our results show that compounds 10 and 11 have the greatest selectivity for tumor cell lines being that of compound 10 higher than that of *Cis*-platin and carboplatin. The selectivities of pentadentate pyridyl ligands complexed to Fe are well below to that reported for *Cis*-platin.

Other researchers [216–219] used Fe (III) ligands and after analyzing them concluded that like Fe (II)-based complexes they also had cytotoxic characteristics against tumor lines in a dose-dependent manner and to some degree a

concentration-dependent selectivity. An important fact to note is that the IC_{50} values reported are mostly higher than those reported in this study.

The increase in ROS levels in a dose- and time-dependent manner is one of the characteristics commonly found by researchers when working with this type of Fe (II) [214,215] and Fe (III) based metallic compounds [217]. Taking also into account the results obtained with the Mn compounds, we decided to investigate the effects that the new Fe-based compounds have on the redox balance of the cell. This analysis was carried out only with the compound that has the lowest IC_{50} value and the highest selectivity for tumor cells, that is, compound 10. As it can be seen in **Figure 14**, this compound increases the levels of ROS in a dose- and time-dependent manner. The fact that the most sensitive cell line induces lower ROS levels indicates that the observed cytotoxic effect may not be solely mediated by intracellular ROS production. To confirm the role of ROS compounds in the cytotoxicity induced by compound 10, we investigated the effect on cytotoxicity of co-incubating the cells with the antioxidant NAC. After treatment, it was observed that NAC does not counteract the effect produced by compound 10 in any of the two cell lines assayed. This seems to indicate that the cytotoxicity produced by compound 10 is not primarily linked to ROS production. It is known that cancer cells have higher basal ROS levels than normal cells [220,221] possibly due to oncogenic stimulation, increased metabolic activity and malfunctioning of the mitochondria [220]. However, it cannot be completely discarded that the increase of ROS levels in cancer cells mediated by compound 10 was highly enough to mask the effect of the antioxidant agent used not being visible at least at the concentrations used.

Searching for other molecular effects of compound 10 on cancer cells we investigated whether this compound was interacting with DNA. Again, the assay was carried out with and without the addition of H_2O_2 as ROS initiator and we observed that our compounds do not have the ability to interact with DNA in the absence of H_2O_2. However, again, when this oxidizing agent is present all compounds acquire this capacity even degrading DNA at the highest concentrations. Other studies have shown that Fe (II) complexes coupled to

pentadentate pyridyl ligands [214] and pentadentate N-donor ligands [215] have also the ability to interact with DNA, to nick it and even some of them to cleave DNA, as is in our study. In the latter study [215] the addition of a ROS initiator such as H_2O_2 was also required to observe the interaction with DNA. These results indicate that the increase of the concentration of ROS in cancer cells induced by our Fe (II) compounds may have an impact on DNA. A striking effect of compound 10 over DNA was the early appearance of a band of linear DNA. If compound 10 was breaking both strands randomly, the possibility of DNA linearization would be very low. A possible explanation of this effect is that each of Fe atoms of the binuclear compound was breaking one of the two strands of DNA.

Analysis of the effect of compound 10 on the cell cycle of tumor cell lines has shown that our compound does not alter the percentage of cells at any cycle phase in the NCI-H460 cell line, whereas a clear antiproliferative effect is observed on the OVCAR-8 cell line due to the arrest of the S and G_2/M phases of the cycle. It is interesting to recall that this cell line is much less sensitive to compound 10 than the NCI-H460 cell line, which would indicate that the cytotoxic effect attributed to compound 10 has a cell cycle-independent character. The effect that other Fe compounds have on the cell cycle is varied. Some compounds [215,217] arrest cells at the G_0/G_1 cell cycle phase with the respective decrease of the other phases while other reports [214,217] have shown that the arrest after treatment with their Fe compounds occurs mainly in the S phase of the cell cycle . The arrest at this cell cycle phase may suggest that there is DNA damage that activates DNA repair mechanisms in the affected cells and, as a result, these cells stop DNA replication. In summary, these results would indicate that the cytotoxic and antiproliferative effect could be attributed to its ability to damage DNA.

Induction of apoptosis has been recognized as a possible outcome of DNA damage in pluricellular organisms [222]. We decided to study whether our compound has the ability to induce apoptosis in the NCI-H460 and OVCAR-8 cell lines. The induction of apoptosis due to treatment with iron-based compounds has been reported by several authors [210–219]. Our results indicate that after treatment

with compound 10 both cell lines increase their levels of both, early and late apoptosis. The late apoptosis values of the NCI-H460 cell line are much higher than those of the OVCAR-8 cell line, which, accordingly, is the most sensitive to this Fe compound.

Since cell migration is an important feature in the late period of cancer progression and that its inhibition is essential for an effective treatment, we decided to evaluate the effect of our compound on the migration capacity of tumor cells. For this study we had to change the cell line model since neither NCI-H460, nor OVCAR-8, had a significant migration capacity to investigate its inhibition. We selected the MDA-MB-231 cell line used previously for NLSPE5. Our results indicate that the migration capacity is significantly suppressed when this cell line is treated with compound 10 although its effect is lower than that observed with NLSPE5. As far as we know, the production of Fe (II) compounds that inhibit cell migration has been reported in only one other case. Xie *et al*. **[210]** produced different Fe (II) complexes coupled to phenanthroline derivatives that also significantly decrease the migration of the Human Umbilical Vein Endothelial cells.

CONCLUSIONS

6. CONCLUSIONS

- The ND-RNase NLSPE5 increases the expression of the epigenetic mark H3K27me3 in the MDA-MB-231 cell line, which would partly explain its pleiotropic effects.

- NLSPE5 significantly reduces the migration and invasion ability of the MDA-MB-231 cells and downregulates N-cadherin protein expression.

- A panel of new Mn compounds containing pyridine-pyrazole and (-)-pinene[5,6]bipyridine rings show cytotoxic activity against OVCAR-8 and NCI-H460 cell lines.

- Among the Mn compounds, Mn8 has a remarkable and selective antitumor activity that is of the same order of magnitude as *Cis*-platin.

- Mn8 and to a lesser extent its ligand, have the capacity to produce ROS in the two cell lines analyzed in a dose- and time- dependent manner. These ROS compounds are involved in the cytotoxic mechanism of Mn8.

- Mn8, but not its ligand, interacts with DNA in the presence of oxidizing agents such as H_2O_2. This interaction could explain the higher cytotoxicity presented by Mn8 with respect to its ligand.

- Neither Mn8 nor its ligand affect cell cycle phase distribution of tumor cell lines.

- The mechanism of cell death by which Mn8 acts is different from that of apoptosis and necrosis and remains to be determined.

- All the binuclear Fe related compounds carrying pyridylic rings tested show IC_{50} values lower than that of *Cis*-platin and carboplatin.

- Of all the Fe compounds tested, compound 10 is the most cytotoxic and selective for tumor cells, showing a selectivity index even higher to that of *Cis*-platin and carboplatin.

- All Fe compounds interact with DNA promoting double strand breaks in the presence of an oxidizing agent such as H_2O_2

- Compound 10 induce intracellular ROS formation in both cell lines tested in a dose- and time-dependent manner. However, we have not demonstrated whether the cytotoxicity produced by compound 10 is primarily linked to ROS production.

- In the OVCAR-8 cell line compound 10 causes cell cycle arrest in the S and G_2/M phases, while for NCI-H460 cell line no significant changes in the cell cycle phase distribution were observed upon incubation with the compound.

- Compound 10 induces cell death by apoptosis and significantly decreases the migration capacity of the breast tumor cell line MDA-MB-231.

REFERENCES

REFERENCES

1. Stewart, J.G. *Anatomical Chart Company. Atlas of Pathophysiology*; 4th ed.; Wolters Kluwer, 2018; ISBN 978-84-17370-10-7.

2. Hanahan, D.; Weinberg, R.A. The Hallmarks of Cancer. *Cell* **2000**, *100*, 57–70, doi:10.1016/S0092-8674(00)81683-9.

3. World Health Organization Cáncer Available online: https://www.who.int/es/news-room/fact-sheets/detail/cancer (accessed on 26 January 2022).

4. Mitchell, R.N.; Kumar, V.; Abbas, A.K.; Aster, J.C. *Compendio Robbins Cotran. Patologia Estructural y Funcional*; Elsevier Health Sciences, 2017; ISBN 9788491131311.

5. Gersten, O.; Wilmoth, J.R. The Cancer Transition in Japan since 1951. *Demogr. Res.* **2002**, *7*, 271–306, doi:10.4054/DemRes.2002.7.5.

6. Omran, A.R. The Epidemiologic Transition: A Theory of the Epidemiology of Population Change. *Milbank Q.* **2005**, *83*, 731–757, doi:10.1111/j.1468-0009.2005.00398.x.

7. Bray, F.; Ferlay, J.; Soerjomataram, I.; Siegel, R.L.; Torre, L.A.; Jemal, A. Global Cancer Statistics 2018: GLOBOCAN Estimates of Incidence and Mortality Worldwide for 36 Cancers in 185 Countries. *CA. Cancer J. Clin.* **2018**, *68*, 394–424, doi:10.3322/caac.21492.

8. ECIS - European Cancer Information System *European Cancer Information System*; 2021;

9. Mitrus, I.; Bryndza, E.; Sochanik, A.; Szala, S. Evolving Models of Tumor Origin and Progression. *Tumour Biol.* **2012**, *33*, 911–917, doi:10.1007/s13277-012-0389-0.

10. Loeb, L.A. Human Cancers Express Mutator Phenotypes: Origin, Consequences and Targeting. *Nat. Rev. Cancer* **2011**, *11*, 450–457, doi:10.1038/nrc3063.

11. Vesely, M.D.; Kershaw, M.H.; Schreiber, R.D.; Smyth, M.J. Natural Innate and Adaptive Immunity to Cancer. *Annu. Rev. Immunol.* **2011**, *29*, 235–271, doi:10.1146/annurev-immunol-031210-101324.

12. Hanahan, D.; Weinberg, R.A. Hallmarks of Cancer: The next Generation. *Cell* **2011**, *144*, 646–674, doi:10.1016/j.cell.2011.02.013.

13. Belden, S.; Flaherty, K.T. MEK and RAF Inhibitors for BRAF-Mutated Cancers. *Expert Rev. Mol. Med.* **2012**, *14*, doi:10.1017/erm.2012.11.

14. Baines, A.T.; Xu, D.; Der, C.J. Inhibition of Ras for Cancer Treatment: The Search Continues. *Future Med. Chem.* **2011**, *3*, 1787–1808, doi:10.4155/fmc.11.121.

15. Viatour, P.; Sage, J. Newly Identified Aspects of Tumor Suppression by RB. *DMM Dis. Model. Mech.* **2011**, *4*, 581–585, doi:10.1242/dmm.008060.

16. Elmore, S. Apoptosis: A Review of Programmed Cell Death. *Toxicol. Pathol.* **2007**, *35*, 495–516, doi:10.1080/01926230701320337.

17. Friedberg, E.C. DNA Damage and Repair. *Nature* **2003**, *421*, 436–440, doi:10.1038/nature01408.

18. Fulda, S. Evasion of Apoptosis as a Cellular Stress Response in Cancer. *Int. J. Cell Biol.* **2010**, *2010*, doi:10.1155/2010/370835.

19. Hayflick, L.; Moorhead, P.S. The Serial Cultivation of Human Diploid Cell Strains. *Exp. Cell Res.* **1961**, *25*, 585–621, doi:10.1016/0014-4827(61)90192-6.

20. Ogrunc, M.; d'Adda di Fagagna, F. Never-Ageing Cellular Senescence. *Eur. J. Cancer* **2011**, *47*, 1616–1622, doi:10.1016/j.ejca.2011.04.003.

21. Nishida, N.; Yano, H.; Nishida, T.; Kamura, T.; Kojiro, M. Angiogenesis in Cancer. *Vasc. Health Risk Manag.* 2006, *2*, 213–219.

22. Sun, W. Angiogenesis in Metastatic Colorectal Cancer and the Benefits of Targeted Therapy. *J. Hematol. Oncol.* **2012**, *5*, 63, doi:10.1186/1756-8722-5-63.

23. Yu, E. mi; Jain, M.; Aragon-Ching, J.B. Angiogenesis Inhibitors in Prostate Cancer Therapy. *Discov. Med.* **2010**, *10*, 521–530.

24. Eggstein, G.R.; Liebner, S.; Wolburg, H. The Blood-Brain Barrier in the Human Glioma. In *Blood-Spinal Cord and Brain Barriers in Health and Disease*; Academic Press, 2003; pp. 561–576 ISBN 9780080528229.

25. Troncoso, D.; Aldana, S.; Chaparro, V.; Rey, L.; Ramírez, A.; Montoya, C.; Valderrama, A.; Cañas, A. Transición Epitelio Mesénquima: De Lo Molecular a Lo Fisiológico. **2017**, 1–10.

26. Cavallaro, U.; Christofori, G. Cell Adhesion and Signalling by Cadherins and Ig-CAMs in Cancer. *Nat. Rev. Cancer 2004 42* **2004**, *4*, 118–132, doi:10.1038/nrc1276.

27. Castaño, Z.; Tracy, K.; McAllister, S.S. The Tumor Macroenvironment and Systemic Regulation of Breast Cancer Progression. *Int. J. Dev. Biol.* **2011**, *55*, 889–897, doi:10.1387/ijdb.113366zc.

28. Torino, F.; Bonmassar, E.; Bonmassar, L.; De Vecchis, L.; Barnabei, A.; Zuppi,

C.; Capoluongo, E.; Aquino, A. Circulating Tumor Cells in Colorectal Cancer Patients. *Cancer Treat. Rev.* 2013, *39*, 759–772.

29. Warburg, O. On the Origin of Cancer Cells. *Science (80-.).* **1956**, *123*, 309–314, doi:10.1126/science.123.3191.309.

30. Unterlass, J.E.; Curtin, N.J. Warburg and Krebs and Related Effects in Cancer. *Expert Rev. Mol. Med.* **2019**, *21*, doi:10.1017/erm.2019.4.

31. Chen, Z.; Lu, W.; Garcia-Prieto, C.; Huang, P. The Warburg Effect and Its Cancer Therapeutic Implications. *J. Bioenerg. Biomembr.* **2007**, *39*, 267–274, doi:10.1007/s10863-007-9086-x.

32. Liberti, M. V.; Locasale, J.W. The Warburg Effect: How Does It Benefit Cancer Cells? *Trends Biochem. Sci.* **2016**, *41*, 211–218, doi:10.1016/j.tibs.2015.12.001.

33. Deberardinis, R.J.; Thompson, C.B. Cellular Metabolism and Disease: What Do Metabolic Outliers Teach Us? *Cell* **2012**, *148*, 1132–1144, doi:10.1016/j.cell.2012.02.032.

34. Eljaszewicz, A.; Wiese, M.; Helmin-Basa, A.; Jankowski, M.; Gackowska, L.; Kubiszewska, I.; Kaszewski, W.; Michalkiewicz, J.; Zegarski, W. Collaborating with the Enemy: Function of Macrophages in the Development of Neoplastic Disease. *Mediators Inflamm.* **2013**, *2013*, doi:10.1155/2013/831387.

35. Vajdic, C.M.; van Leeuwen, M.T. Cancer Incidence and Risk Factors after Solid Organ Transplantation. *Int. J. Cancer* **2009**, *125*, 1747–1754, doi:10.1002/ijc.24439.

36. Guo, W.; Lasky, J.L.; Wu, H. Cancer Stem Cells. *Pediatr. Res.* **2006**, *59*, 59–64, doi:10.1203/01.pdr.0000203592.04530.06.

37. Moharil, R.; Dive, A.; Khandekar, S.; Bodhade, A. Cancer Stem Cells: An Insight. *J. Oral Maxillofac. Pathol.* **2017**, *21*, 463, doi:10.4103/JOMFP.JOMFP_132_16.

38. Kuşoğlu, A.; Biray Avcı, Ç. Cancer Stem Cells: A Brief Review of the Current Status. *Gene* **2019**, *681*, 80–85, doi:10.1016/J.GENE.2018.09.052.

39. Yu, Z.; Pestell, T.G.; Lisanti, M.P.; Pestell, R.G. Cancer Stem Cells. *Int. J. Biochem. Cell Biol.* **2012**, *44*, 2144, doi:10.1016/J.BIOCEL.2012.08.022.

40. López de Andrés, J.; Griñán-Lisón, C.; Jiménez, G.; Marchal, J.A. Cancer Stem Cell Secretome in the Tumor Microenvironment: A Key Point for an Effective Personalized Cancer Treatment. *J. Hematol. Oncol.* **2020**, *13*, 1–22, doi:10.1186/s13045-020-00966-3.

41. Bidram, E.; Esmaeili, Y.; Ranji-Burachaloo, H.; Al-Zaubai, N.; Zarrabi, A.; Stewart, A.; Dunstan, D.E. A Concise Review on Cancer Treatment Methods and Delivery Systems. *J. Drug Deliv. Sci. Technol.* **2019**, *54*, 101350,

doi:10.1016/J.JDDST.2019.101350.

42. Kumar, P. Recent Advancement in Cancer Treatment. In *Design of Nanostructures for Theranostics Applications*; William Andrew Publishing, 2018; pp. 621–651 ISBN 9780128136690.

43. Padma, V.V. An Overview of Targeted Cancer Therapy. *Biomed.* **2015**, *5*, 1–6, doi:10.7603/s40681-015-0019-4.

44. Rosenberg, L.E.; Rosenberg, D.D. Chapter 16 - The Genetics of Cancer. In; Rosenberg, L.E., Rosenberg, D.D.B.T.-H.G. and G., Eds.; Academic Press: San Diego, 2012; pp. 259–288 ISBN 978-0-12-385212-0.

45. Hajdu, S.I. A Note from History: Landmarks in History of Cancer, Part 1. *Cancer* **2011**, *117*, 1097–1102, doi:10.1002/cncr.25553.

46. Hajdu, S.I.; Vadmal, M. A Note from History: Landmarks in History of Cancer, Part 6. *Cancer* **2013**, *119*, 4058–4082, doi:10.1002/cncr.28319.

47. Gropper, M.A.; Miller, R.D.; Eriksson, L.I.; Fleisher, L.A.; Wiener-Kronish, J.P.; Cohen, N.H.; Leslie, K. *Miller's Anesthesia, 2-Volume Set E-Book*; Elsevier Health Sciences, 2020; ISBN 0323612644.

48. Ponnusamy, L.; Mahalingaiah, P.K.S.; Singh, K.P. Epigenetic Reprogramming and Potential Application of Epigenetic-Modifying Drugs in Acquired Chemotherapeutic Resistance. In *Advances in Clinical Chemistry*; Elsevier, 2020; Vol. 94, pp. 219–259 ISBN 9780128208014.

49. Lin, Y.; Mauro, J.C.; Kaur, G. Bioactive Glasses for Cancer Therapy. In *Biomedical, Therapeutic and Clinical Applications of Bioactive Glasses*; Woodhead Publishing, 2018; pp. 273–312 ISBN 9780081021965.

50. Germanas, J.; Pandya, A.G. Alkylating Agents. In *Dermatologic Therapy*; BC Decker, 2002; Vol. 15, pp. 317–324.

51. Puyo, S.; Montaudon, D.; Pourquier, P. From Old Alkylating Agents to New Minor Groove Binders. *Crit. Rev. Oncol. Hematol.* **2014**, *89*, 43–61, doi:10.1016/j.critrevonc.2013.07.006.

52. Khalife, O.; Muhammad, M.; Kenj, M.; Salamoon, M. Alkylating Agents. In *Cyclophosphamide: Clinical Pharmacology, Uses and Potential Adverse Effects*; Nova Science Publishers, Inc., 2015; pp. 1–19 ISBN 9781634635837.

53. Falzone, L.; Salomone, S.; Libra, M. Evolution of Cancer Pharmacological Treatments at the Turn of the Third Millennium. *Front. Pharmacol.* **2018**, *9*, 1300, doi:10.3389/fphar.2018.01300.

54. Kaye, S.B. New Antimetabolites in Cancer Chemotherapy and Their Clinical Impact. *Br. J. Cancer* **1998**, *78*, 1–7, doi:10.1038/bjc.1998.747.

55. Tiwari, M. Antimetabolites: Established Cancer Therapy. *J. Cancer Res. Ther.* **2012**, *8*, 510–519, doi:10.4103/0973-1482.106526.

56. Scholar, E. Antimetabolites. In *xPharm: The Comprehensive Pharmacology Reference*; Elsevier Inc., 2007; pp. 1–4 ISBN 9780080552323.

57. Zehnder •, A.; Graham •, J.; Reavill •, D.R.; McLaughlin, A. Neoplastic Diseases in Avian Species. In *Current Therapy in Avian Medicine and Surgery*; Elsevier, 2016; pp. 107–141.

58. Bharti, A.C.; Vishnoi, K.; Singh, S.M.; Aggarwal, B.B. Pathways Linked to Cancer Chemoresistance and Their Targeting by Nutraceuticals. In *Role of Nutraceuticals in Chemoresistance to Cancer*; Elsevier, 2018; pp. 1–30.

59. Chen, J.-G.; Horwitz, S.B. Differential Mitotic Responses to Microtubule-Stabilizing and -Destabilizing Drugs. *Cancer Res.* **2002**, *62*, 1935–1938.

60. Mirzaei, H.; Emami, S. Recent Advances of Cytotoxic Chalconoids Targeting Tubulin Polymerization: Synthesis and Biological Activity. *Eur. J. Med. Chem.* **2016**, *121*, 610–639, doi:10.1016/J.EJMECH.2016.05.067.

61. Kingston, D.G.I. Tubulin-Interactive Natural Products as Anticancer Agents. *J. Nat. Prod.* **2009**, *72*, 507, doi:10.1021/NP800568J.

62. Van Vuuren, R.J.; Visagie, M.H.; Theron, A.E.; Joubert, A.M. Antimitotic Drugs in the Treatment of Cancer. *Cancer Chemother. Pharmacol.* **2015**, *76*, 1101–1112, doi:10.1007/s00280-015-2903-8.

63. Masawang, K.; Pedro, M.; Cidade, H.; Reis, R.M.; Neves, M.P.; Corrêa, A.G.; Sudprasert, W.; Bousbaa, H.; Pinto, M.M. Evaluation of 2',4'-Dihydroxy-3,4,5-Trimethoxychalcone as Antimitotic Agent That Induces Mitotic Catastrophe in MCF-7 Breast Cancer Cells. *Toxicol. Lett.* **2014**, *229*, 393–401, doi:10.1016/j.toxlet.2014.06.016.

64. Mitchison, T.J. The Proliferation Rate Paradox in Antimitotic Chemotherapy. *Mol. Biol. Cell* **2012**, *23*, 1–6, doi:10.1091/mbc.E10-04-0335.

65. Jordan, M.A.; Wilson, L. Microtubules as a Target for Anticancer Drugs. *Nat. Rev. Cancer* **2004**, *4*, 253–265, doi:10.1038/nrc1317.

66. Kavallaris, M. Microtubules and Resistance to Tubulin-Binding Agents. *Nat. Rev. Cancer* **2010**, *10*, 194–204, doi:10.1038/nrc2803.

67. Kersten, W.; Kersten, H.; Szybalski, W. Physicochemical Properties of Complexes between Deoxyribonucleic Acid and Antibiotics Which Affect Ribonucleic Acid Synthesis (Actinomycin, Daunomycin, Cinerubin, Nogalamycin, Chormomycin, Mithramycin, and Olivomycin). *Biochemistry* **1966**, *5*, 236–244, doi:10.1021/bi00865a031.

68. Umezawa, H.; Maeda, K.; Takeuchi, T.; Okami, Y. New Antibiotics, Bleomycin A and B. *J. Antibiot. (Tokyo).* **1966**, *19*, 200–209.

69. Chen, J.; Stubbe, J. Bleomycins: Towards Better Therapeutics. *Nat. Rev. Cancer* **2005**, *5*, 102–112, doi:10.1038/nrc1547.

70. Bolzán, A.D.; Bianchi, M.S. DNA and Chromosome Damage Induced by Bleomycin in Mammalian Cells: An Update. *Mutat. Res.* **2018**, *775*, 51–62, doi:10.1016/j.mrrev.2018.02.003.

71. Wright, J.C.; Dolgopol, V.B.; Logan, M.; Prigot, A.; Wright, L.T. Clinical Evaluation of Puromycin in Human Neoplastic Disease. *AMA. Arch. Intern. Med.* **1955**, *96*, 61–77, doi:10.1001/archinte.1955.04430010075008.

72. Deshpande, R.A.; Shankar, V. Ribonucleases from T2 Family. *Crit. Rev. Microbiol.* **2002**, *28*, 79–122, doi:10.1080/1040-840291046704.

73. Murchison, E.P. RNAases. In; Maloy, S., Hughes, K.B.T.-B.E. of G. (Second E., Eds.; Academic Press: San Diego, 2013; p. 270 ISBN 978-0-08-096156-9.

74. Cho, S.; Beintema, J.J.; Zhang, J. The Ribonuclease A Superfamily of Mammals and Birds: Identifying New Members and Tracing Evolutionary Histories. *Genomics* **2005**, *85*, 208–220, doi:10.1016/j.ygeno.2004.10.008.

75. D'Alessio, G. New and Cryptic Biological Messages from RNases. *Trends Cell Biol.* **1993**, *3*, 106–109, doi:10.1016/0962-8924(93)90166-X.

76. Castro, J.; Ribó, M.; Benito, A.; Vilanova, M. Approaches to Endow Ribonucleases with Antitumor Activity: Lessons Learned from the Native Cytotoxic Ribonucleases. In *Anti-cancer Drugs - Nature, Synthesis and Cell*; 2016; pp. 135–168 ISBN 978-953-51-2814-4.

77. Úsuga, X.; Rugeles, M. Ribonucleasas: Su Potencial Terapéutico En Infecciones Virales. *Acta Biológica Colomb.* **2006**, *11*, 31–44.

78. Ribó, M.; Benito, A.; Canals, A.; Nogués, M. V.; Cuchillo, C.M.; Vilanova, M. Purification of Engineered Human Pancreatic Ribonuclease. In *Methods in Enzymology*; Academic Press Inc., 2001; Vol. 341, pp. 221–234.

79. Sorrentino, S.; Naddeo, M.; Russo, A.; D'Alessio, G. Degradation of Double-Stranded RNA by Human Pancreatic Ribonuclease: Crucial Role of Noncatalytic Basic Amino Acid Residues. *Biochemistry* **2003**, *42*, 10182–10190, doi:10.1021/bi030040q.

80. Canals, A.; Ribó, M.; Benito, A.; Bosch, M.; Mombelli, E.; Vilanova, M. Production of Engineered Human Pancreatic Ribonucleases, Solving Expression and Purification Problems, and Enhancing Thermostability. *Protein Expr. Purif.* **1999**, *17*, 169–181, doi:10.1006/prep.1999.1112.

81. Castro, J.; Ribo, M.; Benito, A.; Vilanova, M. Mini-Review: Nucleus-Targeted Ribonucleases as Antitumor Drugs. *Curr Med Chem* **2013**, *20*, 1225–1231, doi:10.2174/0929867311320100003.

82. Ribó, M.; Benito, A.; Vilanova, M. Antitumor Ribonucleases. In *Ribonucleases*; Nicholson, A.W., Ed.; Springer Berlin Heidelberg: Berlin, Heidelberg, 2011; pp. 55–88 ISBN 978-3-642-21078-5.

83. Benito, A.; Ribó, M.; Vilanova, M. On the Track of Antitumour Ribonucleases. *Mol. Biosyst.* **2005**, *1*, 294–302, doi:10.1039/b502847g.

84. Gaur, D.; Swaminathan, S.; Batra, J.K. Interaction of Human Pancreatic Ribonuclease with Human Ribonuclease Inhibitor: Generation of Inhibitor-Resistant Cytotoxic Variants. *J. Biol. Chem.* **2001**, *276*, 24978–24984, doi:10.1074/jbc.M102440200.

85. Rutkoski, T.; Raines, R. Evasion of Ribonuclease Inhibitor as a Determinant of Ribonuclease Cytotoxicity. *Curr. Pharm. Biotechnol.* **2008**, *9*, 185–199, doi:10.2174/138920108784567344.

86. Kojima, K. Molecular Aspects of the Plasma Membrane in Tumor Cells. *Nagoya J. Med. Sci.* **1993**, *56*, 1–18, doi:10.18999/nagjms.56.1-4.1.

87. Eller, C.H.; Chao, T.Y.; Singarapu, K.K.; Ouerfelli, O.; Yang, G.; Markley, J.L.; Danishefsky, S.J.; Raines, R.T. Human Cancer Antigen Globo H Is a Cell-Surface Ligand for Human Ribonuclease 1. *ACS Cent. Sci.* **2015**, *1*, 181–190, doi:10.1021/acscentsci.5b00164.

88. Leland, P.A.; Schultz, L.W.; Kim, B.M.; Raines, R.T. Ribonuclease A Variants with Potent Cytotoxic Activity. *Proc. Natl. Acad. Sci. U. S. A.* **1998**, *95*, 10407–10412, doi:10.1073/pnas.95.18.10407.

89. Vasandani, V.M.; Wu, Y.N.; Mikulski, S.M.; Youle, R.J.; Sung, C. Molecular Determinants in the Plasma Clearance and Tissue Distribution of Ribonucleases of the Ribonuclease A Superfamily. *Cancer Res.* **1996**, *56*, 4180–4186.

90. Matoušek, J. Ribonucleases and Their Antitumor Activity. *Comp. Biochem. Physiol. - C Toxicol. Pharmacol.* **2001**, *129*, 175–191, doi:10.1016/S1532-0456(01)90202-9.

91. Rodríguez, M.; Moussaoui, M.; Benito, A.; Cuchillo, C.M.; Nogués, M. V.; Vilanova, M. Human Pancreatic Ribonuclease Presents Higher Endonucleolytic Activity than Ribonuclease A. *Arch. Biochem. Biophys.* **2008**, *471*, 191–197, doi:10.1016/j.abb.2007.12.016.

92. Leland, P.A.; Staniszewski, K.E.; Kim, B.M.; Raines, R.T. Endowing Human Pancreatic Ribonuclease with Toxicity for Cancer Cells. *J. Biol. Chem.* **2001**, *276*, 43095–43102, doi:10.1074/jbc.M106636200.

93. Kuusisto, H. V.; Wagstaff, K.M.; Alvisi, G.; Roth, D.M.; Jans, D.A. Global Enhancement of Nuclear Localization-dependent Nuclear Transport in Transformed Cells. *FASEB J.* **2012**, *26*, 1181–1193, doi:10.1096/fj.11-191585.

94. Benito, A.; Vilanova, M.; Ribo, M. Intracellular Routing of Cytotoxic Pancreatic-Type Ribonucleases. *Curr. Pharm. Biotechnol.* **2008**, *9*, 169–179, doi:10.2174/138920108784567281.

95. Bosch, M.; Benito, A.; Ribó, M.; Puig, T.; Beaumelle, B.; Vilanova, M. A Nuclear Localization Sequence Endows Human Pancreatic Ribonuclease with Cytotoxic Activity. *Biochemistry* **2004**, *43*, 2167–2177, doi:10.1021/bi035729+.

96. Castro, J.; Ribó, M.; Navarro, S.; Nogués, M. V.; Vilanova, M.; Benito, A. A Human Ribonuclease Induces Apoptosis Associated with P21WAF1/CIP1 Induction and JNK Inactivation. *BMC Cancer* **2011**, *11*, 9, doi:10.1186/1471-2407-11-9.

97. Rodríguez, M.; Benito, A.; Tubert, P.; Castro, J.; Ribó, M.; Beaumelle, B.; Vilanova, M. A Cytotoxic Ribonuclease Variant with a Discontinuous Nuclear Localization Signal Constituted by Basic Residues Scattered Over Three Areas of the Molecule. *J. Mol. Biol.* **2006**, *360*, 548–557, doi:10.1016/j.jmb.2006.05.048.

98. Vert, A.; Castro, J.; Ruiz-Martínez, S.; Tubert, P.; Escribano, D.; Ribó, M.; Vilanova, M.; Benito, A. Generation of New Cytotoxic Human Ribonuclease Variants Directed to the Nucleus. *Mol. Pharm.* **2012**, *9*, 2894–2902, doi:10.1021/mp300217b.

99. Tubert, P.; Rodríguez, M.; Ribó, M.; Benito, A.; Vilanova, M. The Nuclear Transport Capacity of a Human-Pancreatic Ribonuclease Variant Is Critical for Its Cytotoxicity. *Invest. New Drugs* **2011**, *29*, 811–817, doi:10.1007/s10637-010-9426-2.

100. Castro, J.; Ribó, M.; Puig, T.; Colomer, R.; Vilanova, M.; Benito, A. A Cytotoxic Ribonuclease Reduces the Expression Level of P-Glycoprotein in Multidrug-Resistant Cell Lines. *Invest. New Drugs* **2012**, *30*, 880–888, doi:10.1007/s10637-011-9636-2.

101. Vert, A.; Castro, J.; Ribó, M.; Benito, A.; Vilanova, M.; Vert, A.; Castro, J.; Ribó, M.; Benito, A.; Vilanova, M.; et al. A Nuclear-Directed Human Pancreatic Ribonuclease (PE5) Targets the Metabolic Phenotype of Cancer Cells. *Oncotarget* **2016**, *7*, 18309–18324, doi:10.18632/oncotarget.7579.

102. Fanara, P.; Hodel, M.R.; Corbett, A.H.; Hodel, A.E. Quantitative Analysis of Nuclear Localization Signal (NLS)-Importin α Interaction through Fluorescence Depolarization: Evidence for Auto-Inhibitory Regulation of NLS Binding. *J. Biol. Chem.* **2000**, *275*, 21218–21223, doi:10.1074/jbc.M002217200.

103. García-Galindo, G. Anàlisi de La Selectivitat per a Cèl·lules Tumorals de Ribonucleases Citotòxiques i Desenvolupament d'eines per Augmentar Aquesta Selectivitat, Universitat de Girona, 2016.

104. García-Galindo, G.; Castro, J.; Matés, J.; Bravo, M.; Ribó, M.; Vilanova, M.; Benito, A. The Selectivity for Tumor Cells of Nuclear-Directed Cytotoxic RNases Is Mediated by the Nuclear/Cytoplasmic Distribution of P27KIP1. *Molecules* **2021**, *26*, doi:10.3390/molecules26051319.

105. Castro, J.; Tornillo, G.; Ceada, G.; Ramos-Neble, B.; Bravo, M.; Ribó, M.; Vilanova, M.; Smalley, M.J.; Benito, A. A Nuclear-Directed Ribonuclease Variant Targets Cancer Stem Cells and Inhibits Migration and Invasion of Breast Cancer Cells. *Cancers (Basel).* **2021**, *13*, doi:10.3390/cancers13174350.

106. Chen, D.; Milacic, V.; Frezza, M.; Dou, Q. Metal Complexes, Their Cellular Targets and Potential for Cancer Therapy. *Curr. Pharm. Des.* **2009**, *15*, 777–791, doi:10.2174/138161209787582183.

107. Zhang, C.X.; Lippard, S.J. New Metal Complexes as Potential Therapeutics. *Curr. Opin. Chem. Biol.* **2003**, *7*, 481–489, doi:10.1016/S1367-5931(03)00081-4.

108. Castro, J.; Manrique, E.; Bravo, M.; Vilanova, M.; Benito, A.; Fontrodona, X.; Rodríguez, M.; Romero, I. A Family of Manganese Complexes Containing Heterocyclic-Based Ligands with Cytotoxic Properties. *J. Inorg. Biochem.* **2018**, *182*, 124–132, doi:10.1016/j.jinorgbio.2018.01.021.

109. Storr, T. *Ligand Design in Medicinal Inorganic Chemistry*; Wiley, 2014; Vol. 9781118488; ISBN 9781118697191.

110. Haas, K.L.; Franz, K.J. Application of Metal Coordination Chemistry to Explore and Manipulate Cell Biology. *Chem. Rev.* **2009**, *109*, 4921–4960, doi:10.1021/cr900134a.

111. Huang, D.; Savage, S.R.; Calinawan, A.P.; Lin, C.; Zhang, B.; Wang, P.; Starr, T.K.; Birrer, M.J.; Paulovich, A.G. A Highly Annotated Database of Genes Associated with Platinum Resistance in Cancer. *Oncogene 2021 4046* **2021**, *40*, 6395–6405, doi:10.1038/s41388-021-02055-2.

112. Simpson, P. V.; Desai, N.M.; Casari, I.; Massi, M.; Falasca, M. Metal-Based Antitumor Compounds: Beyond Cisplatin. *Future Med. Chem.* **2019**, *11*, 119–135, doi:10.4155/fmc-2018-0248.

113. Gheorghe-Cetean, S.; Cainap, C.; Oprean, L.; Hangan, A.; Virag, P.; Fischer-Fodor, E.; Gherman, A.; Cainap, S.; Constantin, A.-M.; Laszlo, I.; et al. Platinum Derivatives: A Multidisciplinary Approach. *J. BUON.* **2017**, *22*, 568–577.

114. Rébé, C.; Demontoux, L.; Pilot, T.; Ghiringhelli, F. Platinum Derivatives Effects on Anticancer Immune Response. *Biomolecules* **2020**, *10*, doi:10.3390/biom10010013.

115. Howell, S.B.; Safaei, R.; Larson, C.A.; Sailor, M.J. Copper Transporters and the Cellular Pharmacology of the Platinum-Containing Cancer Drugs. *Mol.*

Pharmacol. **2010**, *77*, 887–894, doi:10.1124/mol.109.063172.

116. Karasawa, T.; Sibrian-Vazquez, M.; Strongin, R.M.; Steyger, P.S. Identification of Cisplatin-Binding Proteins Using Agarose Conjugates of Platinum Compounds. *PLoS One* **2013**, *8*, e66220, doi:10.1371/journal.pone.0066220.

117. Rancoule, C.; Guy, J.B.; Vallard, A.; Ben Mrad, M.; Rehailia, A.; Magné, N. Les 50 Ans Du Cisplatine. *Bull. Cancer* **2017**, *104*, 167–176, doi:10.1016/j.bulcan.2016.11.011.

118. Galanski, M.; Jakupec, M.; Keppler, B. Update of the Preclinical Situation of Anticancer Platinum Complexes: Novel Design Strategies and Innovative Analytical Approaches. *Curr. Med. Chem.* **2005**, *12*, 2075–2094, doi:10.2174/0929867054637626.

119. Dilruba, S.; Kalayda, G. V. Platinum-Based Drugs: Past, Present and Future. *Cancer Chemother. Pharmacol.* **2016**, *77*, 1103–1124, doi:10.1007/s00280-016-2976-z.

120. Ando, Y.; Shimokata, T.; Yasuda, Y.; Hasegawa, Y. Carboplatin Dosing for Adult Japanese Patients. *Nagoya J. Med. Sci.* **2014**, *76*, 1–9, doi:10.18999/nagjms.76.1-2.1.

121. Boyd, L.R.; Muggia, F.M. Carboplatin/Paclitaxel Induction in Ovarian Cancer: The Finer Points. *Oncol. (United States)* **2018**, *32*, 418–424.

122. Ndagi, U.; Mhlongo, N.; Soliman, M.E. Metal Complexes in Cancer Therapy – An Update from Drug Design Perspective. *Drug Des. Devel. Ther.* **2017**, *11*, 599–616, doi:10.2147/DDDT.S119488.

123. Erikson, K.M.; Syversen, T.; Aschner, J.L.; Aschner, M. Interactions between Excessive Manganese Exposures and Dietary Iron-Deficiency in Neurodegeneration. In Proceedings of the Environmental Toxicology and Pharmacology; Elsevier, May 1 2005; Vol. 19, pp. 415–421.

124. Hurley, L.S.; Keen, C.L. Manganese. In *Trace Elements in Human and Animal Nutrition: Fifth Edition*; 1987; pp. 185–223 ISBN 9780080924687.

125. Wedler, F.C. Biological Significance of Manganese in Mammalian Systems. In *Progress in Medicinal Chemistry*; Elsevier, 1993; Vol. 30, pp. 89–133.

126. Zhou, D.F.; Chen, Q.Y.; Qi, Y.; Fu, H.J.; Li, Z.; Zhao, K. Di; Gao, J. Anticancer Activity, Attenuation on the Absorption of Calcium in Mitochondria, and Catalase Activity for Manganese Complexes of N-Substituted Di(Picolyl)Amine. *Inorg. Chem.* **2011**, *50*, 6929–6937, doi:10.1021/ic200004y.

127. Aschner, M.; Guilarte, T.R.; Schneider, J.S.; Zheng, W. Manganese: Recent Advances in Understanding Its Transport and Neurotoxicity. *Toxicol. Appl. Pharmacol.* **2007**, *221*, 131–147, doi:10.1016/j.taap.2007.03.001.

128. El Mchichi, B.; Hadji, A.; Vazquez, A.; Leca, G. P38 MAPK and MSK1 Mediate Caspase-8 Activation in Manganese-Induced Mitochondria-Dependent Cell Death. *Cell Death Differ.* **2007**, *14*, 1826–1836, doi:10.1038/sj.cdd.4402187.

129. Oubrahim, H.; Stadtman, E.R.; Chock, P.B. Mitochondria Play No Roles in Mn(II)-Induced Apoptosis in HeLa Cells. *Proc. Natl. Acad. Sci. U. S. A.* **2001**, *98*, 9505–9510, doi:10.1073/pnas.181319898.

130. Kovala-Demertzi, D.; Hadjipavlou-Litina, D.; Staninska, M.; Primikiri, A.; Kotoglou, C.; Demertzis, M.A. Anti-Oxidant, in Vitro, in Vivo Anti-Inflammatory Activity and Antiproliferative Activity of Mefenamic Acid and Its Metal Complexes with Manganese(II), Cobalt(II), Nickel(II), Copper(II) and Zinc(II). *J. Enzyme Inhib. Med. Chem.* **2009**, *24*, 742–752, doi:10.1080/14756360802361589.

131. Liu, J.; Guo, W.; Li, J.; Li, X.; Geng, J.; Chen, Q.; Gao, J. Tumor-Targeting Novel Manganese Complex Induces ROS-Mediated Apoptotic and Autophagic Cancer Cell Death. *Int. J. Mol. Med.* **2015**, *35*, 607–616, doi:10.3892/ijmm.2015.2073.

132. Pereira, T.A.; Da Silva, G.E.T.; Hernández, R.B.; Forti, F.L.; Espósito, B.P. Antitumor Activity of Mn(III) Complexes in Combination with Phototherapy and Antioxidant Therapy. *BioMetals* **2013**, *26*, 439–446, doi:10.1007/s10534-013-9626-2.

133. Rich, J.; Rodríguez, M.; Romero, I.; Fontrodona, X.; Van Leeuwen, P.W.N.M.; Freixa, Z.; Sala, X.; Poater, A.; Solà, M. N-Tetradentate Spanamine Derivatives and Their MnII-Complexes as Catalysts for Epoxidation of Alkenes. *Eur. J. Inorg. Chem.* **2013**, *2013*, 1213–1224, doi:10.1002/ejic.201201154.

134. Rich, J.; Rodríguez, M.; Romero, I.; Vaquer, L.; Sala, X.; Llobet, A.; Corbella, M.; Collomb, M.N.; Fontrodona, X. Mn(Ii) Complexes Containing the Polypyridylic Chiral Ligand (−)-Pinene[5,6]Bipyridine. Catalysts for Oxidation Reactions. *J. Chem. Soc. Dalt. Trans.* **2009**, 8117–8126, doi:10.1039/b906435d.

135. Rich, J.; Manrique, E.; Molton, F.; Duboc, C.; Collomb, M.N.; Rodríguez, M.; Romero, I. Catalytic Activity of Chloro and Triflate Manganese(II) Complexes in Epoxidation Reactions: Reusable Catalytic Systems for Alkene Epoxidation. *Eur. J. Inorg. Chem.* **2014**, *2014*, 2663–2670, doi:10.1002/ejic.201402032.

136. Manrique, E.; Poater, A.; Fontrodona, X.; Solà, M.; Rodríguez, M.; Romero, I. Reusable Manganese Compounds Containing Pyrazole-Based Ligands for Olefin Epoxidation Reactions. *Dalt. Trans.* **2015**, *44*, 17529–17543, doi:10.1039/c5dt02787j.

137. Velders, A.H.; Kooijman, H.; Spek, A.L.; Haasnoot, J.G.; De Vos, D.; Reedijk, J. Strong Differences in the in Vitro Cytotoxicity of Three Isomeric Dichlorobis(2-Phenylazopyridine)Ruthenium(II) Complexes. *Inorg. Chem.*

2000, *39*, 2966–2967, doi:10.1021/ic000167t.

138. Khan, A.; Singh, P.; Srivastava, A. Synthesis, Nature and Utility of Universal Iron Chelator – Siderophore: A Review. *Microbiol. Res.* **2018**, *212–213*, 103–111, doi:10.1016/j.micres.2017.10.012.

139. Lieu, P.T.; Heiskala, M.; Peterson, P.A.; Yang, Y. The Roles of Iron in Health and Disease. *Mol. Aspects Med.* **2001**, *22*, 1–87, doi:10.1016/S0098-2997(00)00006-6.

140. Liu, X.; Dong, X.; He, C.; Zhang, X.; Xiang, G.; Ma, X. New Polyazamacrocyclic 3-Hydroxy-4-Pyridinone Based Ligands for Iron Depletion Antitumor Activity. *Bioorg. Chem.* **2020**, *96*, 103574, doi:10.1016/j.bioorg.2020.103574.

141. Akam, E.A.; Tomat, E. Targeting Iron in Colon Cancer via Glycoconjugation of Thiosemicarbazone Prochelators. *Bioconjug. Chem.* **2016**, *27*, 1807–1812, doi:10.1021/acs.bioconjchem.6b00332.

142. Raza, M.; Chakraborty, S.; Choudhury, M.; Ghosh, P.; Nag, A. Cellular Iron Homeostasis and Therapeutic Implications of Iron Chelators in Cancer. *Curr. Pharm. Biotechnol.* **2014**, *15*, 1125–1140, doi:10.2174/1389201015121412021119 15.

143. Kolberg, M.; Strand, K.R.; Graff, P.; Kristoffer Andersson, K. Structure, Function, and Mechanism of Ribonucleotide Reductases. *Biochim. Biophys. Acta - Proteins Proteomics* **2004**, *1699*, 1–34, doi:10.1016/j.bbapap.2004.02.007.

144. Jomova, K.; Valko, M. Importance of Iron Chelation in Free Radical-Induced Oxidative Stress and Human Disease. *Curr. Pharm. Des.* **2011**, *17*, 3460–3473, doi:10.2174/138161211798072463.

145. Vessieres, A. Iron Compounds as Anticancer Agents. In *RSC Metallobiology*; Royal Society of Chemistry, 2019; Vol. 2019-Janua, pp. 62–90 ISBN 9781782629917.

146. Wang, K.; Gao, E. Recent Advances in Multinuclear Complexes as Potential Anticancer and DNA Binding Agents. *Anticancer. Agents Med. Chem.* **2014**, *14*, 147–169, doi:10.2174/1871520611313999031 3.

147. Curado, N.; Contel, M. Heterometallic Complexes as Anticancer Agents. In *RSC Metallobiology*; Royal Society of Chemistry, 2019; Vol. 2019-Janua, pp. 143–168 ISBN 9781782629917.

148. Dvořák, Z.; Štarha, P.; Šindelář, Z.; Trávníček, Z. Evaluation of in Vitro Cytotoxicity of One-Dimensional Chain [Fe(Salen)(L)] n Complexes against Human Cancer Cell Lines. *Toxicol. Vitr.* **2012**, *26*, 480–484, doi:10.1016/j.tiv.2012.01.006.

149. Horn, A.; Fernandes, C.; Parrilha, G.L.; Kanashiro, M.M.; Borges, F. V.; De Melo,

E.J.T.; Schenk, G.; Terenzi, H.; Pich, C.T. Highly Efficient Synthetic Iron-Dependent Nucleases Activate Both Intrinsic and Extrinsic Apoptotic Death Pathways in Leukemia Cancer Cells. *J. Inorg. Biochem.* **2013**, *128*, 38–47, doi:10.1016/j.jinorgbio.2013.07.019.

150. Studier, F.W.; Moffatt, B.A. Use of Bacteriophage T7 RNA Polymerase to Direct Selective High-Level Expression of Cloned Genes. *J. Mol. Biol.* **1986**, *189*, 113–130, doi:10.1016/0022-2836(86)90385-2.

151. Ribó, M.; Benito, A.; Canals, A.; Nogués, M. V.; Cuchillo, C.M.; Vilanova, M. Purification of Engineered Human Pancreatic Ribonuclease. *Methods Enzymol.* **2001**, *341*, 221–234, doi:10.1016/S0076-6879(01)41154-2.

152. Pace, C.N.; Vajdos, F.; Fee, L.; Grimsley, G.; Gray, T. How to Measure and Predict the Molar Absorption Coefficient of a Protein. *Protein Sci.* **1995**, *4*, 2411–2423, doi:10.1002/pro.5560041120.

153. Martínez-Ferraté, O.; López-Valbuena, J.M.; Belmonte, M.M.; White, A.J.P.; Benet-Buchholz, J.; Britovsek, G.J.P.; Claver, C.; Van Leeuwen, P.W.N.M. Novel Iminopyridine Derivatives: Ligands for Preparation of Fe(Ii) and Cu(Ii) Dinuclear Complexes. *Dalt. Trans.* **2016**, *45*, 3564–3576, doi:10.1039/c5dt04358a.

154. Cailleau, R.; Young, R.; Olivé, M.; Reeves, W.J. Breast Tumor Cell Lines from Pleural Effusions. *J. Natl. Cancer Inst.* **1974**, *53*, 661–674, doi:10.1093/jnci/53.3.661.

155. Hinterleitner, T.A.; Saada, J.I.; Berschneider, H.M.; Powell, D.W.; Valentich, J.D. IL-1 Stimulates Intestinal Myofibroblast COX Gene Expression and Augments Activation of Cl- Secretion in T84 Cells. *Am. J. Physiol. - Cell Physiol.* **1996**, *271*, doi:10.1152/ajpcell.1996.271.4.c1262.

156. Carney, D.N.; Gazdar, A.F.; Bepler, G.; Guccion, J.G.; Marangos, P.J.; Moody, T.W.; Zweig, M.H.; Minna, J.D. Establishment and Identification of Small Cell Lung Cancer Cell Lines Having Classic and Variant Features. *Cancer Res.* **1985**, *45*, 2913–2923, doi:10.1016/s0169-5002(86)80023-x.

157. Mitra, A.K.; Davis, D.A.; Tomar, S.; Roy, L.; Gurler, H.; Xie, J.; Lantvit, D.D.; Cardenas, H.; Fang, F.; Liu, Y.; et al. In Vivo Tumor Growth of High-Grade Serous Ovarian Cancer Cell Lines. *Gynecol. Oncol.* **2015**, *138*, 372–377, doi:10.1016/j.ygyno.2015.05.040.

158. Breslin, S.; O'Driscoll, L. Three-Dimensional Cell Culture: The Missing Link in Drug Discovery. *Drug Discov. Today* **2013**, *18*, 240–249, doi:10.1016/j.drudis.2012.10.003.

159. Fang, Y.; Eglen, R.M. Three-Dimensional Cell Cultures in Drug Discovery and Development. *SLAS Discov.* **2017**, *22*, 456–472, doi:10.1177/1087057117696795.

160. Elliott, N.T.; Yuan, F. A Review of Three-Dimensional in Vitro Tissue Models for Drug Discovery and Transport Studies. *J. Pharm. Sci.* **2011**, *100*, 59–74, doi:10.1002/jps.22257.

161. Edmondson, R.; Broglie, J.J.; Adcock, A.F.; Yang, L. Three-Dimensional Cell Culture Systems and Their Applications in Drug Discovery and Cell-Based Biosensors. *Assay Drug Dev. Technol.* **2014**, *12*, 207–218, doi:10.1089/adt.2014.573.

162. Vert, A. Molecular Mechanism of PE5-Induced Cytotoxicity and Generation of New Cytotoxic Nuclear-Directed Ribonuclease Variants, Universitat de Girona (UdG), 2014.

163. Donaldson-Collier, M.C.; Sungalee, S.; Zufferey, M.; Tavernari, D.; Katanayeva, N.; Battistello, E.; Mina, M.; Douglass, K.M.; Rey, T.; Raynaud, F.; et al. EZH2 Oncogenic Mutations Drive Epigenetic, Transcriptional, and Structural Changes within Chromatin Domains. *Nat. Genet.* **2019**, *51*, 517–528, doi:10.1038/s41588-018-0338-y.

164. Vettese-Dadey, M.; Grant, P.A.; Hebbes, T.R.; Crane-Robinson, C.; Allis, C.D.; Workman, J.L. Acetylation of Histone H4 Plays a Primary Role in Enhancing Transcription Factor Binding to Nucleosomal DNA in Vitro. *EMBO J.* **1996**, *15*, 2508–2518, doi:10.1002/j.1460-2075.1996.tb00608.x.

165. Kornberg, R.D.; Lorch, Y. Twenty-Five Years of the Nucleosome, Fundamental Particle of the Eukaryote Chromosome. *Cell* **1999**, *98*, 285–294, doi:10.1016/S0092-8674(00)81958-3.

166. Kundu, T.K.; Palhan, V.B.; Wang, Z.; An, W.; Cole, P.A.; Roeder, R.G. Activator-Dependent Transcription from Chromatin in Vitro Involving Targeted Histone Acetylation by P300. *Mol. Cell* **2000**, *6*, 551–561, doi:10.1016/S1097-2765(00)00054-X.

167. Chavez, K.J.; Garimella, S. V.; Lipkowitz, S. Triple Negative Breast Cancer Cell Lines: One Tool in the Search for Better Treatment of Triple Negative Breast Cancer. *Breast Dis.* **2010**, *32*, 35–48, doi:10.3233/BD-2010-0307.

168. Anders, C.K.; Carey, L.A. Biology, Metastatic Patterns, and Treatment of Patients with Triple-Negative Breast Cancer. *Clin. Breast Cancer* **2009**, *9*, S73, doi:10.3816/CBC.2009.s.008.

169. Weatherburn, D.C.; Mandal, S.; Mukhopadhyay, S.; Bhaduri, S.; Lindoy, L.F. Manganese. In *Comprehensive Coordination Chemistry II*; Pergamon, 2004; Vol. 5, pp. 1–125 ISBN 9780080437484.

170. Wu, A.J.; Penner-Hahn, J.E.; Pecoraro, V.L. Structural, Spectroscopic, and Reactivity Models for the Manganese Catalases. In *Chemical Reviews*; American Chemical Society, 2004; Vol. 104, pp. 903–938.

171. Mullins, C.S.; Pecoraro, V.L. Reflections on Small Molecule Manganese Models

That Seek to Mimic Photosynthetic Water Oxidation Chemistry. *Coord. Chem. Rev.* **2008**, *252*, 416–443, doi:10.1016/j.ccr.2007.07.021.

172. Dismukes, C.G.; Reedijk, J. Bioinorganic Catalysis. *Reedijk J Marcel Dekker, New York, USA* **1993**, 317.

173. Huang, X.; Wang, Z.; Wu, Y.; Fan, T.; Wang, S.; Wang, X. Variety of Molecular Conformation of Plasmid PUC18 DNA and Solenoidally Supercoiled DNA. *Sci. China. Ser. C, Life Sci.* **1996**, *39*, 571–583.

174. Torre, L.A.; Siegel, R.L.; Ward, E.M.; Jemal, A. Global Cancer Incidence and Mortality Rates and Trends - An Update. *Cancer Epidemiol. Biomarkers Prev.* 2016, *25*, 16–27.

175. Sung, H.; Ferlay, J.; Siegel, R.L.; Laversanne, M.; Soerjomataram, I.; Jemal, A.; Bray, F. Global Cancer Statistics 2020: GLOBOCAN Estimates of Incidence and Mortality Worldwide for 36 Cancers in 185 Countries. *CA. Cancer J. Clin.* **2021**, *71*, 209–249, doi:10.3322/caac.21660.

176. Mathew, M.; Verma, R.S. Humanized Immunotoxins: A New Generation of Immunotoxins for Targeted Cancer Therapy. *Cancer Sci.* **2009**, *100*, 1359–1365, doi:10.1111/j.1349-7006.2009.01192.x.

177. Ngollo, M.; Lebert, A.; Daures, M.; Judes, G.; Rifai, K.; Dubois, L.; Kemeny, J.L.; Penault-Llorca, F.; Bignon, Y.J.; Guy, L.; et al. Global Analysis of H3K27me3 as an Epigenetic Marker in Prostate Cancer Progression. *BMC Cancer* **2017**, *17*, 1–8, doi:10.1186/s12885-017-3256-y.

178. Mironova, N.; Patutina, O.; Brenner, E.; Kurilshikov, A.; Vlassov, V.; Zenkova, M. The Systemic Tumor Response to RNase A Treatment Affects the Expression of Genes Involved in Maintaining Cell Malignancy. *Oncotarget* **2017**, *8*, 78796–78810, doi:10.18632/oncotarget.20228.

179. Saxena, S.K.; Sirdeshmukh, R.; Ardelt, W.; Mikulski, S.M.; Shogen, K.; Youle, R.J. Entry into Cells and Selective Degradation of TRNAs by a Cytotoxic Member of the RNase A Family. *J. Biol. Chem.* **2002**, *277*, 15142–15146, doi:10.1074/jbc.M108115200.

180. Lee, Y.S.; Shibata, Y.; Malhotra, A.; Dutta, A. A Novel Class of Small RNAs: TRNA-Derived RNA Fragments (TRFs). *Genes Dev.* **2009**, *23*, 2639–2649, doi:10.1101/gad.1837609.

181. Tong, L.; Zhang, W.; Qu, B.; Zhang, F.; Wu, Z.; Shi, J.; Chen, X.; Song, Y.; Wang, Z. The TRNA-Derived Fragment-3017A Promotes Metastasis by Inhibiting NELL2 in Human Gastric Cancer. *Front. Oncol.* **2021**, *10*, 3468, doi:10.3389/fonc.2020.570916.

182. Pellakuru, L.G.; Iwata, T.; Gurel, B.; Schultz, D.; Hicks, J.; Bethel, C.; Yegnasubramanian, S.; De Marzo, A.M. Global Levels of H3K27me3 Track with Differentiation in Vivo and Are Deregulated by MYC in Prostate Cancer.

Am. J. Pathol. **2012**, *181*, 560–569, doi:10.1016/j.ajpath.2012.04.021.

183. Hsieh, I. yun; He, J.; Wang, L.; Lin, B.; Liang, Z.; Lu, B.; Chen, W.; Lu, G.; Li, F.; Lv, W.; et al. H3K27me3 Loss Plays a Vital Role in CEMIP Mediated Carcinogenesis and Progression of Breast Cancer with Poor Prognosis. *Biomed. Pharmacother.* **2020**, *123*, 109728, doi:10.1016/J.BIOPHA.2019.109728.

184. Chen, X.; Song, N.; Matsumoto, K.; Nanashima, A.; Nagayasu, T.; Hayashi, T.; Ying, M.; Endo, D.; Wu, Z.; Koji, T. High Expression of Trimethylated Histone H3 at Lysine 27 Predicts Better Prognosis in Non-Small Cell Lung Cancer. *Int. J. Oncol.* **2013**, *43*, 1467–1480, doi:10.3892/IJO.2013.2062.

185. Vinci, M.; Box, C.; Zimmermann, M.; Eccles, S.A. Tumor Spheroid-Based Migration Assays for Evaluation of Therapeutic Agents. In *Methods in Molecular Biology*; Humana Press, Totowa, NJ, 2013; Vol. 986, pp. 253–266.

186. Ciołczyk-Wierzbicka, D.; Laidler, P. The Inhibition of Invasion of Human Melanoma Cells through N-Cadherin Knock-Down. *Med. Oncol.* **2018**, *35*, 1–9, doi:10.1007/s12032-018-1104-9.

187. Derycke, L.D.M.; Bracke, M.E. N-Cadherin in the Spotlight of Cell-Cell Adhesion, Differentiation, Embryogenesis, Invasion and Signalling. *Int. J. Dev. Biol.* **2004**, *48*, 463–476, doi:10.1387/IJDB.041793LD.

188. Wu, Z.; Xue, S.; Zheng, B.; Ye, R.; Xu, G.; Zhang, S.; Zeng, T.; Zheng, W.; Chen, C. Expression and Significance of C-Kit and Epithelial-Mesenchymal Transition (EMT) Molecules in Thymic Epithelial Tumors (TETs). *J. Thorac. Dis.* **2019**, *11*, 4602–4612, doi:10.21037/jtd.2019.10.56.

189. Loessner, D.; Stok, K.S.; Lutolf, M.P.; Hutmacher, D.W.; Clements, J.A.; Rizzi, S.C. Bioengineered 3D Platform to Explore Cell-ECM Interactions and Drug Resistance of Epithelial Ovarian Cancer Cells. *Biomaterials* **2010**, *31*, 8494–8506, doi:10.1016/j.biomaterials.2010.07.064.

190. Karlsson, H.; Fryknäs, M.; Larsson, R.; Nygren, P. Loss of Cancer Drug Activity in Colon Cancer HCT-116 Cells during Spheroid Formation in a New 3-D Spheroid Cell Culture System. *Exp. Cell Res.* **2012**, *318*, 1577–1585, doi:10.1016/j.yexcr.2012.03.026.

191. Adcock, A.F. Three-Dimensional (3D) Cell Cultures in Cell-Based Assays for in-Vitro Evaluation of Anticancer Drugs. *J. Anal. Bioanal. Tech.* **2015**, *06*, 1–12, doi:10.4172/2155-9872.1000249.

192. Trédan, O.; Galmarini, C.M.; Patel, K.; Tannock, I.F. Drug Resistance and the Solid Tumor Microenvironment. *J. Natl. Cancer Inst.* **2007**, *99*, 1441–1454, doi:10.1093/jnci/djm135.

193. Dasari, S.; Bernard Tchounwou, P. Cisplatin in Cancer Therapy: Molecular Mechanisms of Action. *Eur. J. Pharmacol.* 2014, *740*, 364–378.

194. Sciot, R.; Eyken, P. Van; Desmet, V.J. Transferrin Receptor Expression in Benign Tumours and in Hepatoblastoma of the Liver. *Histopathology* **1990**, *16*, 59–62, doi:10.1111/j.1365-2559.1990.tb01061.x.

195. Calzolari, A.; Oliviero, I.; Deaglio, S.; Mariani, G.; Biffoni, M.; Sposi, N.M.; Malavasi, F.; Peschle, C.; Testa, U. Transferrin Receptor 2 Is Frequently Expressed in Human Cancer Cell Lines. *Blood Cells, Mol. Dis.* **2007**, *39*, 82–91, doi:10.1016/j.bcmd.2007.02.003.

196. Ansari, K.I.; Grant, J.D.; Kasiri, S.; Woldemariam, G.; Shrestha, B.; Mandal, S.S. Manganese(III)-Salens Induce Tumor Selective Apoptosis in Human Cells. *J. Inorg. Biochem.* **2009**, *103*, 818–826, doi:10.1016/j.jinorgbio.2009.02.004.

197. Li, M.X.; Chen, C.L.; Zhang, D.; Niu, J.Y.; Ji, B.S. Mn(II), Co(II) and Zn(II) Complexes with Heterocyclic Substituted Thiosemicarbazones: Synthesis, Characterization, X-Ray Crystal Structures and Antitumor Comparison. *Eur. J. Med. Chem.* **2010**, *45*, 3169–3177, doi:10.1016/j.ejmech.2010.04.009.

198. Zhang, F.; Lin, Q.Y.; Zheng, X.L.; Zhang, L.L.; Yang, Q.; Gu, J.Y. Crystal Structures, Interactions with Biomacromolecules and Anticancer Activities of Mn(II), Ni(II), Cu(II) Complexes of Demethylcantharate and 2-Aminopyridine. *J. Fluoresc.* **2012**, *22*, 1395–1406, doi:10.1007/s10895-012-1078-5.

199. Al-Anbaky, Q.; Al-Karakooly, Z.; Kilaparty, S.P.; Agrawal, M.; Albkuri, Y.M.; Rangumagar, A.B.; Ghosh, A.; Ali, N. Cytotoxicity of Manganese (III) Complex in Human Breast Adenocarcinoma Cell Line Is Mediated by the Generation of Reactive Oxygen Species Followed by Mitochondrial Damage. *Int. J. Toxicol.* **2016**, *35*, 672–682, doi:10.1177/1091581816659661.

200. Hille, A.; Ott, I.; Kitanovic, A.; Kitanovic, I.; Alborzinia, H.; Lederer, E.; Wölfl, S.; Metzler-Nolte, N.; Schäfer, S.; Sheldrick, W.S.; et al. [N,N′-Bis(Salicylidene)-1,2-Phenylenediamine]Metal Complexes with Cell Death Promoting Properties. *J. Biol. Inorg. Chem.* **2009**, *14*, 711–725, doi:10.1007/s00775-009-0485-9.

201. Farghadani, R.; Rajarajeswaran, J.; Mohd Hashim, N.B.; Abdulla, M.A.; Muniandy, S. A Novel β-Diiminato ManganeseIII Complex as the Promising Anticancer Agent Induces G0/G1 Cell Cycle Arrest and Triggers Apoptosis via Mitochondrial-Dependent Pathways in MCF-7 and MDA-MB-231 Human Breast Cancer Cells. *RSC Adv.* **2017**, *7*, 24387–24398, doi:10.1039/c7ra02478a.

202. Slator, C.; Molphy, Z.; McKee, V.; Kellett, A. Triggering Autophagic Cell Death with a Di-Manganese(II) Developmental Therapeutic. *Redox Biol.* **2017**, *12*, 150–161, doi:10.1016/j.redox.2017.01.024.

203. Xu, Q.; Zhan, G.; Zhang, Z.; Yong, T.; Yang, X.; Gan, L. Manganese Porphyrin-Based Metal-Organic Framework for Synergistic Sonodynamic Therapy and Ferroptosis in Hypoxic Tumors. *Theranostics* **2021**, *11*, 1937–1952,

doi:10.7150/thno.45511.

204. Gao, E.J.; Su, J.; Zhang, S.; Zhou, H.; Zhan, Y.; Qiu, X.; Ding, Y.Q.; Sun, N.; Zhu, M.C. Synthesis, Structures, Fluorescence Studies and Cytotoxicity of a New Manganese(II) Complex. *Inorg. Nano-Metal Chem.* **2017**, *47*, 1509–1519, doi:10.1080/24701556.2017.1357603.

205. Zhao, P.; Zhong, W.; Ying, X.; Yuan, Z.; Fu, J.; Zhou, Z. Manganese Chloride-Induced G0/G1 and S Phase Arrest in A549 Cells. *Toxicology* **2008**, *250*, 39–46, doi:10.1016/j.tox.2008.05.016.

206. HERNROTH, B.; HOLM, I.; GONDIKAS, A.; TASSIDIS, H. Manganese Inhibits Viability of Prostate Cancer Cells. *Anticancer Res.* **2018**, *38*, 137 LP – 145.

207. Oubrahim, H.; Boon Chock, P.; Stadtman, E.R. Manganese(II) Induces Apoptotic Cell Death in NIH3T3 Cells via a Caspase-12-Dependent Pathway. *J. Biol. Chem.* **2002**, *277*, 20135–20138, doi:10.1074/jbc.C200226200.

208. Abbaspour, N.; Hurrell, R.; Kelishadi, R. Review on Iron and Its Importance for Human Health. *J. Res. Med. Sci.* **2014**, *19*, 164–174.

209. McDonald, A.R.; Que, L. High-Valent Nonheme Iron-Oxo Complexes: Synthesis, Structure, and Spectroscopy. *Coord. Chem. Rev.* **2013**, *257*, 414–428, doi:10.1016/j.ccr.2012.08.002.

210. Xie, L.; Luo, Z.; Zhao, Z.; Chen, T. Anticancer and Antiangiogenic Iron(II) Complexes That Target Thioredoxin Reductase to Trigger Cancer Cell Apoptosis. *J. Med. Chem.* **2017**, *60*, 202–214, doi:10.1021/acs.jmedchem.6b00917.

211. Poh, H.T.; Ho, P.C.; Fan, W.Y. Cyclopentadienyl Iron Dicarbonyl (CpFe(CO)2) Derivatives as Apoptosis-Inducing Agents. *RSC Adv.* **2016**, *6*, 18814–18823, doi:10.1039/c5ra23891a.

212. Pradhan, N.; Pratheek, B.M.; Garai, A.; Kumar, A.; Meena, V.S.; Ghosh, S.; Singh, S.; Kumari, S.; Chandrashekar, T.K.; Goswami, C.; et al. Induction of Apoptosis by Fe(Salen)Cl through Caspase-Dependent Pathway Specifically in Tumor Cells. *Cell Biol. Int.* **2014**, *38*, 1118–1131, doi:10.1002/cbin.10308.

213. Pilon, A.; Brás, A.R.; Côrte-Real, L.; Avecilla, F.; Costa, P.J.; Preto, A.; Helena Garcia, M.; Valente, A. A New Family of Iron(II)-Cyclopentadienyl Compounds Shows Strong Activity against Colorectal and Triple Negative Breast Cancer Cells. *Molecules* **2020**, *25*, 1592, doi:10.3390/molecules25071592.

214. Wong, E.L.M.; Fang, G.S.; Che, C.M.; Zhu, N. Highly Cytotoxic Iron(II) Complexes with Pentadentate Pyridyl Ligands as a New Class of Anti-Tumor Agents. *Chem. Commun.* **2005**, 4578–4580, doi:10.1039/b507687k.

215. Kwong, W.L.; Lok, C.N.; Tse, C.W.; Wong, E.L.M.; Che, C.M. Anti-Cancer Iron(II)

Complexes of Pentadentate N-Donor Ligands: Cytotoxicity, Transcriptomics Analyses, and Mechanisms of Action. *Chem. - A Eur. J.* **2015**, *21*, 3062–3072, doi:10.1002/chem.201404749.

216. Fei, B.L.; Xu, W.S.; Gao, W.L.; Zhang, J.; Zhao, Y.; Long, J.Y.; Anson, C.E.; Powell, A.K. DNA Binding and Cytotoxicity Activity of a Chiral Iron(III) Triangle Complex Based on a Natural Rosin Product. *J. Photochem. Photobiol. B Biol.* **2015**, *142*, 77–85, doi:10.1016/j.jphotobiol.2014.11.008.

217. Kim, K.K.; Singh, R.K.; Strongin, R.M.; Moore, R.G.; Brard, L.; Lange, T.S. Organometallic Iron(Iii)-Salophene Exerts Cytotoxic Properties in Neuroblastoma Cells via Mapk Activation and Ros Generation. *PLoS One* **2011**, *6*, e19049, doi:10.1371/journal.pone.0019049.

218. Ansari, K.I.; Kasiri, S.; Grant, J.D.; Mandal, S.S. Fe(III)-Salen and Salphen Complexes Induce Caspase Activation and Apoptosis in Human Cells. *J. Biomol. Screen.* **2011**, *16*, 26–35, doi:10.1177/1087057110385227.

219. Lange, T.S.; Kim, K.K.; Singh, R.K.; Strongin, R.M.; McCourt, C.K.; Brard, L. Iron(III)-Salophene: An Organometallic Compound with Selective Cytotoxic and Anti-Proliferative Properties in Platinum-Resistant Ovarian Cancer Cells. *PLoS One* **2008**, *3*, e2303, doi:10.1371/journal.pone.0002303.

220. Pelicano, H.; Carney, D.; Huang, P. ROS Stress in Cancer Cells and Therapeutic Implications. *Drug Resist. Updat.* **2004**, *7*, 97–110, doi:10.1016/j.drup.2004.01.004.

221. XJ, W.; X, H. Targeting ROS: Selective Killing of Cancer Cells by a Cruciferous Vegetable Derived pro-Oxidant Compound. *Cancer Biol. Ther.* **2007**, *6*, 646–647, doi:10.4161/CBT.6.5.4092.

222. Norbury, C.J.; Zhivotovsky, B. DNA Damage-Induced Apoptosis. *Oncogene* **2004**, *23*, 2797–2808, doi:10.1038/sj.onc.1207532.